Summer 2022

Seasonal Assessments of Bioregeneration in Slow Sand Filters Amended with Granular Activated Carbon

Katherine R. Morsefield
University of New Hampshire

Seasonal Assessments of Bioregeneration in Slow Sand Filters Amended with Granular Activated Carbon

BY

KATHERINE ROSE MORSEFIELD

B.S. Biology, Bowling Green State University, 2019

THESIS

Submitted to the University of New Hampshire

in Partial Fulfillment of

the Requirements for the Degree of

Master of Science

In

Civil & Environmental Engineering

September 2022

This thesis has been examined and approved in partial fulfillments of the requirements for the degree of Master of Science in Civil & Environmental Engineering by:

Thesis Director, M. Robin Collins, PhD, P.E., Professor of Civil and Environmental Engineering

Paula Mouser, PhD, P.E., Associate Professor of Civil and Environmental Engineering

Jeffrey Hall, PhD, Research Scientist II

On May 25th, 2022

Original approval of signatures are on file with the University of New Hampshire Graduate School.

Acknowledgements

I would like to acknowledge a number of individuals who made this research project possible. I am grateful to Dr. Robin Collins for introducing me to engineering concepts and projects related to slow sand filtration. I would like to personally thank Dan Wells, the superintendent at the Winthrop Utilities District, for all of his assistance and cooperation throughout the duration of this study. Lastly, I'd like to acknowledge Peter Dwyer, Damon Burt, Kellen Sawyer and Todd Lang for their assistance both in the field and in the laboratory.

My fellow colleagues, students, friends, and family also played a monumental role in the completion of this project. Without their continued support, this would not have been possible. I am especially grateful for my parents as they have always encouraged me and believed in me.

Katie Morsefield

June, 2022

TABLE OF CONTENTS

List of Tables

List of Figures

List of Abbreviations

SSF	Slow sand filtration
GAC	Granular activated carbon
DOC	Dissolved organic carbon
BDOC	Biodegradable organic carbon
HDLR	Hydraulic loading rate
ES	Effective size
U.C.	Uniformity coefficient
NOM	Natural organic matter
THFMP	Trihalomethane formation potential
NTU	Nephelometric turbidity units
THM	Trihalomethane
SOC	Synthetic organic chemical
DBP	Disinfection byproduct
MW	Molecular weight
PAC	Powder activated carbon
EAC	Extruded activated carbon
F400	Filtrasorb® 400
TOC	Total organic carbon
PPCPs	Pharmaceutical and personal care products
BAC	Biologically activated carbon
EBCT	Empty bed contact time
ATP	Adenosine triphosphate
DNA	Deoxyribonucleic acid
EPS	Extracellular polymeric substance
HSSF	Household slow sand filtration
I-HSSF	Intermittent household slow sand filtration
C-HSSF	Continuous household slow sand filtration
AWWSC	American Water Works Service Company
CGE	Compagnie Générale des Eaux
G/GA	Glucose/glutamic acid
UV	Ultraviolet
ABS	Absorbance
pH	Potential hydrogen
PCR	Polymerase chain reaction
TBE	Tris/Borate/EDTA
iTOL	Interactive tree of life
ICP-AES	Inductively coupled plasma atomic emission spectroscopy
PCOA	Principle coordinate analysis

ABSTRACT

Seasonal Assessments of Bioregeneration in Slow Sand Filters Amended with Granular Activated Carbon

by
Katherine Rose Morsefield
University of New Hampshire, September 2022

The application of slow sand filtration (SSF) has conventionally proven to be a reliable and relatively inexpensive means of producing potable drinking water for decades. As technologies in drinking water treatment continue to advance, innovations to the design and operation of slow sand filtration have the ability to transform its contribution in municipal and industrial settings. SSF amended with granular activated carbon (GAC) has been on the rise in recent decades due to its ability to improve the removal of organic material, while allowing SSF to maintain its innate treatment simplicity.

A slow sand filter amended with granular activated carbon in Winthrop, Maine has demonstrated the potential to preserve the life span of the GAC sublayer for over one and a half decades. From the time when GAC was initially installed in 2005, it has not required the addition of human regenerative interferences to maintain elevated removals of organic precursor measured by dissolved organic carbon (DOC). This study aimed to investigate the biologically active components and seasonal microbial patterns within filter sublayers that may contribute to the GAC bioregenerative process. Specific goals of this study were to explore mechanisms contributing to the maintenance of GAC adsorption sites, explore impacts of seasonal temperature variations on biodegradable and non-biodegradable organic carbon removals by

slow sand filters amended with GAC, and to explore impacts of seasonal temperature variations on microbial communities.

Removals associated with biodegradable organic carbon (BDOC) and non-biodegradable organic carbon (BDOC) showed significant removals after several years of filter run-time, as well as differences in removals based on various GAC "ages." Biomass and microbial community composition showed sensitivity to filter media type, location within the filter, and influence of temperature variations. Metals accumulations and content on various media showed significant accumulations of Iron on sand media and Calcium on GAC media. Results suggest calcium cation accumulation on the GAC sublayer may be correlated to higher removals of organic carbon on GAC.

1. INTRODUCTION

1.1 Overview of Slow Sand Filtration with a GAC Sublayer

The implementation and use of granular amendments in conventional slow sand filtration has demonstrated the ability to improve treatment performance and enhance removal of natural organic matter. Granular activated carbon (GAC) has the ability to enhance adsorption of natural organic matter while preserving the simplicity of conventional slow sand filtration processes. Previous studies have highlighted the ability of GAC to maintain elevated removals of dissolved organic carbon after several years of use without the need for replacement or regeneration. The present study investigates mechanisms contributing to the renewal of GAC adsorption sites, along with microbial variation within GAC sublayers and adjacent media layers.

The GAC "Sandwich" modification was first studied at the University of New Hampshire in 1987 (Collins et al., 1987) and later studied in greater depth by Tom Page (Page,1997). This modification to conventional slow sand filters involves an 8-15 centimeter layer of granular activated carbon that is placed in the middle of a previously established slow sand filter bed. Conventional slow sand filters require slow filtration rates and this application to the GAC sublayer allows for greater contact time, ultimately augmenting adsorption. The GAC "sandwich" design allows for the upper layer of sand, also known as the schmutzdecke, to act as a biological mechanism in removing dissolved organic matter and particulates, while the GAC sublayer acts as a non-backwashed adsorber (Page, 1997).

Advantages to GAC sandwich modifications to conventional SSF includes installation within pre-existing SSF structures without the addition of piping systems and framework. Due to GAC

acting as a non-backwashed adsorber, system backwashes are not required for this type of system design creating less maintenance for system operators. GAC sandwich modifications implemented in conventional slow sand filter designs can provide various benefits in drinking water treatment and remain a viable option for small communities.

1.2 Research Statement

The genesis of this study was associated with a granular activated carbon layer that was installed in a slow sand filter in Winthrop, Maine in the year 2005. This study aimed to investigate why slow sand filters amended with granular activated carbon have continued to achieve elevated removals of dissolved organic carbon without the replacement or regeneration of the GAC sublayer.

1.3 Research Objectives and Approach

The main objective of this research was to evaluate biologically active components, chemically active components, and seasonal microbial patterns within filter sublayers that may contribute to the GAC bioregenerative process. Extensive biological and chemical analyses were performed to assess potential factors contributing to the bioregenerative process of the GAC sublayer.

Specific goals of this study were to:

- Explore the impact of seasonal temperature variation on biodegradable and non-biodegradable organic carbon removals by slow sand filters amended with GAC
- Explore mechanisms contributing to the maintenance of GAC adsorption sites over an extended period of time

- Explore the impact of seasonal temperature variation on biomass production and microbial communities

Sampling events occurred at the Slow Sand Water Filtration Plant in Winthrop, Maine at various dates based on seasonal patterns. Media samples were collected from Filter #1 to perform ATP biomass analyses, DNA extraction and sequencing analyses, and metals extractions. Aqueous samples were collected to assess general water quality parameters, total organic carbon, dissolved organic carbon, and biodegradable organic carbon.

2. LITERATURE REVIEW

2.1 Overview of Slow Sand Filtration

Slow sand filtration has been implemented worldwide for centuries. The treatment process provides excellent municipal water treatment for areas in which source water is low in color, turbidity, and algae. The design of this system provides a simple, yet economically reliable operation for small communities.

2.1.1 History of Conventional Slow Sand Filters

Conventional slow sand filtration has been implemented all over the world due to its ability to provide exceptional treated water quality in combination with the simplicity of its design. The modern use and design of slow sand filters as a municipal drinking water treatment system originated in design by James Simpson in 1829 for the Chelsea Water Company in London (Baker,1949; Unger, 2006; Arora, 2017). With acceptance in Europe in the latter half of the 19th century, the United States followed in accepting SSF as a method of municipal drinking water treatment. The first slow sand filter implemented for municipal use in the United States was designed by James Kirkwood in Poughkeepsie, New York and was installed in 1872 (Unger, 2006). The traditional design schematic used today is demonstrated in Figure 2-1 and has been incorporated in drinking water treatment for over 100 years.

Initially, slow sand filters were appreciated for their ability to provide a mechanical means of straining out suspended solids and turbidity. The effectiveness of SSF to decrease the risk of waterborne diseases was determined prior to greater knowledge of relationships between pathogens causing the disease and elements of the disease itself (Manz, 2004).

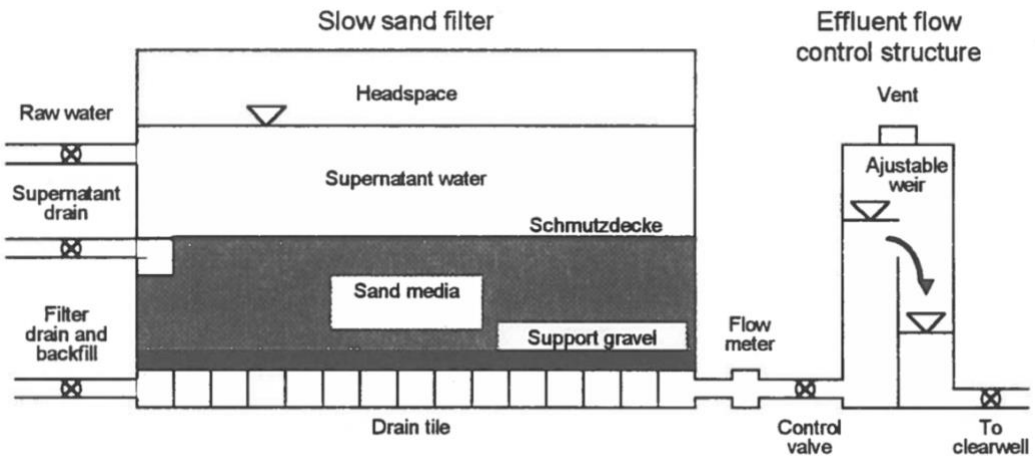

Figure 2-1. Overview of a conventional slow sand filter (adapted from Collins et al., 1991; Page, 1997).

Per Huisman & Wood (1974), slow sand filtration became a legal requirement for all potable water extracted from the Thames River in 1852 when Jon Snow linked the outbreak of cholera and typhoid to waterborne contamination. This connection was further investigated when a cholera epidemic occurred in Altona and Hamburg, Germany. In this event, Hamburg delivered water untreated to its community, while Altona delivered a filtered water supply to the community, avoiding the spread of waterborne disease. (Arora, 2017).

2.1.2 Design and Operation

The design and operation of a traditional slow sand filter is simple and cost effective. The purification of water is accomplished through a combination of physiochemical and biological processes when untreated water slowly percolates through a bed of porous sand (Partinoudi et al., 2006) The main elements of a slow sand filter include a supernatant water layer, filter medium, an underdrain system assimilated with support gravel, and a flow control system as shown in Figure 2-2.

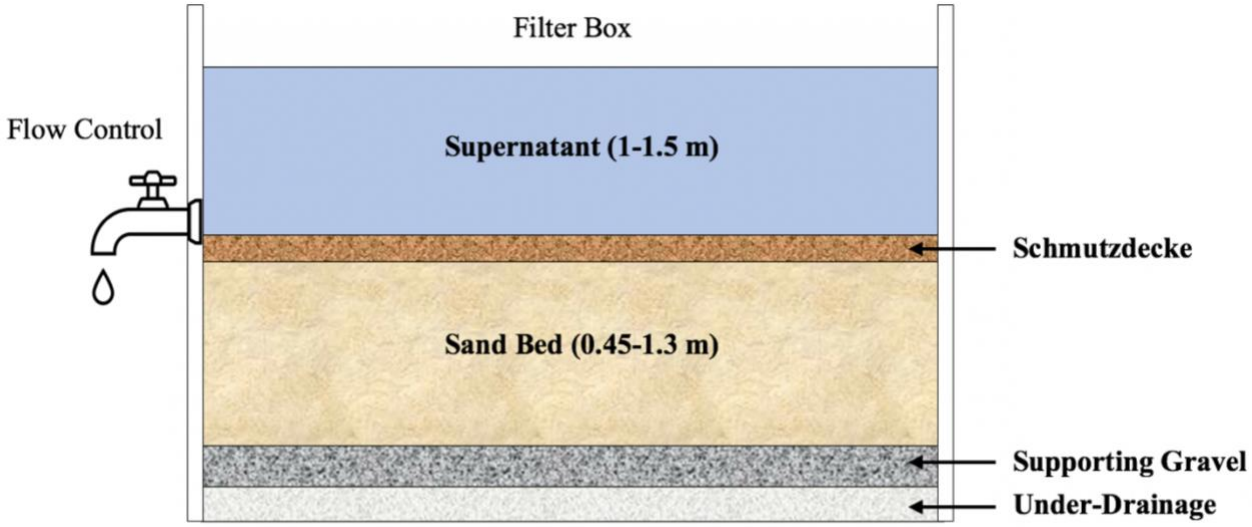

Figure 2-2. Slow sand filter configuration breakdown (values adapted from M.R. Collins, 2022).

- *Supernatant Water Layer*: The supernatant water serves two major purposes; providing a constant head above the filter and allowing the filter to overcome the opposition of the filter bed to produce downward flow of water through the sand bed.

- *Filter Medium*: Sand is one of the most common filter mediums used in this system due to its low cost, resilience, and accessibility. There are four major design elements of the sand bed mentioned by Unger (2006) which include:

    1. Plan area (A), determined by design flow rate (Q) and hydraulic loading rate (HLR)
    2. Depth
    3. Effective size (ES) of sand media (d_{10})
    4. Uniformity coefficient (UC) of sand media (d_{60}/d_{10})

- *Underdrain System*: The underdrain system typically consists of a gravel support layer that serves as a passageway for water from the filter bed. This system also serves as a layer of support for the filter bed.

- *Flow Control System*: The purpose of a flow control system is to regulate the speed at which water passes through the sand bed, ultimately determining the filtration rate for the system to operate effectively and efficiently.

There are several features which distinguish slow sand filtration from a variety of drinking water treatment methods. The application of slow filtration rates paired with moderately long filter run times makes SSF a unique treatment method that is cost effective and simple. Page (1997) also mentions the small effective size of the sand medium and univariant sand media at all depths are distinguishable characteristics. Lastly, the lack of pre-treatment needed for influent water sources prior to reaching the filter bed in combination without needing to perform backwashing of the filter bed makes the effort level relatively low in terms of operation. General design parameters for SSF and its operation are provided in Table 2-1 adapted from the Slow Sand Filtration Tech Brief (2000).

The design parameters for SSF are highly dependent upon the influent water quality. Raw water quality tends to limit the use of slow sand filters due to their innate ability to capture and remove suspended and particulate matter within the upper layer of the filter but lack the ability to remove organic contaminants and synthetic organic chemicals (Logsdon, 1990). Algae content is another parameter which must be considered in the design process. Per Huisman & Wood

(1974), the amount and nature of algae depends on source water temperature, turbidity, nutrient concentration, and amount of sunlight present. When surface waters contain turbidity levels less than 10 NTU and color less than 5 CU, slow sand filtration is considered an effective water treatment technology (Campos et al., 2002).

Table 2-1. Typical Design Parameters and Operation of SSF(adapted from Slow Sand Filtration Tech Brief, 2000).

Design parameters	Recommended range of values
Filtration rate	0.15 $m^3/m^2 \cdot h$ (0.1–0.2 $m^3/m^2 \cdot h$)
Area per filter bed	Less than 200 m^2 (in small community water supplies to ease manual filter cleaning)
Number of filter beds	Minimum of two beds
Depth of filter bed	1 m (minmum of 0.7 m of sand depth)
Filter media	Effective size (ES) = 0.15–0.35 mm; uniformity coefficient (UC) = 2-3
Height of supernatant water	0.7–1 m (maximum 1.5 m)
Underdrain system	
Standard bricks Precast concrete slabs Precast concrete blocks with holes on the top Porous concrete	Generally no need for further hydraulic calculations
Perforated pipes (laterals and manifold type)	Maximum velocity in the manifolds and in laterals = .3 m/s Spacing between laterals = 1.5 m Spacing of holes in laterals = 0.15 m Size of holes in laterals =3 mm

Source: Vigneswaran, S. and C. Visvanathan. 1995

To overcome raw water quality constraints for operational purposes, pre-treatment applications can be considered. Pre-treatment techniques commonly used in slow sand filtration include micro-straining, roughing filters, and pre-ozonation. Gravel roughing filters can be used to assist in removal of turbidity and algae (Collins et al., 1993). Further modifications made in the design of SSF to overcome these limitations include the use of geotextile filter mats to limit schmutzdecke scraping and pre-ozonation to encourage biological growth (Collins et al., 1993; Unger 2006).

2.1.3 SSF Maintenance

During filter operation, the long hydraulic detention time of the supernatant water layer above the sand bed leads to the development of the schmutzdecke. The schmutzdecke layer is a thin,

slimy matting of organic material that is high in biological activity and will be discussed in greater depth in *Section 2.2*. As this layer begins to form in a slow sand filter, this is known as the ripening period. Microorganisms entrap and digest organic matter contained in the raw water influent. The operation and success of slow sand filters rely on the schmutzdecke formation, as research has shown this layer undertakes a governing role in filtration. In SSF, the mechanism involved in the purification of water is mainly a biological process, therefore, its efficiency depends on a balanced community in the schmutzdecke and often requires operation at a constant rate (SSF Tech Brief, 2000).

Due to the application of low filtration rates in SSF, the extent of operation can vary. The amount of time a slow sand filter can operate is dependent upon environmental and source water conditions. The length of operation can last from 60 days to more than 15 years (Arora, 2017). As material begins to accumulate in the schmutzdecke, the filter surface can become clogged. When a filter becomes clogged, this results in an increase in hydraulic resistance to flow and an increase in headloss (Huisman & Wood, 1974). In order to determine the proper maintenance needed to keep slow sand filters in service, headloss is measured on a regular basis to determine when a filter needs to be cleaned.

Periodic maintenance requires slow sand filters to be removed from service and undergo a cleaning process. Filters are cleaned by lowering the water level in order to scrape and remove the schmutzdecke layer along with the top few centimeters of the sand bed. The scraped sand can be reused and this process requires a wash paired with a hydro-cyclone or shaker process in order to reduce most of the suspended solids (Arora, 2017). The washed sand can then be placed in the

sunlight to dry until it is ready for reuse. The length of time between filter cleanings can range from several weeks to a year and is dependent upon the raw water quality and the hydraulic loading rate (Page 1997; SSF Tech Brief, 2000). Once a filter has been cleaned, a ripening period is necessary in order for microbial communities to reestablish the schmutzdecke layer. The length of downtime during cleaning can affect the ripening period and this amount of time could be hours to several weeks depending on the age of the filter media and raw water quality (Cullen and Letterman, 1985).

Harrowing is a method commonly used to clean slow sand filters and is much more efficient than the traditional scraping technique. In West Hartford, Connecticut, operators developed the harrowing method via a comb-tooth harrow connected to a tractor (Collins et al., 1991). The harrow is placed on the top of the filter once the water level is drained to a significant level in order to rake the sand medium. Similar to filter scraping, the schmutzdecke layer and top few centimeters of the sand bed are discharged at the filter surface, as opposed to exiting through the filter bed. This method requires less time and labor to complete and it also allows for filters to maintain the schmutzdecke bacterial layer population while minimizing filter downtime (Collins et al., 1991). According to Visscher (1990), re-sanding a slow sand filter bed becomes necessary every few years when successive scrapings have reduced the sand bed to 0.5-0.6 m. The frequency at which re-sanding and the depth of the sand bed that needs to be refilled depends on the scraping frequency, which can vary from eight to ten years (Collins et al., 1991).

2.1.4 Removal Mechanisms in Slow Sand Filtration

There are a variety of complex forces which contribute to the removal mechanisms demonstrated in SSF. Slow sand filters are capable of removing an array of contaminants at various capacities. There are two main mechanisms involved within the slow sand filtration process and these include both physio-chemical mechanisms and biological mechanisms. This combination allows for conventional SSF processes to remove pathogenic microorganisms such as bacteria, cysts, viruses, and parasites (Poynter & Slade, 1977).

There are two main physical processes involved in slow sand filtration and these include mechanisms of straining and transport. Straining involves the removal of particles larger than grain pore size independent of the applied filtration rate, and can take place at the sand surface (Huisman & Wood, 1974). As water begins to pass through the schmutzdecke layer, followed by the top sand layer, biological matter has the aptitude to break down organic matter causing particles to be physically strained through filter layers. Transport mechanisms can include particle removal from sedimentation, diffusion, interception, inertial forces, and centrifugal forces (Arora, 2017). According to Ives (1970), the significance of various transport mechanisms displayed in SSF can be dependent upon flow rates, particle size, grain size, and temperature. Sedimentation in particular can be considered a characteristic of slow sand filtration. Due to the innate simplicity in design used in combination with a supernatant water layer, this system can promote undisturbed settling amongst filter layers. Sedimentation can occur within pore spaces of slow sand filters and can remove particles smaller than the pore space through settling on the sand grains (Haig et al., 2011).

The formation of the schmutzdecke plays an important biological role in SSF. The schmutzdecke can be divided into two regions, a filter cake or slime layer above the sand followed by a biologically active region in the sand bed (Unger, 2006). Two filtration mechanisms can occur with the presence of a cake layer and this includes cake filtration and depth filtration. In cake filtration, the solid versus fluid suspension to be treated passes through a medium with applied pressure, allowing the flow of suspending fluid (Tien & Bai, 2003). This allows for retention of suspended particles to form a cake on the upstream side of the medium (Tien & Bai, 2003). As filtration processes continue, the cake layer thickens shifting to the mechanism that involves filtration with depth. Depth filtration involves the separation of suspended particles from its carrying fluid within the depth of the filter medium (Sutherland, 2008). Depth filtration is a mechanism which can be combined with cake filtration mechanisms.

Adsorption is another removal mechanisms in SSF and occurs due to a surface process leading to a transfer of molecules and particulates from fluid bulk to a solid surface (Artioli, 2008). Due to this being a physio-chemical process, it favors the removal of dissolved substances and colloidal suspensions (Arora, 2017). Per Huisman and Wood (1974), the success of adsorption mechanisms through SSF is determined by Van der Waals forces, which are typically attractive in nature, and their electrostatic interactions. These interactions are particularly important between the substances to be removed and the sand grains. During the ripening period, adhesion can also play a large role in the success of adsorption. Particles of organic origin will be deposited on the filter surface as ripening occurs and these deposits quickly become the breeding ground for bacteria and other microorganisms (Huisman & Wood, 1974). This allows for the formation of the schmutzdecke layer. Further removals can be achieved as adsorption

mechanisms occur simultaneously with biodegradation. Langmuir and Freundlich isotherm equations are typically used to measure adsorption which is described as the equilibrium of substances attached on the surface with concentrations in the fluid (Artioli, 2008). These particular equations place emphasis and dependence on temperature and temperature is an important factor affecting adsorption removal mechanisms. From a biological and ecological standpoint, adsorption also plays a fundamental role. According to Artioli (2008), adsorption accounts for the transport of substances within ecosystems and can trigger essential processes such as ionic exchange and enzymatic processes.

Biologically active components in slow sand filter layers can also contribute to the removal process. The main components contributing to biological activity in slow sand filters occur as a result of the formation of the schmuztdecke, a thin biofilm layer, on the top sand layer. This creates microbial competition and a diverse microbial community with a variety of organisms performing different functions (Duncan, 1988). It has been proposed by Bellamy et al., 1985b that extracellular organisms can produce sticky biofilms on the filter surface by the attachment of microorganisms and can enhance removals in SSF. The formation of the schmutzdecke layer will be discussed in greater detail in Section 2.3.

Studies have also verified the removal of natural organic matter (NOM) in slow sand filtration. As mentioned previously, adsorption mechanisms and biodegradation are processes which occur simultaneously. Collins et al., 1989 discovered that removals of NOM occur predominantly in the schmutzdecke layer and top sand layer where both of these mechanisms are occurring simultaneously. Collins & Vaughan (1996) attempted to distinguish adsorption from

biodegradation and found that both mechanisms are imperative to NOM removal in biologically active filters. Studies have also indicated biomass and biological activity within slow sand filter sublayers play significant roles in dissolved organic carbon (DOC) removals and trihalomethane formation potential (THMFP) removals (Page, 1997). Biological removal mechanisms of NOM within SSF were studied more in depth by Collins and coworkers (1989) where methods of laminar and massive transfers from bulk fluid to media surfaces were applied. Metabolism of NOM was found to occur due to anabolic and catabolic reactions from extracellular enzymes. From this study, it was concluded that the utilization of NOM in slow sand filtration could assist in the renewal of adsorption sites to continue enhancing the removal of organics.

2.1.5 Advantages and Limitations to Conventional Slow Sand Filtration

The implementation and operation of SSF is advantageous in a variety of ways. A major advantage of SSF compared to other conventional treatment methods is the simplicity in design and construction. The absence of chemical and mechanical application allows for operator design and involvement to be limited, while also decreasing maintenance costs. Without a need for pumps, backwashing, and chemical treatments, this makes SSF reliable with no requirements for close supervision during operation.

SSF replaces the four main steps used in conventional drinking water treatment (coagulation/flocculation, sedimentation filtration, and disinfection) yet still produces and provides excellent treated water quality. Slow sand filtration reduces bacteria, cloudiness, and organic chemicals ultimately eliminating the need for disinfection (SSF Tech Brief, 2000). According to the Slow Sand Filtration Tech Brief (2000), slow sand filters have continually

demonstrated effectiveness in removing suspended particles with effluent turbidities below 1.0 nephelometric turbidity units (NTU), achieving 90 to 99+ percent removals in bacteria and viruses, as well as providing nearly complete removal of Giardia lamblia cysts and Cryptosporidium oocysts. Table 2-2 displays water quality parameters and removals associated with slow sand filtration.

Table 2-2. Water quality parameter and removal capacities of slow sand filtration (adapted from Collins,1998; Slow Sand Filtration Tech Brief, 2000).

Water Quality Paramenter	Removal Capacity
Turbidity	<1.0 NTU
Coliforms	1-3 log units
Enteric Viruses	2-4 log units
Giardia Cysts	2-4+log units
Cryptosporidium Oocysts	>4 log units
Dissolved Organic Carbon	<15-25%
Biodegradable	
Dissolved Organic Carbon	<50%
Trihalomethane Precursors	<20-30%
Heavy Metals	
Zn, Cu, Cd, Pb	>95-99%
Fe, Mn	>67%
As	<47%

Source: Adapted from Collins, M.R. 1998.

Some disadvantages to conventional slow sand filtration include a relatively large land area requirement paired with a slow hydraulic loading rate in order to maintain bacterial removal characteristics. In most communities, the availability of large land acreage is limited and can be quite expensive. Another disadvantage to SSF is that it is most successful when used for source waters that contain low algal content and low turbidity. Source waters that contain a turbidity level greater than 10 NTU may require the use of roughing filters as a pretreatment method to

reduce turbidity (Unger 2006; SSF Tech Brief, 2000) Pre-treatment methods are able to expand the scope of where SSF can be implemented, however, this creates an increase in time and costs for maintenance related to the removal of the schmutzdecke layer.

Lastly, SSF has limited ability to remove extremely colloid-size particles and dissolved organic compounds associated with color, taste, excessive trihalomethane (THM) precursor concentrations, and heavy metals, especially during colder temperatures (Manz, 2004; SSF Tech Brief, 2000). A GAC sandwich filter is a slow sand filter amended with a layer of GAC, which assists in removing organic material. This modification is discussed in greater detail in *Section 2.2* and serves as the main focus of the present study. This modified slow sand filter can effectively remove pesticides, total organic carbon and THM precursors (SSF Tech Brief, 2000). Slow sand filtration continues to remain the most appropriate filtration option for reduced systems and smaller communities despite its limitations.

2.2 GAC Sandwich Modification to Slow Sand Filtration

The implementation and use of granular amendments in conventional slow sand filtration has demonstrated the ability to improve treatment performance and enhance removal of natural organic matter. Granular activated carbon (GAC) has the ability to advance adsorption of natural organic matter while preserving the simplicity of conventional slow sand filtration processes. The main objective of this research is to explore the bioregenerative capacities of the GAC layer and how its properties may increase bed life of the GAC sublayer.

2.2.1 GAC Sandwich Description

The configuration of a slow sand filter amended with a GAC layer involves a base layer of sand, an intermediate GAC layer, a top sand layer. The term “sandwich” evolved from the fact that this configuration is simply the incorporation of a GAC layer in the middle of a conventional slow sand filter. The typical configuration of a slow sand filter amended with GAC is highlighted in Figure 2-3.

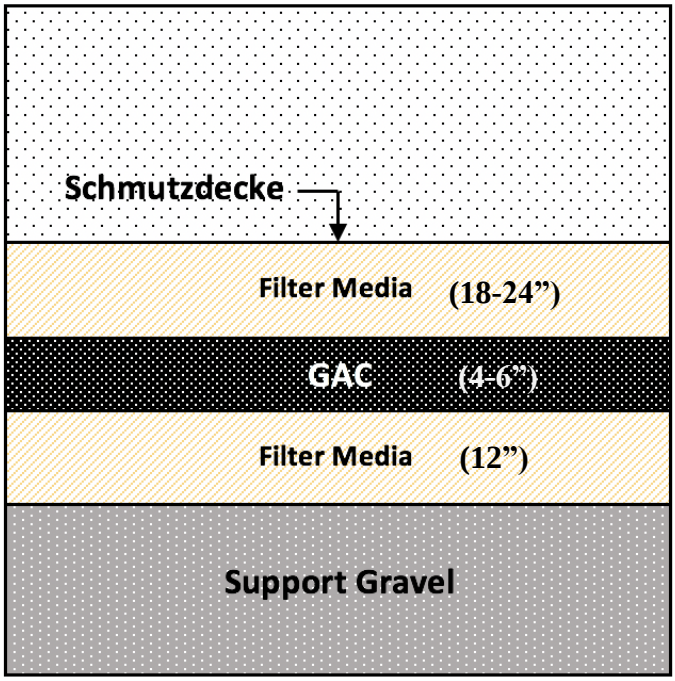

Figure 2-3. Configuration of a slow sand filter amended with granular activated carbon (values adapted from M.R. Collins, 2022).

This type of filter uses a top sand layer approximately 18 inches in depth, followed by a GAC layer ranging from 4-6 inches in depth, and a base sand layer approximately 12 inches in depth. (SSF Tech Brief, 2000). The sandwiched configuration of GAC between the layers of a conventional slow sand filter provides the advantages of slow sand filtration in combination with granular activated carbon adsorption mechanisms in a solitary unit.

SSFs modified with a GAC sublayer was first studied at the University of New Hampshire in 1987 (Collins et al., 1987) and in greater depth at the university by Tom Page (Page, 1997). In comparison to single medium filters, the GAC sandwich SSF system is multi-functional and has the ability to enhance biodegradation (Page, 1997; Campos et al., 2002; Li et al., 2018). The upper layer of sand acts a biological mechanism reducing the incoming particulate and dissolved organic carbon (DOC) loading onto the GAC, while the GAC can act as a non-backwashed adsorber (Page, 1997). The slow filtration rate requirement for the operation of conventional slow sand filters allows for a long contact time with the GAC, thus efficiently enhancing adsorption within the GAC layer. The lower sand layer serves as a support to the GAC layer and inhibits finer GAC particles from passing into the effluent, as well as microorganisms (Bauer et al., 1995). GAC sandwich modification to SSF can effectively remove pesticides, total organic carbon (TOC), THM precursors, and has the capability to support enhanced biodegradation. (Page, 1997; SSF Tech Brief, 2000).

2.2.2 Properties of Granular Activated Carbon

The application of granular activated carbon in drinking water treatment systems has increased the removal of both synthetic organic chemicals (SOCs) and dissolved naturally occurring organic materials (NOMs) due to its adsorptive properties. Synthetic organic chemicals are of particular concern within the drinking water treatment operation due to their adverse effects on human health, while natural organic materials are a major antecedent to the formation of disinfection byproducts (DBPs) (Karanfil & Kilduff, 1999). According to the United States Environmental Protection Agency (USEPA), GAC adsorption has been declared one of the best available technologies for removing both SOCs and NOMs (EPA, 2022).

Activated carbon can be produced from a variety of carbonaceous materials including wood, coal, lignin, coconut shells, and sugar (Karanfil & Kilduff, 1999; Lu et al., 2020). This results in the creation of a microporous adsorbent that contains a high surface area along with a broad range of surface functional groups. (Karanfil & Kilduff, 1999). The adsorptive effectiveness and capacity is determined by the volume of well-developed pores and the pore-size distribution relative to the molecular weight (MW) of organic matter (Karanfil & Kilduff, 1999; Nowotny et. al, 2007).

The chemical structure of activated carbon also plays a dominant role in how surface functional groups can influence the adsorptive properties of granular activated carbon, as well as its ability to be reactivated and reused once it reaches exhaustion. The structure is primarily comprised of carbon atoms that are ordered in parallel stacks of hexagonal layers, which are crosslinked and tetrahedrally bonded (Kilduff & Karanfil, 1999). Within this carbon matrix, elements such as oxygen, hydrogen, and nitrogen can be found. Typically, there are three main forms of activated carbon used in a variety of liquid phase treatments and these are shown in Figure 2-4. These include a) granular activated carbon (GAC), b) powder activated carbon (PAC), and c) extruded activated carbon (EAC) (Wholesale Activated Carbon, 2022). Once activated carbon has reached exhausted bed volume capacity, several techniques can be used to reactivate the carbon for reuse as described in greater detail later.

a) GAC b) PAC c) EAC

Figure 2-4. Three main forms of activated carbon used in gas and liquid phase adsorption. (adapted from Wholesale Activated Carbon, 2022)

The GAC used in this present study is Calgon's Filtrasorb® 400 (F400). The type of contaminants to be removed by F400 GAC include taste and odor compounds, organic color, total organic carbon (TOC), industrial organic compounds such as TCE and PCE, PFAS, and selected heavy metals (Patil et al., 2013; Filtrasorb® 400 Granular Activated Carbon Data Sheet, 2019). Some benefits to using Calgon F400 as the GAC of choice listed within the Filtrasorb® 400 Granular Activated Carbon Data Sheet (2019) include:

- High density carbon resulting in greater adsorption capacity per unit volume.
- Carbon granules are uniformly activated through the entire granule resulting in excellent adsorption properties and constant adsorption kinetics.
- Carbon bed segregation is retained after repeated abrasions, ensuring the adsorption profile remains undisturbed to maximize bed life.

This particular type of carbon is produced using select grades of bituminous coal through a process known as reagglomeration. The process of reagglomeration produces a highly active and durable granular product that is able to endure abrasion impacts. F400 abrasion impacts can include repeated backwashing, hydraulic transport, and reactivation for reuse (Filtrasorb® 400 Granular Activated Carbon Data Sheet, 2019). The activation of carbon is carefully controlled in order to produce significant volumes of both low and high energy pores for effective adsorption. Typical properties of Calgon F400 Carbon is displayed below in Table 2-3 and is typically applied in down-flow packed bed operations using gravity or pressure systems. Specifications and design considerations for GAC Sandwich SSF systems depend upon the operating conditions, desired treatment objectives, and the compounds being adsorbed. Calgon F400 is formulated to comply with all the applicable provisions of the AWWA Standard for Granular Activated Carbon (B604) and is produced in the United States.

While backwashing of GAC cannot occur once placed in a conventional slow sand filter, conditioning and backwashing prior to placing media online is crucial to the performance of granular activated carbon. Before placing fresh media online, there are three important factors as to why this is necessary: (1) separates the media by size, therefore, subsequent backwashing will return the media to the same relative position in the bed; (2) assists in removing any remaining air from the bed; (3) contributes to the removal of fine media which can lead to excessive pressure drop and flow restriction (Filtrasorb® 400 Granular Activated Carbon Data Sheet, 2019). Proper implementation of backwashing prior to granular activated carbon use in SSF is a crucial step in order to collect the most representative and meaningful contaminants within the filter bed.

Table 2-3. Filtrasorb® 400 GAC specifications and properties (adapted from Filtrasorb® 400 Granular Activated Carbon Data Sheet, 2019).

Specifications[1]	FILTRASORB 400
Iodine Number, mg/g	1000 (min)
Moisture by Weight	2% (max)
Effective Size	0.55–0.75 mm
Uniformity Coefficient	1.9 (max)
Abrasion Number	75 (min)
Screen Size by Weight, US Sieve Series	
On 12 mesh	5% (max)
Through 40 mesh	4% (max)

[1]Calgon Carbon test method

Typical Properties*	FILTRASORB 400
Apparent Density (tamped)	0.54 g/cc
Water Extractables	<1%
Non-Wettable	<1%

*For general information only, not to be used as purchase specifications.

2.2.3 GAC Removal Mechanisms

One main property of granular activated carbon that makes it advantageous when applied to SSF is its adsorption capacity. Clean carbon surfaces are oleophilic, which creates a strong attraction for organic compounds and non-polar contaminants via van der Waals forces (Patil et al., 2013). Granular activated carbon has been hypothesized to provide a more favorable surface for the attachment and accumulation of microorganisms than typical filter media. It is expected that the GAC sublayer should reach a point of exhaustion and be ready for replacement at the time of re-sanding (Page, 1997). However, slow adsorption mechanisms, removals attributed to biodegradation, and the bioregeneration process may account for removals on the GAC sublayer over extended periods of time.

A pseudo steady-state of operation and removal is eventually reached in GAC amended filters that are operated for long durations of time without the application of regenerative processes. Studies have shown that steady-state removals of natural organic matter (NOM) measured by total organic carbon (TOC) and trihalomethane formation potential (THFMP) can range from 10% to 40% (Roberts & Summers 1982; Glaze & Wallace, 1984; Carlson et al; 1994; Wang et al; 1995; Page, 1997). Pseudo steady-state removals have also been reported in the literature for dissolved organic carbon (DOC) removals ranging from 1-4 mg DOC/L GAC/h (Eberhardt 1976; AWWA, 1981; Maloney et al.,1984; Glaze & Wallace, 1984; Page, 1997). As removal mechanisms in GAC are related to both adsorption and biodegradation mechanisms, Figure 2-5 obtained from Sontheimer et al., 1988 and Carlson et al., 1994 displays a theoretical representation of DOC removals by adsorption and biodegradation processes.

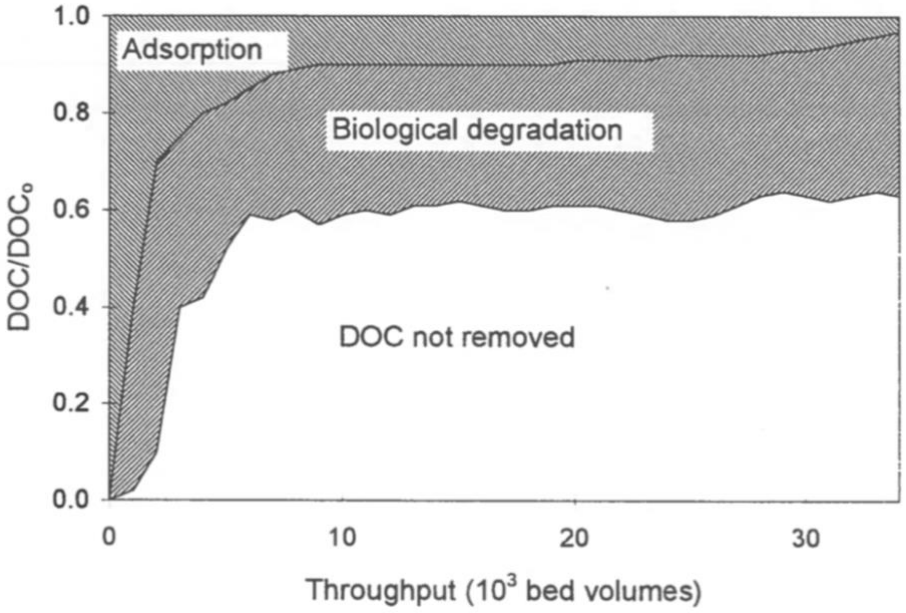

Figure 2-5. Theoretical representation of DOC removals by adsorption and biodegradation (adapted from Sontheimer et al. 1988 and Carlson et al., 1994).

Adsorption mechanisms dominate within the initial period while bacteria populations are in the acclimation phase (Page, 1997). According to Sontheimer et al., (1988), biological degradation begins to occur within the first five to twenty days of filter operation and becomes more significant as adsorption sites within the GAC are saturated over time. Once steady-state conditions plateau, it is suspected that majority of the adsorption capacity is exhausted. Once this occurs, biodegradation is then considered the predominant removal mechanism (Roberts & Summers, 1982). Removal over extended periods of time may also be accounted for with slow mass transfer into the micropore regions of granular activated carbon (Peel & Benedek, 1983).

Slow adsorption within micropore regions of GAC could be another probable mechanism contributing to the pseudo steady-state removal phase. A dual rate kinetic model was developed by Peel and Benedek (1980) to assist in predicting this mode of TOC adsorption. This particular model assumes carbon particles consist of both macropores and micropores. The slow adsorption approach to equilibrium is assumed to occur within the micropore region (Page, 1997). This kinetic model was later verified in a study by Peel & Benedek (1983). Long-term pilot studies involving relatively bio refractory feed streams to GAC columns verified that the close agreement between experimental break through curves and predictions from the model suggest that long-term removal of organics is principally caused by adsorption mechanisms (Peel, 1979; Peel & Benedek, 1983).

GAC sandwich models have also been applied in more recent filtration studies in attempts to remove pharmaceutical and personal care products (PPCPs) and antibiotics from source waters. Li et al., (2018) evaluated lab-scale GAC sandwich slow sand filters with various GAC layer

depths. The main compounds used in this study were DEET, paracetamol, caffeine, and triclosan at concentrations of 25 ug/L. In this study, the target PPCPs were significantly removed by using GAC sandwich SSF than sand alone (Li et al., 2018). Filter 2, which consisted of 10 cm of sand, 10 cm of GAC, and 30 cm of sand at a flow rate of 5 cm/h, had an average removal of 99.5% for targeted PPCPs. (Li et al., 2018). It was also determined that there were no significant differences of PPCP removals when flow rates were altered between 10 cm/h and 20 cm/h for the three GAC sandwiched filters used in this study. Xu et al., 2021 compared antibiotic removals in sand, GAC, GAC sandwich, and anthracite-sand dual biofilters at bench-scale to mimic filtration processes typically seen in drinking water treatment. This study was conducted for a duration of three months to emphasize biofilter performance and the removal of five antibiotics: amoxicillin, clarithromycin, oxytetracycline, sulfamethoxazole, and trimethoprim. Target antibiotics were significantly removed by GAC-associated biofilters corresponding to an average of greater than 90% removals, while sand and anthracite-sand biofilters showed removals corresponding to less than 20% (Xu et al., 2021).

Along with slow adsorption mechanisms, there has been evidence of enhanced biodegradation in slow sand filters amended with granular activated carbon. As discussed in *Section 2.2.2*, there are several biological and chemical properties associated with granular activated carbon that contribute to the advantages of using GAC as a biological support medium in SSF. The process in which GAC is created results in a microporous adsorbent which contains a high surface area and broad range of surface functional groups (Karanfil & Kilduff, 1999). The functional groups created through the production of GAC, particularly -OH and -COOH on the activated carbon surface have demonstrated the ability to enhance microbial attachment (Stewart et al., 1990;

Kutics & Suzuki, 1992; Page, 1997). The natural roughness and porosity of GAC has also been shown to provide a greater surface area for attachment of microorganisms within the GAC sublayer. Activated carbon can also be partially regenerated by microorganisms while the carbon bed remains in operation (Page, 1997). Evidence supporting bioregeneration within a GAC sublayer will be discussed in greater detail in *Section 2.2.4*.

2.2.4 Bioregeneration of GAC Adsorption Sites

The removal and adsorption mechanisms that occur with the application of granular activated carbon are important to understand, as they can be essential in predicting the long-term performances associated with slow sand filters sandwiched with GAC. After several months of operation, filters amended with GAC eventually transition into biologically active carbon (BAC) filters. BAC filters have the ability to remove organic pollutants as well as inorganic nutrients via methods of adsorption, enhanced biodegradation, and bioregeneration.

During any type of treatment which involves the incorporation of granular activated carbon, the sites on GAC that are available for adsorption decrease over time as pollutants and other natural organic matter are adsorbed. This results in the adsorptive capacities of carbon surfaces greatly decreasing causing GAC to eventually be replaced or regenerated. A naturally occurring phenomenon, known as bioregeneration, has been shown to increase the service life of activated carbons and transpires as a result of combined biological aspects and GAC adsorption treatments. Bioregeneration of activated carbon is typically defined as the renewal of GAC adsorption sites by microorganisms for continued adsorption (Aktaş & Çeçen, 2007)

According to (Aktaş & Çeçen, 2007) bioregeneration is dependent upon several factors including biodegradability, adsorbability and desorbability of sorbate, activated carbon characteristics, and the nature of the microbial community. In theory, there are two plausible mechanisms in which bioregeneration can potential occur within a GAC sublayer. The first mechanism includes the idea of bioregeneration transpiring due to a concentration gradient within the filter. This includes the biodegradation of organic compounds being released from activated carbon followed by a desorption process due to a concentration gradient between the activated carbon surfaces and bulk liquids (Aktaş & Çeçen, 2007). The second mechanism involves the process of bioregeneration transpiring due to the presence of exo-enzymes. Several investigators have hypothesized that the bioregeneration process involves the use of extracellular enzymes (Perotti & Rodman, 1979; Kim et al., 1997; Sirotkin et al., 2001). Based on this theory, bioregeneration occurs as a result of exoenzymes, which are excreted by microorganisms. These microorganisms then diffuse into activated carbon pores causing a reaction with the adsorbed substrates.

Coinciding with the idea of biologically active GAC, these methods take advantage of the pre-established microbial communities within SSF sublayers. Another proposed theory provided by Sublette et al. (1982), includes the theory that activated carbon provides a surface for microorganisms to attach to which can protect them from shock loadings of toxic and inhibitory materials, all while these microorganisms are simultaneously regenerating the activated carbon. Biologically active GAC has been hypothesized to greatly extend the service life of a GAC bed for removal far beyond the point at which adsorptive capacities would normally be exhausted. (Page 1997). It has been shown that pre-ozonation significantly enhances biological activity on GAC by improving the biodegradability of organics in the water (Singer, 1988; Langlais et al.,

1991). Combination of ozonation and GAC filtration is commonly referred to as the BAC process.

As mentioned previously, there are several factors influencing and affecting the success of bioregenerative processes. Some additional factors include the reversibility of adsorption, the presence of microorganisms present along with their ability to metabolize the adsorbate, and whether microbial growth conditions are optimal (Aktaş & Çeçen, 2007). It is also important to note that the porous structure of activated carbon and empty bed contact times can also influence bioregeneration. (Klimenko et al., 2002) discovered that mesoporous activated carbon was more efficiently bioregenerated than microporous activated carbon. The contact time of activated carbon with substrate can also influence and affect bioregeneration and is supported by several investigators. (Aktaş & Çeçen, 2007) highlighted that a higher empty bed contact time (EBCT) insinuates a lower concentration within the filter liquid phase. This allows for a larger driving force correlating to desorption and biodegradation of sorbed compounds.

2.2.5 Advantages and Limitations to GAC Sandwich Modification

There are numerous advantages to incorporating a GAC sublayer within existing slow sand filter structures. The first being that the GAC sublayer can easily be incorporated into the existing structure without the use of additional pipework and construction. Due to the GAC acting as a non-backwashed adsorber, there is no need for backwashing to be incorporated into the operation of the system. This implementation eliminates the potential for media stratification and mixing of saturated GAC with unsaturated GAC, enhancing the breakthrough profile (Page, 1997). The GAC layer can also contribute to an increase in biomass production, which can also enhance

biodegradation of pollutants due to the carbon layer remaining undisturbed within the "sandwich" modification. Incorporation of a GAC sublayer in Slow Sand Filtration Facilities in Manchester, New Hampshire and particularly at the Slow Sand Filtration Plant in Winthrop, Maine, have also shown elevated removals of dissolved organic carbon (DOC) after fifteen plus years of service without the need for regeneration or replacement.

Disadvantages associated with the use of GAC include the replacement and regeneration of the carbon after bed volumes have been exhausted. With any type of treatment, the sites available for adsorption onto activated carbon decreases, resulting in the loss of the adsorptive capacity of GAC. GAC regeneration requires large capital investments and operating costs (Aktaş & Çeçen, 2007). The regeneration process is also a plausible method to treat GAC that has been exhausted, however, this has been known to alter GAC properties and cause adsorption capacities to be reduced after each regeneration cycle.

2.3 The Sand-Water Interface

The schmutzdecke has been described as a complex, biological layer formed at the subsurface of a slow sand filter. This particular layer plays a crucial role in the production and purification of potable drinking water treatment. The microbial community formed within the schmutzdecke layer is responsible for creating an initial zone of biological activity and can provide degradation of soluble organics within the raw water source.

2.3.1 Development of Schmutzdecke Layer

The optimal performance of slow sand filters can only be achieved when the filter is fully

matured and acclimated with a steady biomass population. (Arora, 2017). The development of the schmutzdecke layer depends on available microbes in raw water sources, food and oxygen supply, residence time, and wetting of the sand bed (Ranjan & Prem, 2018). It is formed in the first few weeks of operation, otherwise known as the ripening period. Ripening periods depend on the nature of the raw water quality, temperature, and filtration velocity (Duncan, 1988). Typically, the ripening period will range from about one week to several months. Warm temperatures and high nutrients will decrease ripening periods (Hendricks, 1991). A steady state biomass population is achieved when there is an equilibrium between the microorganism populations and the substrate availability under appropriate water quality conditions.

Huisman and Wood (1974) describe the schmutzdecke layer as a thin, slimy matting of material organic in origin, consisting of filamentous algae and other forms of life including but not limited to, diatoms, protozoa, rotifers, and bacteria. This layer is intensively active due to various microorganisms entrapping, digesting, and breaking down organic matter contained in the water passing through (Huisman & Wood, 1974). The bacterial activity is most prominent in this upper layer of the filter bed and gradually decreases with depth as food sources become scarcer. Figure 2-6 obtained from Partinoudi et al., (2006), displays the schmutzdecke biomass development within the upper layer of a filter. When the schmutzdecke layer begins to merge with deeper biological layers present within the slow sand filter, biological mechanisms continue to occur (Ranjan & Prem, 2018).

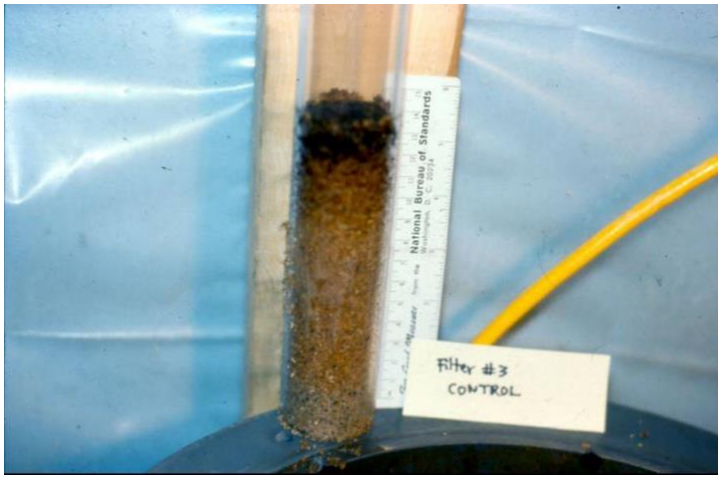

Figure 2-6. Schmutzdecke biomass development (adapted from Partinoudi et al., 2006).

According to Huisman and Wood (1974), there are four dominant processes which contribute to the purification of raw water and filtration processes within the schmutzdecke and biological zones:

- *Hostile environment:* Typical environmental conditions found within slow sand filters consist of temperatures below 30ºC. For intestinal bacteria to successfully multiply, this would include environmental temperatures similar to the human body, around 37ºC. (Ranjan & Prem, 2018). Therefore, intestinal bacterial populations are unable to thrive in typical environmental conditions associated with slow sand filters.

- *Competition for food:* Food is a requirement for metabolic processes in microorganisms. Oxidation processes which occur during metabolism consume organic matter within the raw water, including dead organisms (Ranjan & Prem, 2018). Within upper layers of slow sand filters, particularly the schmutzdecke, there is greater competition for food as

there is more biomass accumulation. At lower depths, food becomes scarcer and many microorganisms starve.

- *Predation:* Several studies have shown that predatory organisms exist within filter sublayers and will feed off other microorganisms present within the upper layer of filter beds. (Unger & Collins, 2008).

- *Excretion of poison or toxins:* Microorganisms in SSF can produce various substances that act as chemical and biological poisons that affect intestinal bacteria (Ranjan & Prem, 2018).

The combined effects of these four dominating processes as the schmutzdecke ripens and matures with a steady biomass population can allow for biological activity to continue within the schmutzdecke layer and various filter sublayers. Bellamy et al., (1985a) reported that as filtration progresses, biological growth continues to occur in the sand bed and gravel layer. However, the filter is not as effective in removing bacteria during this period. Throughout this study it was determined that a new sand bed has the ability to remove 85% of coliform bacteria present in raw water sources, whereas a fully acclimated and mature sand bed has the ability to remove more than 99% of the coliform bacteria (Bellamy et al., 1985a). An additional study conducted by Hirschi and Sims (1991) conveyed that the development of the schmutzdecke layer is an essential process in the removal of pollutants from raw water sources.

2.3.2 Effect of Temperature on SSF Performance

The biomass population can change dynamically by responding promptly to changes in temperature, influent organic concentration and dissolved oxygen (Duncan, 1988). Several studies have shown that the efficiency of slow sand filtration may be increased when temperatures increase. Temperature has been found to influence the speed at which chemical reactions take place as well as the metabolic rates of bacteria and microorganisms present within the filter (Ranjan & Prem, 2018).

As mentioned previously, the schmutzdecke layer can take several weeks to a few months to ripen. Palmateer et al., (1998) studied the development of biofilms within the schmutzdecke and discovered that it took approximately 16 days to develop biofilm at 85-90% coverage at 21ºC. It was also noted that raw water that is more biologically active will result in quicker biofilm development and thus filter operation will be more efficient (Palmateer et al., 1998). In a study conducted by Partinoudi et al., (2006) assessing temperature influences on slow sand filtration performance, it was determined that the preferential microbial removal occurred when the study was conducted at warmer temperatures. A robust correlation between increasing bacillus spore log removal trends and increasing phospholipid biomass can be seen in Figure 2-7, adapted from Partinoudi et al., (2006). In conclusion, microbial removals were shown to be more efficient at warmer temperatures.

As water temperatures begin to decrease, satisfactory biochemical oxidation of organic matter is not able to take place as efficiently by microbes within the biological layer (Ranjan & Prem, 2018). At low temperatures, bacterial activity within the schmutzdecke layer starts to slow down. Per Ranjan & Prem (2018), the activity of bacteria that consume protozoa and nematodes

abruptly decreases, allowing for slower metabolic rates of intestinal bacteria which can enhance their ability to be present within the filter bed. At lower temperatures, the numbers of *E.coli* and other microbes are also greatly reduced. The factor by which the numbers of these microbes are present can typically range from 100-1000, but have the potential to fall as low as 2 at temperatures of 2ºC or less (Ranjan & Prem, 2018).

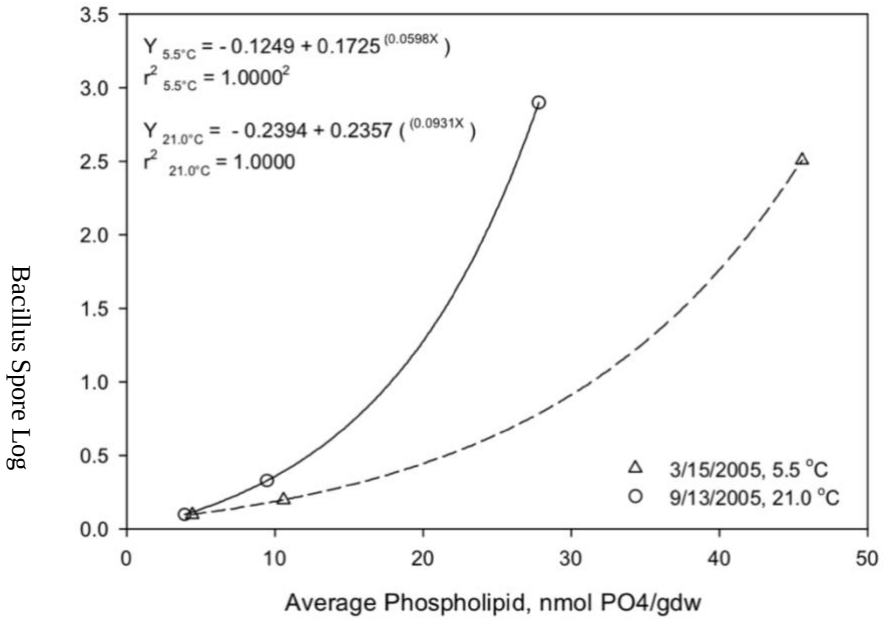

Figure 2-7. Correlation between bacillus spore log removal and phospholipid biomass concentration (adapted from Partinoudi et al., 2006).

2.3.3. Quantification of Biomass in the Schmutzdecke Layer

The fundamental physio-chemical and biological mechanisms controlling water purification and headloss development in slow sand filtration remains poorly defined, despite its current and historical importance (Campos et al., 2002). As the filtration process progresses, biomass has been shown to accumulate in the schmutzdecke layer and contributes to headloss development. The quantification of biomass growth within schmutzdecke layers and adjacent sand layers and

the factors affecting the formation of this layer could improve the understanding of the complex biological interactions operating in SSF (Campos et al., 2002).

Microbial biomass in the schmutzdecke and sand filter bed has been quantified using a variety of microbial methods. Multiple reports include single measurements of the net biomass production at the end of a filter run prior to filter cleaning. This sample collection accentuates significant amounts of variability within schmutzdecke and variability of sand biomass accumulation in operational slow sand filters. (Campos et al., 2002).The various methods used to quantify biomass concentrations in the schmutzdecke layer confound inter-study comparisons of biomass development and behavior in SSF due to the inconsistent units and sampling intervals (Campos et al., 2002). The collection of representative samples from the schmutzdecke layer and adjacent sand media during filter operation is difficult in practice due to limited access to filter layers within slow sand filters. The lack of simple routine measurements for biomass quantification have resulted in a limited amount of field-scale investigations focusing on the biological mechanisms involved in the SSF process.

Collins et al., (1993) quantified bacterial populations in the schmutzdecke layer by measuring biomass and bacterial counts within media covered slow sand filters. It was determined that bacterial populations decreased with depth, while filter biomass was significantly correlated to bacteria counts. Another study conducted by Seger & Rothman (1996) placed emphasis on biological activity in uncovered slow sand filters that were both ozonated and non-ozonated. Biomass activity was measured using adenosine triphosphate (ATP) luciferin-luciferase methods in combination with total cell count by epifluorescence microscopy. Balen (2018) used ATP

extraction techniques paired with deoxyribonucleic acid (DNA) extraction techniques as a method to enumerate biofilter biomass in a lab-scale study to evaluate strategies used to increase biofilter performance in the presence of low-carbon source waters. This study concluded that biofilter active biomass was increased within biofilters that were amended with organic substrates. High levels of ATP concentrations were achieved in biofilters amended with organic substrates, suggesting that organic carbon is a growth-limiting nutrient (Balen, 2018).

Campos et al., (2002) studied temporal and spatial dynamics of biomass development in full-scale SSF beds at the Walton Water Treatment Works, operated by Thames Utilities Ltd. in the United Kingdom. During the experimental period which occurred between the months of May and August, water temperatures increased from 12-13ºC ranging to 18-19ºC. To measure biomass, a chloroform-fumigation extraction technique was adapted from standard laboratory procedures (Campos et al., 2002). Sand biomass increased significantly with temporal and seasonal variations between May and August for an uncovered SSF bed and can be shown in Figure 2-8 obtained from Campos et al., (2002).

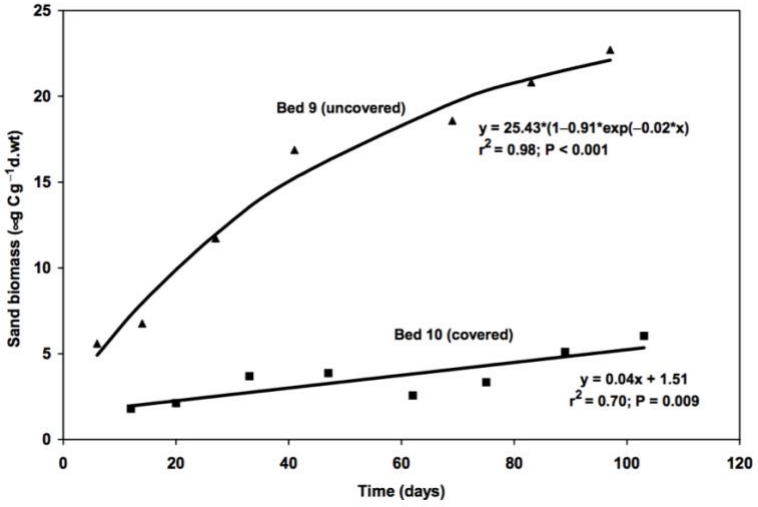

Figure 2-8. Correlation between sand biomass production and seasonal variations (adapted from Campos et al., 2002).

As this current study is attempting to look at temporal and seasonal variations of biomass production in the schmutzdecke and adjacent filter layers, it is important to note that Campos et al., (2002) discovered that biomass accumulation in the schmutzdecke layer was highly variable, but did not show any significant or consistent patterns in spatial or temporal development. The biomass development in the schmutzdecke can be detailed by Campos et al., (2002) in Figure 2-9.

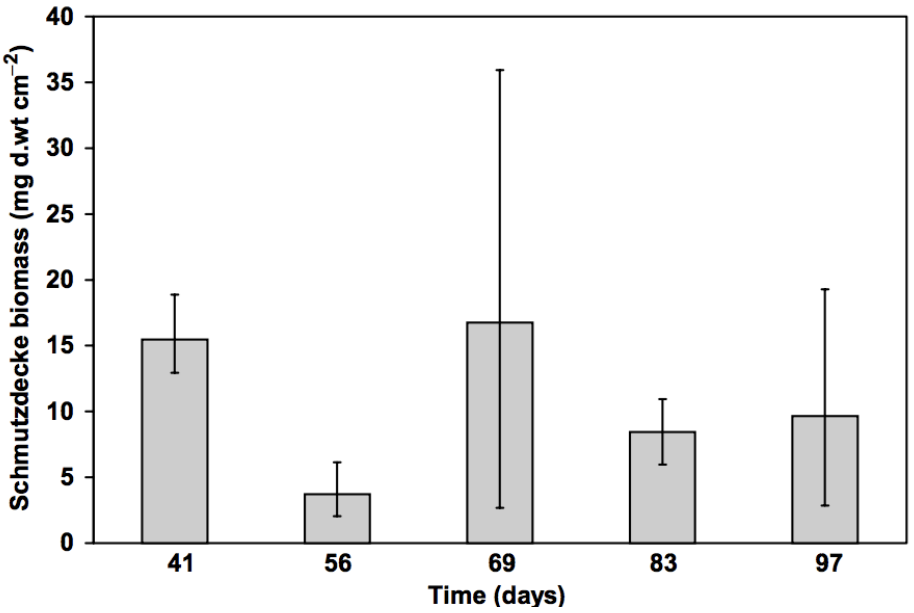

Figure 2-9. Schmutzdecke biomass variability (adapted from Campus et al., 2002).

A series of studies conducted by Unger & Collins (2008) verified that Escherichia coli (*E.coli*) removals in slow rate biological filters primarily occurred within the schmutzdecke layer and were shown to be statistically correlated to operational and design parameters for SSF. In this study, four analyses were used to quantify filter media biomass accumulation: phospholipid measurement for biomass, total carbohydrate and total protein measurements, and a carbon dioxide monitor was applied to monitor biological activity (Unger & Collins, 2008). Page (1997)

measured biomass via phospholipid extraction techniques using pilot-scale filters in Milo, Maine This study concluded that established biomass levels did not appear to vary significantly with seasonal changes and that the greatest levels of biomass occurred in the schmutzdecke and top sand layers.

While a variety of biomass quantification techniques exist and have been used in an array of experimental studies conducted within schmutzdecke and sand layers, lack of consistent sampling techniques and application of dependable laboratory methods creates gaps in this area of study. Consistent techniques can assist in gaining a greater understanding of the complex mechanisms, both physio-chemical and biological, involved in SSF.

2.3.4 Limitations of the Schmutzdecke Layer

While the development of the schmutzdecke provides many advantages to slow sand filtration removals, there are also limitations associated with biomass accumulation on the top of the sand bed. As the schmutzdecke layer begins to thicken, flow rates through the filter are reduced (Ranjan & Prem, 2018). This process eventually leads to clogging of the filter subsurface and in turn, filter subsurface must be cleaned. The clogging of porous media results from a decrease in the capacity of a treatment system to filter water. Clogging can occur as a result of three main processes: physical, chemical, and biological (Baveye et al., 1998). In SSF, the particular clogging mechanism observed is due to microbial activity on the subsurface layer. According to Baveye et al., (1998), microbial clogging could occur from cell accumulations in the pore space, the production of extracellular polymer substances (EPS), release in the pore space by gaseous byproducts, and the accumulation of insoluble precipitates that can be microbially mediated.

Harrowing is one method used to scrape the schmutzdecke surface and top few centimeters of the sand bed to prevent clogging in SSF, as mentioned in *Section 2.1.3*. After a filter is cleaned, water is recirculated in the filter to begin the process of new biofilm accumulation. Per Ranjan & Prem (2018), it has also been noted that the schmutzdecke can contribute to the total head loss within filter beds due to the schmutzdecke acting as a porous filter medium in open filters. Adenerian & Akanmu (2013) reported that the schmutzdecke layer is removed when the head loss becomes excessive and outflow rates decrease. Harrowing provides a limitation to SSF as scraping the schmutzdecke causes the ripening period to begin again, which can be variable depending upon temperature and biomass production rates.

2.4 Temperature Influences on Slow Sand Filtration & GAC

As mentioned previously, the development of the schmutzdecke layer plays a functional role in the removal of organics in slow sand filtration. Microbes that accumulate on the surface interface utilize the organics as a food source and this enhances the service life of fixed bed slow sand filters amended with GAC through the conversion to BAC filters. As temperatures in raw water sources decrease, slow sand filters become less effective at removing microorganisms from cold water due to a decline in biological activity within the filter bed (SSF Tech Brief, 2000). Biologically active filters aid in reducing biodegradable organic matter, including micro-pollutants, through a complex coexistence of adsorption and biodegradation processes. Due to these processes being dependent upon temperature, treatment plants located in temperate and polar regions are subject to seasonal temperature variations (Moona et al., 2019).

2.4.1 Microbial Growth Potential, Removal, and Biomass Production

According to Logsdon et al., (2002), colder temperatures appear to be a significant limiting factor for the implementation of SSF in North America. Colder temperatures can cause microbiological removal efficacy to decrease due to a reduction in biofilm production. Few studies have been conducted on the basis of SSF performance during colder temperatures. Typically, any comparisons for SSF performance in winter and summer conditions are confounded by raw water quality variations between summer and winter seasons (Partinoudi et al., 2006). LeCraw (2003) highlighted personal communications between the Environmental Protection Agency and Canadian officials, which concluded the idea that slow sand filtration is not as effective in capturing source water microorganisms during colder temperatures.

Partinoudi et al. (2006) hypothesized that the presence of extracellular polymeric substances (EPS) produced by SSF biofilm assists in increasing particle attachment at the filter subsurface, ultimately increasing removal efficiency. It was also speculated that biomass production may significantly decrease at cold temperatures, consequently reducing the EPS within the filter. In this study, samples were analyzed for biomass, EPS, carbohydrates, proteins, biological activity, chlorophyll, seston and metal ions (Partinoudi et al., 2006). As this study focused on noticeable variations in biomass production with seasonal changes, higher removals were observed in the presence of increasing phospholipid biomass concentrations. Most of the biomass was located in the upper region of the pilot slow sand filters and the highest microbial removals were obtained at the highest phospholipid biomass concentrations during warmer temperatures (Partinoudi et al., 2006). The lowest microbial removals were obtained during colder temperatures at lower phospholipid biomass concentrations, signifying that temperature influences biomass production.

A strong correlation was also seen between microbial removals and biological respiration. Microbial removal rates for biological respiration were generally 2.5x ,more efficient in warm temperatures (21ºC) than in cold temperatures (5.5ºC) (Partinoudi et al., 2006). During warm temperatures, microbial removals were also shown to increase more rapidly indicating that a more efficient type of biomass or biological activity was present at those temperatures (Partinoudi et al., 2006).

Several studies have indicated the influence of temperature on the effectiveness of slow sand filtration processes involved the inactivation of certain viruses such as bacteriophage MS2, poliovirus, hepatitis A, *Escherichia coli* (E.coli), and fecal indicator organisms. Nasser and Oman (1999) conducted a study in which various groundwater samples were enumerated with strains of hepatitis A, poliovirus 1, and *E.coli* to observe the effects of temperature on inactivation rates. It was found that the inactivation of hepatitis A and poliovirus-1 was greater at high temperatures (20-30ºC) as compared to low temperatures (4-10ºC). (Nasser & Oman, 1999). The results of this study indicated that the inactivation of viral agents found in natural source waters is dependent upon the water quality, temperature, microorganism type, and greater microbial activity occurring at higher temperatures (Nasser & Oman, 1999). Schuster et al., (2005) analyzed information pertaining to waterborne outbreaks occurring in Canada between the years of 1974 and 2001 to try to define apparent trends. It was discovered that severe weather, close proximity to animal populations, and treatment system malfunctions were linked to reported disease outbreaks (Schuster et al., 2005).

Poynter and Slade (1977) focused on poliovirus removals by SSF and indicated that increased removals occurred with increasing water temperatures. This study was conducted over a four year period and accredited increased removals of poliovirus with higher temperatures due to increases in biological activity occurring within the SSF process. The increased activity of microorganisms living in slow sand filters, usually microorganisms that prey on or inactivate viruses, was the probable cause of higher virus removals at higher temperatures (Poynter & Slade, 1977). An additional study focused on temperature influences for MS2 and E.coli removals showed an approximate 2 log increase in removals in warmer SSF experiments that included temperatures ranging from 13ºC to 16ºC as compared to experiments conducted at 10ºC (Dullemont et al., 2006). In conclusion, enhanced microorganism removals in this study were also attributed to the increased biological activity that occurs in SSF at warmer temperatures (Dullemont et al., 2006).

Relationships between temperature, fecal indicator organism removal, and filtration rates have also been studied in slow sand filtration processes. Bellamy et al., (1985a) discovered that temperatures decreasing from 17ºC to 5ºC and below caused a descent in coliform removals from 99% to roughly 90% in the presence of colder waters. Total coliform removals were also discovered to be adversely influenced by increases to filtration rates when rates were altered from 0.04 m/hr to 0.4 m/hr (Bellamy et al., 1985a). At the Thames Water Utility in London, Toms & Bayley (1988) conducted studies focused on the impact of filtration rates and temperatures. It was observed that low temperatures create a limitation on the capacity of filters to remove fecal indicator organisms (Toms & Bayley, 1988). At temperatures below 4ºC and a filtration rate of 0.3m/hr, average concentrations achieved included less than 50 E.coli/ 100 mL

in comparison to a filtration rate of 0.2 m/hr only achieving a concentration of 10 E.coli / 100 mL.

A more recent study conducted on household slow sand filtration (HSSF) by Lubarsky et al., 2022 focused on intermittent and continuous household systems to investigate extracellular polymeric substance (EPS) composition, biomass, dissolved oxygen, and microbial community development. The study was conducted for 48 days using a continuous HSSF (C-HSSF) and an intermittent HSSF(I-HSSF) to place emphasis on bacterial removals from river water, particularly *E.coli* and fecal coliform detection, changes in turbidity, and apparent color removals. Results demonstrated an increase of carbohydrates from 21.4 to 101.2 $mg \cdot g^{-1}$ for C-HSSF and 22.5 to 93.9 $mg \cdot g^{-1}$ for I-HSSF and an increase in proteins from 34.9 to 217 $mg \cdot g^{-1}$ for C-HSSF and 34.9 to 307.8 $mg \cdot g^{-1}$ for I-HSSF (Lubarsky et al., 2022). Improvements related to the efficiency of HSSF systems was observed throughout the duration of this study as there was a 3.23 log removal of *E.coli*, a 2.98 log removal for total coliforms, increase in turbidity removals from 60% to 95%, and an increase in apparent color removals from 50% to 90% (Lubarsky et al., 2022).

Temperature variations also were monitored throughout the duration of this study. During week four, there was substantial amount of rainfall causing external temperatures to drop by 2ºC. Temperatures dropped to 18.6ºC in the C-HSSF and 15.5ºC in the I-HSSF and this drop was correlated to a decrease in EPS carbohydrates and proteins within samples collected during week four (Lubarsky et al., 2022). It was later confirmed that the temperature variations did not affect the overall performance of household slow sand filters. As slow sand filtration systems are

applied in an array of settings for the removal of organics and bacteria from raw water sources, the implementation of this system continues to provide several benefits in drinking water treatment processes.

2.4.2 DOC and BDOC Removals by SSF Amended with GAC

The influence of raw water temperatures on the removal of dissolved organic carbon (DOC) and biodegradable organic carbon (BDOC) have been studied at various water treatment plants where several biological processes are involved. It has been indicated that the behavior of slow sand filtration differs from that of GAC filtration. As mentioned previously, GAC amendments to SSF can significantly enhance the removal of organic precursors quantified by DOC and BDOC.

Welté & Montiel (1996) studied the removal of DOC and BDOC performances on the treatment chain at the Ivry Treatment Plant, which supplies approximately 30% of drinking water to the city of Paris. In this study, it was determined that SSF performance is optimal and more efficient at temperatures above 15ºC. A total DOC removal of 28% was observed at 6ºC as compared to a total removal of 43% at 15C (Welté & Montiel,1996). A comparison was made between raw water, SSF water, and GAC waters. As displayed by Welté & Montiel (1996) in Table 2-4 below, the efficiency of SSF for BDOC removal is very high, displaying rates at 76% for 15ºC.

Granular activated carbon has displayed a lower removing efficiency compared to SSF at 15ºC, however, the efficiency optimum for GAC filters in BDOC removals occurred at temperature ranges between 5ºC and 10ºC (Welté & Montiel,1996). The results of this study suggest that the

behaviors involved in slow sand filtration versus slow sand filtration amended with a GAC sublayer could differ when it comes to removals of biodegradable and dissolved organic carbon.

Table 2-4. BDOC and DOC removals for SSF and GAC Filtration displayed as percentages (adapted from Welté & Montiel, 1996).

Temperature	6ºC		9ºC		15ºC	
Removals	*BDOC*	*DOC*	*BDOC*	*DOC*	*BDOC*	*DOC*
Slow Sand Filtration	21%	4.7%	19%	6.1%	76%	42%
GAC after Ozonation	34%	7.0%	56%	25%	51%	26%

Research on slow sand filters amended with granular activated carbon began at the University of New Hampshire in 1987 and a more in depth understanding of the DOC removal process by enhanced SSF began in the mid-1990s by Tom Page. (Graham & Collins, 2014). A comparative pilot study was conducted with a control slow sand filter, a 7.5 inch GAC amended slow sand filter, and a 15 inch GAC amended slow sand filter. DOC removals reached pseudo steady-state removals of 12%, 28%, and 46% respectively, and filter run time occurred for over 300 days. (Page 1997; Graham & Collins, 2014). The removals associated with the biodegradable organic carbon (BDOC) fraction were comparatively similar for the control and GAC amended pilot filters, indicating that elevated removals of DOC by granular activated carbon amended filters were due to adsorption mechanisms. This is displayed in Figure 2-10 obtained from Tom Page (1997).

Respectively, the pseudo steady-state removals by adsorption for the 7.5 inch GAC amended filter was 16% and for the 15 inch GAC amended filter removals were 36% (Page, 1997). As mentioned previously, adsorption is a primary removal mechanism in slow sand filters amended

with GAC and a property of granular activated carbon. Adsorption is the dominant mechanism in DOC removal within the first 10,000-15,000 GAC bed volumes (BVs) and has been shown to be dependent upon temperature (Graham & Collins, 2014). As steady-state removals by adsorption are achieved, biodegradation begins to achieve proportional removals of dissolved organic carbon as temperatures begin to increase above 10ºC (Graham & Collins, 2014).

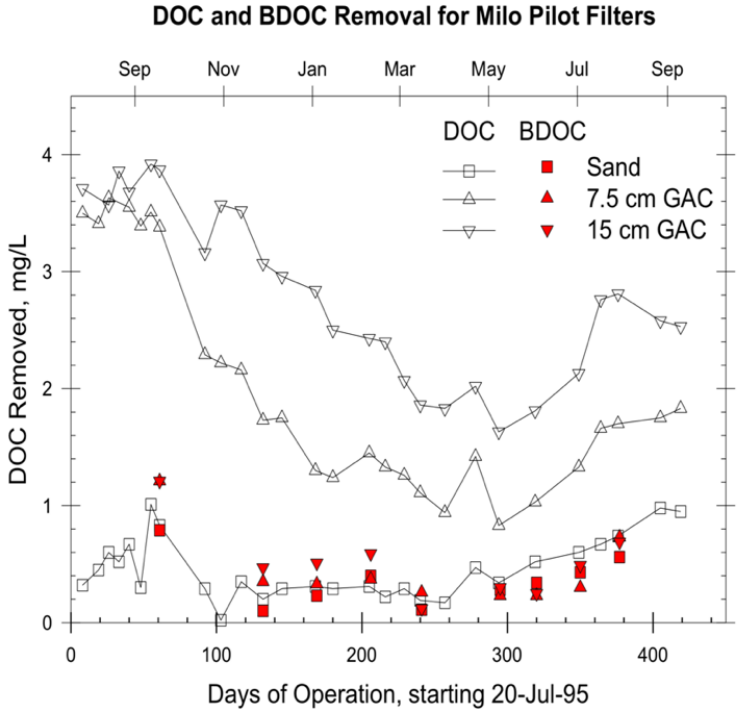

Figure 2-10. Removals associated with DOC and BDOC in GAC amended pilot filters studied in Milo, Maine (adapted from Page, 1997).

A summary depiction of DOC removals observed by both adsorption and degradation within the GAC amended pilot filters as a function of bed volumes is demonstrated by Page (1997) in Figure 2-11. Due to DOC removals occurring by adsorption after 400+ days of filter run time, roughly equivalent to 12,000 - 23,000 bed volumes, there is evidence present to support slow adsorption mechanisms and bioregeneration in the GAC sublayer (Page, 1997; Graham & Collins, 2014).

Slow adsorption mechanisms are suggested by the steady-state adsorption rates being proportional to the empty bed contact time (EBCT) of the GAC (Graham & Collins, 2014). Evidence suggests the bioregeneration mechanism occurring due to increasing adsorption rates with the increase in temperature. DOC removals have been associated with temperature fluxes and are summarized in Figure 2-12 adapted from Page (1997). While both bioregeneration and adsorption mechanisms are fundamental processes in DOC removal mechanisms observed in SSF, relative importance is a function of temperature and further investigations are needed to determine the effect of temperature on these mechanisms.

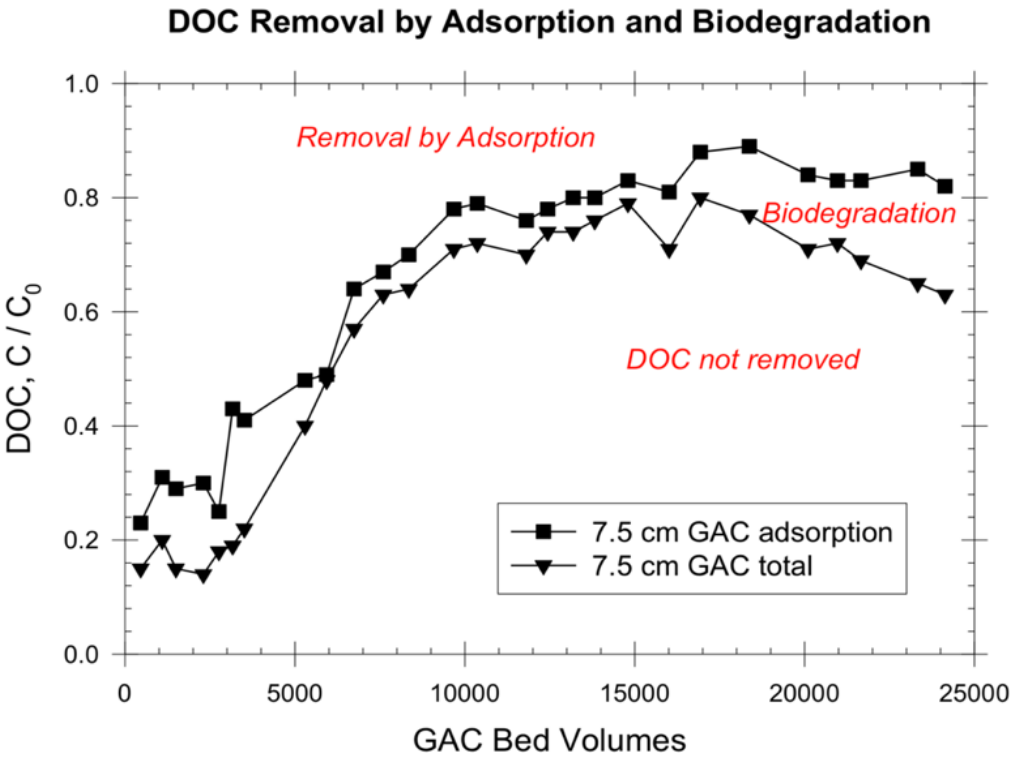

Figure 2-11. Summary depiction of DOC removals observed by adsorption and biodegradation in pilot filters amended with GAC (adapted from Page, 1997).

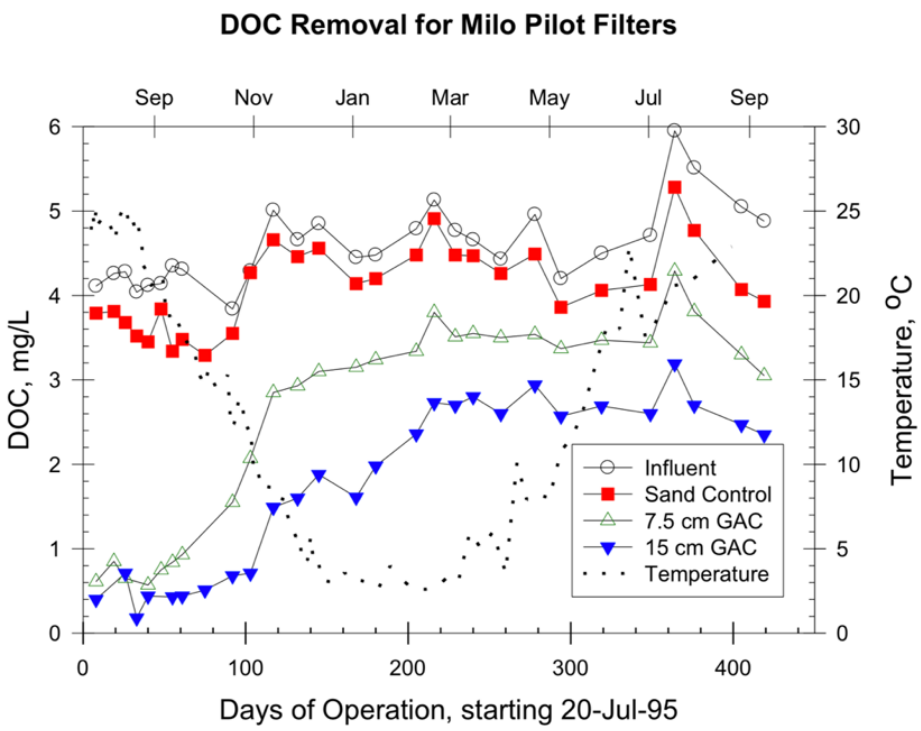

Figure 2-12. DOC removals associated with temperature variations (adapted from Page, 1997).

2.5 Adsorption of Heavy Metals Accumulation on Filter Media & GAC

Granular activated carbon (GAC) is applied to conventional slow sand filters to adsorb organic compounds that may be harmful to humans and to improve the quality of potable water. While operating in this capacity, both sand media and GAC can accrue metals concentrations in substantial quantities. Metals such as iron, manganese, aluminum, and calcium have been found to accumulate on sand and GAC surfaces due to their natural ubiquity in source waters.

2.5.1 Metals Accumulation and Adsorption on Granular Media

Heavy metals are well-known sources of environmental pollution due to their natural toxicity, persistence within environmental settings, and their ability to bioaccumulate. Sources of metals accumulation are commonly associated with industrial discharges, but other important sources to

consider include, but are not limited to road run-off, landfill leachate, and municipal sludge (Marquis et al., 1976; Ellis, 1988, Pradhan & Levine, 1992). Heavy metals can remain persistent in the environment due to the nature of their speciation. The removal of heavy metals in slow sand filtration can be applied through a variety of processes which can include chemical precipitation, adsorption, biological uptake, ion exchange, and reverse osmosis.

Muhammad et al., (1998) focused on a controlled lab setting in conjunction with pilot filter studies to determine the performance and mechanisms of the removal of heavy metals by SSF. Lab scale SSFs were created using a sand grade of 0.20 – 0.70 millimeters, filter depth of 1.2 meters, and flow rates od 0.1m/hr. The removal of four representative dissolved heavy metals (Cu, Cr, Pb, and Cd) were studied and results showed that SSF is an effective method in removing heavy metals from water. Removals associated with this study included 99.6% for Copper, 97.2% for Chromium, 100% for Lead, and 96.6% for Cadmium with the application of a TOC dose applied at 12 mg/L. Potential mechanisms for removal in this study were identified as settlement, adsorption to both organic matter and sand, and microbial uptake (Muhammad, 1998).

Another study conducted by Collins & Vaughan (1996) focused on sand media coatings and the characterization of NOM removal by biofiltration. Metals analyses using hot nitric acid and hydrochloric extraction techniques characterized concentrations on sand coatings per gram dry weight for Iron (Fe), Aluminum (Al), Calcium (Ca), and Manganese (Mn) for various local slow sand filters and rapid sand filters in West Hartford, Connecticut and Portsmouth, New Hampshire. It was discovered that the highest concentrations of Iron and Manganese were found

on sand coatings used at the West Hartford SSF. In the rapid sand filters in Portsmouth, there were low concentrations of iron, manganese, and calcium within sand coatings, but high concentrations of Aluminum. Overall, the equivalent metals concentrations ranked from highest to lowest were Portsmouth RSF, West Hartford SSF, followed by Portsmouth SSF. These values obtained from Collins & Vaughan (1996) can be observed in Table 2-5. This study verified that a correlation could be found by relating metal content of sand coatings to various removal trends.

Table 2-5. Metals concentrations from various sand coatings displayed in mg-kg/dry weight (adapted from Collins & Vaughan, 1996).

	WH-SSF	**Port-SSF**	**Port-RSF**
Fe	3732 ± 257	2986 ± 452	641 ± 67
Mn	200 ± 13	45 ± 1	10 ± 1
Ca	270 ± 19	283 ± 39	5 ± 1
Al	1695 ± 117	1148 ± 91	7149 ± 60
Avg metal milliequivalents/kg dry wt	343	250	818

Metals accumulation and adsorption can also occur on and within the GAC sublayer. Granular activated carbon is implemented into SSF designs due to its adsorptive capacities and abilities to enhance the removal of NOM. Due to the simplicity of SSF designs in combination with slow filtration rate applications, build up and accumulation of organics and trace metals on the GAC sublayer can occur gradually over time. Mechanisms for the build-up of organics on granular activated carbon include precipitation on the surface of GAC, adsorption of metallo-organic complexes in the presence of natural organic matter, chelation with NOM, particle deposits, and

ion exchange onto the GAC surface (Dagois et al., 1992; Cannon et al., 1993). While the adsorptive function of GAC provides many benefits to SSF, it will reach a point of exhaustion after months to years of service. Methods can be applied to regenerate the adsorptive capacities of GAC for reuse in SSF and will be discussed in *Section 2.5.2*.

2.5.2 Thermal Regeneration of GAC

The thermal regeneration of granular activated carbon is being increasingly considered as a cost-effective, alternative method to disposal as the discarding of field-spent GAC has become more difficult and expensive. As GAC becomes exhausted of its adsorptive capacities, it can no longer assist in producing required drinking water treatment standards. Spent carbons can be landfilled, incinerated, or thermally regenerated for reuse purposes.

The process of thermal regeneration encompasses four main processes, including a pyrolytic stage and an oxidative stage. DeWolfe et al., (1992) describes the thermal regeneration process beginning with drying GAC at temperatures below 200ºC, followed by the vaporization of volatile adsorbates and the decomposition of unstable adsorbates at temperatures between 200-500ºC to form volatile fragments. The next step being the pyrolytic stage involves spent carbon being exposed to temperatures up to 800ºC under inert conditions (Miguel et al., 2001). This allows char to form on the activated carbon surface. The oxidation of the pyrolyzed residue is performed by applying steam and controlled gasification at temperatures above 700ºC. This stage results in the elimination of the charred residue subsequently exposing the original carbon pore structure (Waer et al., 1992)

The success of thermal generation largely depends upon the characteristics of the field-spent carbon and the conditions used to maximize recovery of original carbon characteristics without generating large carbon losses. This includes the recovery of the virgin pore structure and original adsorptive capacity to be restored (Frederick, 1999). However, studies have shown that the accumulation of heavy metals and the presence of particular metals on the GAC sublayer can negatively affect thermal regeneration processes.

2.5.3 Effect of Calcium Loading on Field-Spent GAC

As mentioned previously, metals accumulation on the GAC surface can occur when the GAC serves as a filter adsorber in conventional slow sand filter designs. Metals can become loaded onto GAC via chemical precipitation, chelation with natural organic matter, adsorption of metallo-organic complexes in the presence of NOM, particle deposits, or ion exchange onto the GAC surface (Dagois et al., 1992; Cannon et al., 1993). Metals such as iron, manganese, aluminum, and calcium have been discovered to accumulate onto GAC due to their natural presence in source waters as well as their presence in chemical treatments used at drinking water treatment facilities. In drinking water treatment, metals accumulation has become increasingly important due to the impact that accumulated metals can have on the thermal reactivation of GAC (Cannon et al., 1993).

Research conducted by Cannon et al., (1993) showed that GAC can accumulate metals in significant quantities, and particularly large accumulations of calcium. Thermal regenerations were conducted on field-spent carbons with a service life of nearly 4 years from the American Water Works Service Company (AWWSC) and the Compagnie Générale des Eaux (CGE) Water

Treatment Plants. It was discovered that the field-spent GAC contained 0.4-7.0 percent calcium, 0.3-3.7 percent aluminum, 0.1-0.5 percent iron, and 0.02-0.6 percent manganese. As Cannon et al., (1993) demonstrates in Figure 2-13, various GAC sources were regenerated and extracted for metals content.

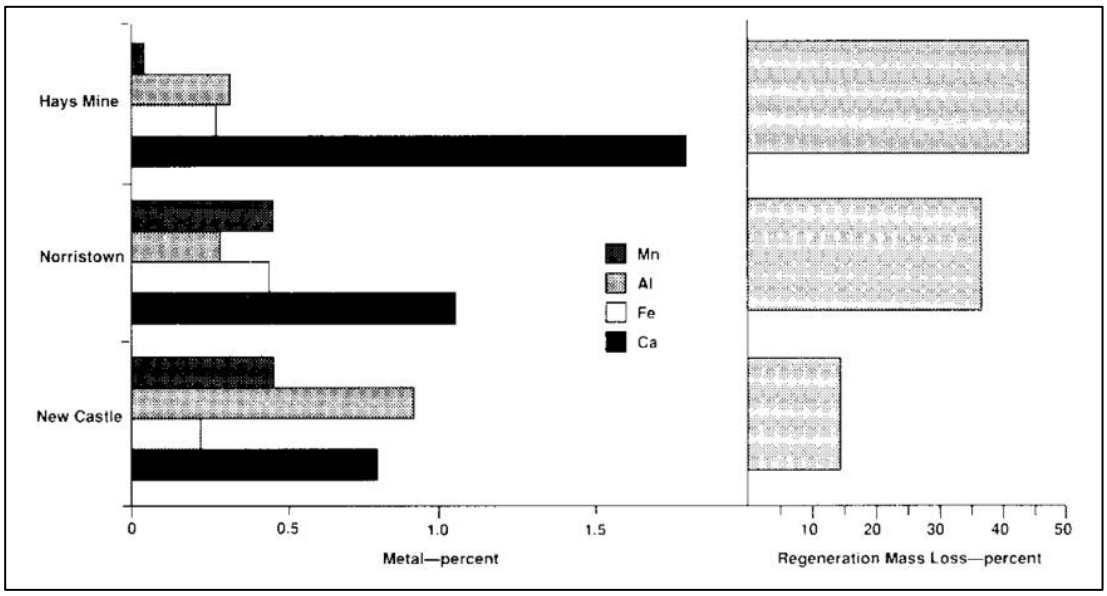

Figure 2-13. Metals content and regeneration mass loss of spent GACs from AWWSC and CGE water treatment plants (adapted from Cannon et al., 1993).

The goal of Cannon's study was to determine how accumulated metals affect the processes involved in thermal regeneration and whether thermal regeneration had the ability to restore GAC to its virgin properties despite the metals concentrations. Several regeneration variables were tested including pyrolysis temperature, oxidation temperature, oxidant gas, oxidant flow rate, and oxidant extent. Cannon et al., (1993) discovered that proper regeneration of field loaded calcium intact could restore the spent GAC, including similar pore structure and surface areas exhibited by virgin GACs. Consequently, when calcium appeared inside field-spent GAC, it caused micropores to be converted to smaller mesopores during thermal oxidation. A guiding

question that came as a result of this research was whether treatment facilities should invest in regeneration costs of GAC, replace existing GAC sublayers with virgin GAC, or dispose of it in a landfill.

It was later discovered that the accumulation of metals affects the process of thermal regeneration, as some of them have been reported to catalyze the reaction between solid carbon and the oxidizing agents (Kaptejin et al., 1986; Knappe et al., 1992; Cannon et al., 1993). Of particular focus, calcium catalysis during regeneration has been found to have more significant effects than any other metal that significantly loads onto water treatment GACs (Cannon et al., 1993). The presence of catalytic metals have the ability to affect the regeneration process in one of two ways. Miguel et al. (2001) explains the first factor being that catalytic metals can increase the reactivity of the carbons, meaning both lower temperatures and reduced reaction times are necessary in order to achieve a certain degree of gasification. Secondly, catalytic metals can affect the development of carbon porosity during the regeneration process, ultimately forming larger pores.

It has also been discovered that calcium commonly accumulates on GAC when it is chelated by natural organic matter, as it is drawn into the pores of GAC (Knappe et al., 1992). Accumulation via precipitation can also occur due to GAC particles serving as a nuclei for this process. When calcium accumulates on GAC, calcium significantly catalyzes the regeneration reaction leading to accelerated internal mass loss (Knappe et al., 1992). Within this study, optimal conditions used for the regeneration of GAC were applied to carbon presenting internally loaded calcium. Regeneration processes applied to GAC with internally loaded calcium led to severe over-

regeneration (Knappe et al., 1992). Thus, signifying that the pore structure and adsorptive capacity of GAC are adversely affected by the application of regeneration. Research conducted in this study verified that calcium loaded GACs did not have the capability to be regenerated to yield GAC properties equivalent to virgin GAC properties.

3. Experimental Approach and Methodology

3.1 Experimental Approach

Specific goals of this study were to assess mechanisms contributing to the maintenance of GAC adsorption sites and the impact of seasonal variation on microbial communities within SSF sublayers. In order to assess the impacts of seasonal variation on filter sublayers, media samples and aqueous samples were obtained for biomass analyses and several aqueous analyses. Aqueous and media samples were obtained from the Slow Sand Filtration Plant in Winthrop, Maine at various dates incorporating seasonal temperature changes for laboratory analyses summarized in Table 3-1.

Table 3-1. Aqueous and Media Sample Collection from Winthrop (ME).

Date	Aqueous Samples	Aqueous Analyses	Media Samples	Media Analyses
August 2021	Raw Water Effluent Filter #1	Water Quality TOC/DOC BDOC Non-BDOC	Schmutzdecke Sand Above GAC GAC	ATP Biomass DNA Extractions Metals Concentrations
September 2021	Raw Water Effluent Filter #1 Effluent Filter #2 Effluent Filter #3	Water Quality TOC/DOC BDOC Non-BDOC	Schmutzdecke Mid-Sand Sand Above GAC GAC	ATP Biomass DNA Extractions
February 2022	Raw Water Effluent Filter #1 Sand Above GAC (Filter #1) Effluent Filter #2 Effluent Filter #3	Water Quality TOC/DOC BDOC Non-BDOC	Schmutzdecke	ATP Biomass DNA Extractions
May 2022	Raw Water Effluent Filter #1 Effluent Filter #2 Sand Above GAC (Filter #3) Effluent Filter #3	Water Quality TOC/DOC BDOC Non-BDOC	Schmutzdecke Mid-Sand Sand Above GAC GAC	ATP Biomass Metals Concentrations

3.2 Aqueous Sampling and Analyses

3.2.1 Sampling Techniques

Aqueous samples were collected from the influent water source to the filters, also known as the raw water source, and three filter effluents at the Slow Sand Water Filtration Plant in Winthrop, Maine. Aqueous samples from all three filters were obtained for general water quality parameters, total organic carbon (TOC), dissolved organic carbon (DOC), and biodegradable organic carbon (BDOC) analyses.

Both the influent water source and the three effluent water sources had various ports in the basement of the filtration plant. For TOC and DOC analyses, aqueous samples from each valve were taken using autoclaved 40 mL glass TOC vials. Source water was used to rinse the vials three times to ensure excess contaminants were cleaned for the raw water source and three filter effluent sources. Vials were filled up with source water after rinsing was complete. Aqueous samples were stored in a cooler during transportation and placed in the 4ºC refrigerator upon arrival in the laboratory at the University of New Hampshire. Aqueous samples obtained for BDOC laboratory procedures involved the use of several 1liter and 5 liter Nalgene carboys. The same rinsing technique was applied to the carboys to ensure any excess soap was removed from the carboys prior to sampling.

Aqueous sample extraction above the GAC sublayer was completed using a metal corer attached to a peristaltic pump via black tubing. The metal corer was inserted into the top layer of filter media until it came to a halt, which signified that the bottom of the sand layer had been reached.

The peristaltic pump was turned on and ran consistently for a few minutes prior to sample collection in order to flush out any media particles and/or contaminants within the tubing.

3.2.2 Total Organic Carbon / Dissolved Organic Carbon

Total organic carbon (TOC) and dissolved organic carbon (DOC) were typically measured from the raw water source, the aqueous samples above the GAC sublayer, and the three effluent water sources in Slow Sand Water Filtration Plant in Winthrop, Maine. TOC and DOC were measured through a GE Sievers 5310C Laboratory TOC Analyzer. For DOC analysis, samples were filtered through a Whatman® GF/F 0.7 μm filter.

3.2.3 Biodegradable Organic Carbon

An aqueous sample is applied to bioacclimated sand for five to seven days in a batch reaction using the Summers/Shaker Batch Bioreactor Method. The readily biodegradable portion of dissolved organic matter is expected to be consumed by microbial activity. The sample must be agitated in order to promote mixing and biodegradation. By incorporating the use of fixed flora, this promotes a rapid response. The difference between the initial and final DOC is operationally defined as Biodegradable Organic Carbon (BDOC).

Prior to the start of the BDOC procedure, two 4 inch diameter PVC columns were set-up which included stainless steel screens, Masterflex pumps, tubing, and a carboy for reservoir. For this procedure, the local water source used within the reservoir was from the Oyster River and supplied by the Durham Drinking Water Treatment Plant. The sand within these columns were then bioacclimated with the untreated, natural water from the Durham Water Treatment Plant for

at least 3-4 weeks prior to initial experimental set-up. The reservoir was rinsed and replaced at least once every two weeks and the target water was recirculated 1-3 days prior to testing.

Sand preparation for the BDOC analysis occurred immediately before use. Sand was removed from the recirculating columns and placed in a plastic tub for transportation back to the laboratory. The sand was rinsed with dechlorinated tap water until the UV absorbance of the final rinse water was less than 0.05 *abs*. Aqueous samples being used for testing were stored in the 4 ºC fridge prior to test application and were removed from the fridge in order to warm to 20 ± 1 ºC. Aqueous samples were not required to be filtered prior to application.

For this procedure, 1 L amber glass bottles with TFE lined caps were used in duplicates to hold sand media along with the aqueous samples. The bottles were washed with detergent, rinsed, washed with chromic acid, and dried in a muffle furnace prior to the start of the experiment. A glucose/glutamic acid (G/GA) solution was used as the control in the BDOC procedure. To prepare the stock solution, 104 mg of glucose ($C_6H_{12}O_6H_2O$) and 104 mg of glutamic acid ($C_5H_9NO_4$) was weighed and added to 200 mL of deionized water. The stock solution was then diluted using 20 mL of the G/GA solution and placed in 2000 mL of deionized water. The stock solution was prepared immediately before use in this procedure and aqueous samples for this method included the raw water source, the aqueous sample above the GAC sublayer, and the three effluent water sources from the Slow Sand Water Filtration Plant in Winthrop, Maine.

Approximately 150 g of wet sand was added to each reactor bottle. Sand was washed with 300 mL of sample to displace any remaining water and decanted off and then 500 mL of sample was

added to the reactor. Roughly 400 mL of headspace should be present to ensure an oxygen source is being provided for the organisms. Once sample application was complete for all reactor bottles, each bottle was swirled and sampled for initial DOC. These samples were collected in 40 mL autoclaved glass TOC vials which were previously labeled according to each sample. The bottles were then placed on a shaker table ~ 150 RPM, in the environmental room to incubate at 20ºC. To prevent algal growth, the lights were kept off. Samples were obtained from each reactor on day 1, day 2, day 5, and day 7 to be analyzed for UV_{254} and TOC/DOC. When the test is complete, the used sand is returned to the bioacclimating columns.

3.2.4 UV_{254}

Ultraviolet absorbance was measured throughout the duration of the BDOC laboratory procedure. Using a Hach DR5000 spectrophotometer set to a single wavelength of 254 nm, samples were typically evaluated at day 0, day 1, day 2, day 5, and day 7 throughout the BDOC procedure. A 1 cm cuvette was rinsed with RO water prior to each sample analysis and was dried using a kimtech wipe prior to being placed in the spectrophotometer. UV_{254} readings were recorded in absorbance (abs) units.

3.2.5 pH and Temperature

Potential hydrogen (pH) and water temperatures were measured daily at the Slow Sand Filtration Plant in Winthrop, Maine using the Thermo Scientific Orion™ Dual Star™ pH and ISE Benchtop Meter. The pH electrode and meter are calibrated with pH buffer standards of 4.01, 7.00, and 10.01 prior to sample readings. To prepare the sample, roughly 30 mL of sample is added to a 50 mL beaker. The pH electrode, ATC probe, and stirrer probe are rinsed with

deionized water, blotted dry and placed into the sample. The stirrer probe is turned on and the meter will flash *stabilizing* followed by *ready*. The pH and temperature of the sample are then able to be recorded. Daily plant sheets were provided from the facility on a monthly basis and data was collected to be used throughout the duration of this study.

3.2.6 Turbidity

Turbidity of the raw water and treated waters from Filter #1, #2, and #3 were measured daily at the Slow Sand Water Filtration Plant in Winthrop, Maine using the Hach 2100N Bench Top Turbidimeter. Samples are prepared by collecting a representative sample in a container to fill a sample cell to the fill line ~ approximately 30 mL. The sample cell must be capped in order to prevent spillage of sample into the instrument and a thin bead of silicone oil must be applied to coat the cell. An oiling cloth is then used to spread the oil in a uniform manor prior to placing the sample cell into the instrument. The sample compartment must always be closed during measurement. The appropriate range, ratio, and unit settings are selected in order to provide accurate measurements. Samples are read and recorded in nephelometric turbidity units (NTUs). Daily plant sheets were provided from the facility on a monthly basis and data was collected to be used throughout the duration of this study.

3.3 Filter Media Sampling and Analyses

3.3.1 Sampling Techniques

Filter #1 in Slow Sand Water Filtration Plant in Winthrop, Maine was drained to a level in which the filter surface was accessible. Media samples from the schmutzdecke layer were obtained using a plastic scoop in combination with a scraping method to ensure appropriate amounts of

active biomass were being sampled. Once media was scraped, samples were placed in two ounce *Nasko* Whirl-Pak® sampling bags with write-on blocks used for labeling. Schmutzdecke samples were typically acquired from three different locations along the filter surface and collected in duplicates or triplicates per location.

To obtain samples within various media layers in Filter #1, a location within the middle of Filter #1 was chosen. A conventional posthole digger was used to reach various media depths beyond the schmutzdecke layer. During sampling events in which various sand media was collected, this involved grab samples from the middle sand layer, roughly 8 inches below the filter surface, and grab samples from the sand just above the GAC sublayer, roughly 13 inches below the filter surface. During sampling events in which granular activated carbon media was acquired, the posthole digger was used to reach a filter depth of roughly 15 inches below the filter surface.

All filter media sampled by layer were collected in duplicates or triplicates and stored in two ounce *Nasko* Whirl-Pak® sampling bags. Samples were then stored in a cooler during transportation and stored in a 4^{o}C refrigerator prior to the start of media analyses in the laboratory. Media samples from Filter #1 at the Slow Sand Water Filtration Plant in Winthrop, Maine were analyzed within twenty-four to forty-eight hours after collection for ATP biomass characterization and DNA biomass analysis.

3.3.2 Deposit and Surface Analysis Characterization by ATP

Total biomass activity, measured by adenosine triphosphate (ATP) concentrations, was quantified using the Deposit & Surface Analysis (Option B Measured Deposit Method) from the

Luminultra® Microbial Monitoring kit. The deposit and surface analysis standard operating procedure included the use of a rehydrating Luminase enzyme and an Ultracheck calibration (RLU_{ATP1}). If RLU_{ATP1} was less than 5,000 a new bottle of Luminase was to be rehydrated. To prepare samples for biomass quantification, approximately 1.0 gram of wet sample media was weighed and immediately placed into a 5 mL UltraLyse 7 tube for ATP extraction. The tube was shaken vigorously by hand to promote homogenized mixing and then sat for a minimum of 5 minutes to ensure complete extraction. Using a fixed volume micropipette, 1 mL of the UltraLyse 7 extraction solution was diluted into a 9 mL UltraLute dilution tube. The cap was placed on the tube and inverted three times to dilute any interferences within the sample. Total ATP was then measured using a luminometer in conjunction with the firefly luciferase assay. A pipette was used to extract 100 uL of the Luciferase enzyme and placed into an assay tube containing 100 uL of the solution from the UltraLute tube.

A PhotonMaster luminometer was used to read light output from the samples. Results were displayed in relative light units (RLU), which were converted by the LumiCalc software to picogram of total ATP per gram of media (pg ATP/g). For consistency purposes in reporting ATP data, the results were converted to ng ATP/gdw and ng tATP/cm^2 (*See Appendix A*). For that, a known mass of wet media was dried in a muffle furnace at 99º C for 24 hours and re-weighed to determine the dry to wet ratio. For example, the results for sand media displayed a gram dry weight ratio of 87% and GAC media displayed a gram dry weight ratio of 52%. Typical sand media and GAC densities were used to convert gram dry weight values to surface area. Calculations included a density of 2.65 g/cm^3 with an effective particle size of 0.57 mm for sand media and a density of 0.54 g/cm^3 with an effective particle size of 0.65 mm for GAC.

3.3.3 Biomass Characterization by DNA Sequencing Analysis

Total nucleic acid was extracted for metabarcoding from the media samples obtained from Slow Sand Filter #1 at the Slow Sand Water Filtration Plant in Winthrop, Maine. Deoxyribonucleic acid (DNA) extractions were performed used the Qiagen DNEasy® PowerSoil® Pro DNA Extraction kit. PowerBead Pro tubes were spun briefly to ensure that the beads settled to the bottom and approximately 250 mg of media was added along with 800 uL of Solution CD1. The solution was vortexed briefly to ensure mixing. PowerBead Pro tubes were placed horizontally on a Vortex Adapter at maximum speed for 10 minutes, then centrifuged at 15,000 g rpm x g for 1 minute. The supernatant is transferred to clean 2 mL Microcentrifuge Tubes, which were provided in the kit.

The remaining steps listed in the Quick-Start Protocol were performed on the Qiagen QIAcube Connect. QIAcube Connect is able to isolate highly pure nucleic acids using a spin-column based lyse, bind, wash, and elute procedure. The large touch screen on this device and the barcode scanner are used to select the protocol needed. In this case, the DNEasy® PowerSoil® Pro Kit was scanned using the barcode provided on the kit and instructions were followed by on-screen prompts. Once the extraction process was complete, samples were stored in the -80ºC freezer until ready for polymerase chain reaction (PCR) amplification processes and agarose gel set-up.

Gene amplification, purification, and sequencing for metabarcoding analyses were conducted using standard methods to target and amplify the V4–V5 region prokaryote 16s rRNA gene. Cocktail reagents used included dH_2O, Platinum PCR 2x MasterMix, Forward (F) primer 515F (Parada et al., 2016) and Reverse (R) primers 926R (Quince et al., 2011; Parada et al., 2016).

These forward and reverse primers with the Nextera Illumina adapter sequence attached were provided by the Hubbard Center of Genomics Laboratory at the University of New Hampshire. Standard PCR protocol included an Aliquot cocktail consisting of 17 uL of dH_2O, 25 uL of Platinum PCR mix, and 3 uL of each F and R primers, and 2 uL of the extracted DNA samples for a volume total of 50 uL. Concentration readings were not taken throughout the duration of this study and samples were directly applied to the amplification process. After sample preparation, the SimpliAmp™ Thermal Cycler was programmed for a general PCR cycle. Denaturation began at 94ºC for 3 minutes. The remaining steps included denaturation at 94ºC for 45 seconds, annealing at 50ºC for 60 seconds, and extension at 72ºC for 60 seconds. These steps were repeated 25 times. A final extension period occurred at 72ºC for 10 minutes and then samples were held at 4ºC until collected from the thermal cycler. Once the PCR cycle was complete, samples were stored in the -80ºC freezer later analysis by agarose gel.

A 2% agarose-Tris/Borate/EDTA (TBE) buffer gel was used to ensure amplification was successful. Agarose gels are observed under transilluminator to confirm fragments are properly sized with the control ladder and are typically around 500 bp. Amplified samples were given to the Hubbard Center for Genomics Studies Laboratory to attach indexes and the Illumina adapter sequence. Samples with indexes were loaded onto the Illumina NovaSeq 6000 using SP chemistry version 1.5 for paired end 250 base pair sequencing for metabarcoding data analyses.

Metabarcoding data was analyzed using the QIIME2™ microbiome bioinformatics platform. The DADA2 pipeline was used for sequence denoising and sequence variant reconstruction tables. The application of this code allowed for forward and reverse reads of raw sequence data to be

truncated to 240 base-pairs (bp) by trimming the forward primer by 19 bp and the reverse primer by 20 bp. Samples were then re-merged in order to produce visual outputs and statistical analyses based on taxonomy, alpha, and beta diversities. Sequence variants were able to be viewed as relative abundance, otherwise known as percent relative frequencies per sample. Microbiome data analysis of media samples obtained from Slow Sand Filter #1 in Winthrop, Maine included taxonomy plots, interactive trees of life (iTOL), alpha diversity, beta diversity, principal coordinate analyses, and statistical analyses.

3.3.4 Metals Quantification by ICP-AES

Media samples from the schmutzdecke layer, sand above the GAC, and GAC were sent to ACE Products & Consulting LLC in Ravenna, Ohio for metals quantification using inductively coupled plasma atomic emission spectroscopy (ICP-AES) techniques.

The digestion of various media samples for metals extraction was performed using EPA Method 3050B. This method is applicable to soils, sludges, and solid waste samples. Media samples were vigorously digested in nitric acid and hydrogen peroxide, followed by a dilution using either nitric or hydrochloric acid.

EPA Method 6010B was used to measure characteristic emission spectra by optical spectrometry. After digestion, samples are nebulized and the resulting aerosol is transported to the plasma torch. Method detection limits must be established for all wavelengths utilized for each type of matrix commonly analyzed. The matrix used for the MDL calculation must contain analytes of known concentrations within 3-5 times the anticipated detection limit. Each sample

was evaluated for the presence and concentration of the following metals: aluminum, antimony, arsenic, barium, beryllium, cadmium, calcium, chromium, cobalt, copper, iron, lead, lithium, magnesium, manganese, nickel, potassium, selenium, silver, sodium, strontium, thallium, tin, vanadium, and zinc. The metals concentrations of particular focus for this study included: Iron (*Fe*), Manganese (*Mn*), Calcium (*Ca*), and Aluminum (*Al*).

3.4 Quality Assurance / Quality Control

Quality assurance and quality control procedures were applied throughout the duration of this study to ensure results were properly quantified. Quality assurance and quality control methods were performed as outlined in US EPA approved methods, Standard Operating Procedures and Methods, or instruction manuals provided by instrument manufacturers. The Standard Operating Procedures used in this study are provided in *Appendix A*. Sample preservation and requirements were followed strictly throughout the course of this experiment, as well as limits of detection and quantification.

4. RESULTS AND DISCUSSION

4.1 Assessment of Seasonal Variations on BDOC and Non-BDOC Removals

The origin of this study began when a Slow Sand Filter in Winthrop, Maine began demonstrating the ability to preserve the adsorption life span of a GAC sublayer for over one and a half decades. Initial studies at this treatment facility began when the first GAC sublayer was installed in 2005 and did not require the addition of GAC regenerative interferences to maintain elevated removals measured by dissolved organic carbon (DOC) after years of continuous filter run time.

4.1.1 DOC and Non-BDOC Removals

Throughout the duration of this study in conjunction with previous studies, aqueous samples have been obtained from all three filter effluents, as well as the raw water source at the treatment facility in Winthrop, Maine. In November of 2019, Christian Rodriquez obtained aqueous samples from the raw water source as well as Filter #1 and #3 effluents, while in August of 2021, aqueous samples were only collected from the raw water source and the Filter #1 effluent. For the remainder of the study, aqueous samples were collected from the raw water source and all three filter effluents to measure DOC and Non-BDOC removals based on various GAC ages. A summary of various raw water quality parameters and characteristics from this current study are summarized in Table 4-1.

Table 4-1. Raw Water Quality Characteristics and Parameters from Winthrop, ME.

Sampling Period	Average Water Temperature	Average pH	Average Turbidity (Raw Water)	Average Turbidity (Finished Water)
August 2021	21.7 ºC	7.16	0.57 NTU	0.079 NTU
September 2021	21.3 ºC	7.31	0.45 NTU	0.085 NTU
February 2022	4.8 ºC	7.05	0.49 NTU	0.070 NTU
May 2022	11.6 ºC	7.12	0.53 NTU	0.062 NTU

A summary of the aqueous samples obtained from Winthrop, Maine for DOC/BDOC analysis at various dates for the raw water source and three filter effluents are summarized in Table 4-2. The various GAC ages and their year of installation are as follows: Filter #1-2006, Filter #2-2020, and Filter #3-2011. The various removals associated with the biodegradable fraction removed are displayed, while the removals associated with the non-biodegradable organic fraction are also displayed.

Table 4-2. Winthrop, ME SSFs DOC/BDOC Results—Nov. 2019; Aug. 2021; Sept. 2021; Feb. 2022; May.2022

Source	Date	Average Temp °C	DOC (mg/L)	DOC Removed (mg/L)	BDOC (mg/L)	BDOC Removed (mg/L)	Non-BDOC Removed (mg/L)
Raw	11/6/19 8/4/21 9/27/21 2/23/22 5/19/22	10.8 (est.) 21.7 21.3 4.8 11.6	5.55 5.45 5.05 4.69 5.23		1.23 0.85 1.14 0.83 1.27		
Filter #1 (GAC-2006)	11/6/19 8/4/21 9/27/21 2/23/22 5/19/22	10.8 (est.) 21.7 21.3 4.8 11.6	2.57 4.36 2.84 3.32 3.36	2.98 1.09 2.21 1.37 1.87	0.25 0.65 0.23 0.39 0.24	0.98 0.20 0.91 0.44 1.03	2.00 0.89 1.30 0.93 0.84
Filter #2 (GAC-2020)	9/27/21 2/23/22 5/19/22	21.7 21.3 11.6	0.50 0.47 0.33	4.55 4.22 4.90	0 0 0	1.14 0.83 1.27	3.41 3.39 3.65
Filter #3 (GAC-2011)	11/6/19 9/27/21 2/23/22 5/19/22	10.8 (est.) 21.3 4.8 11.6	2.77 2.91 3.05 3.39	2.78 2.14 1.64 1.84	0.20 0.40 0.21 0.32	1.03 0.74 0.62 0.95	1.75 1.40 1.02 0.89

From a perusal of the trends noted that the removals associated with GAC are still significant after several years of filter run-time and in many instances are exceeding the biodegradable fraction. Filter #2, with the “freshest” GAC layer, is removing the measurable biodegradable

organic carbon fraction, yet very large non-BDOC removals were observed. This is most likely due to the GAC in Filter #2 being only within the first two years of "aging".

As discovered by Page (1997), the primary DOC removal mechanism by the pilot control slow sand filter was by biodegradation, which was also a function of temperature or season. The GAC amended slow sand filter was able to significantly enhance NOM removals as compared to the control slow sand filter. It was noted that the rate of biodegradation improved with temperatures greater than 7-12ºC (Page, 1997). Cumulative mass loadings and batch isotherm tests also suggested that biodegradation mechanisms improved the adsorbability of DOC in influent water (Page, 1997). It was also confirmed that the majority of DOC removals occurred within the first few minutes of empty bed contact time (EBCT), therefore SSF provides sufficient contact time for the removal of the BDOC fraction (Page, 1997). Unger and Collins (1997) redefined the schmutzdecke where most of the SSF removals take place, within the first 5-7 minutes of EBCT.

Results from the current study suggest that the GAC sandwich configuration remains a viable treatment option after several years of filter run-time and can continue to enhance NOM removals after several years of installation. Bed volume calculations, which can be found in *Appendix B*, were conducted in order to assess the amount of particular loading onto the GAC sublayer. Filter #1, in which the GAC was installed in 2006, has an adsorption capacity of approximately 73,000 bed volumes. According to Page (1997), the useful operating time of a GAC sandwich filter is roughly 5 years but can be dependent upon organic loading and treatment objectives.

4.1.2 Control Sand and GAC Removals

In order to gain a greater understanding of removals occurring by the sand and GAC sublayers, a peristaltic pump and slotted probe were used to extract aqueous samples above the GAC layer. In February of 2022, aqueous samples were extracted above the GAC layer in Filter #1 and the same extraction process was used to obtain samples from Filter #3 in May of 2022.

The TOC removals for sand only, sand and GAC, and GAC only for Filter #1 and #3 are summarized in Table 4-3 and Table 4-4. The sand layer was directly measured as a result of extracting samples above the GAC, while GAC removals were measured by differences between the sand only and the overall performance of Filters #1 and #3, which includes sand and GAC layers.

Table 4-3. Winthrop, ME SSFs DOC/BDOC Results – Sand & GAC Removals Filter #1 (Feb. 23, 2022)

Source	Date	Average Temp °C	DOC (mg/L)	DOC Removed (mg/L)	BDOC (mg/L)	BDOC Removed (mg/L)	Non-BDOC Removed (mg/L)
Raw	2/23/22	4.8	4.69		0.83		
Sand ONLY	2/23/22	4.8	3.95	0.74	0.49	0.34	0.40
Filter #1 (Sand + GAC-2006)	2/23/22	4.8	3.32	1.37	0.39	0.44	0.93
Δ GAC	2/23/22	4.8		**0.63**	0.34	**0.10**	**0.53**

In Table 4-3, removals associated with GAC include 0.63 mg/L of DOC removed, 0.10 mg/L of BDOC removed, and 0.53 mg/L of Non-BDOC removed. In Filter #3, the removals associated with GAC include 0.56 mg/L of DOC removed, 0.10 mg/L of BDOC removed, and 0.46 mg/L of

Non-BDOC removed. The significant non-BDOC fraction removal occurs primarily within the GAC, essentially highlighting the adsorption capacity of GAC even after roughly fifteen and eleven year of continuous operation.

Table 4-4. Winthrop, ME SSFs DOC/BDOC Results – Sand & GAC Removals Filter #3 (May. 19, 2022)

Source	Date	Average Temp °C	DOC (mg/L)	DOC Removed (mg/L)	BDOC (mg/L)	BDOC Removed (mg/L)	Non-BDOC Removed (mg/L)
Raw	5/19/22	11.6	5.23		1.27		
Sand ONLY	5/19/22	11.6	3.95	1.28	0.42	0.85	0.43
Filter #3 (Sand + GAC-2011)	5/19/22	11.6	3.39	1.84	0.32	0.95	0.89
Δ GAC	5/19/22	11.6		**0.56**	0.85	**0.10**	**0.46**

4.2 Assessing Biomass Characteristics as Functions of Seasonal and Media Influences

Various media samples were obtained from slow sand filters in Winthrop, Maine in order to assess temperature influences and inorganic compositions. Samples were analyzed for biomass production, microbial community composition, and metals concentrations corresponding to schmutzdecke media, sand above the GAC, and granular activated carbon media.

4.2.1 ATP Biomass Analysis as a Function of Temperature

Seasonal variations were explored using a deposit and surface area analysis laboratory method to measure ATP biomass within various filter layers. Several studies have indicated that ATP biomass production increases during warmer temperatures and decreases during colder temperatures. Various media samples were obtained from Filter #1 and #3 throughout the

duration of this study and included sampling events from August 2021, September 2021, February 2022, and May 2022. Samples were obtained by Christian Rodriguez from Filter #2 in November 2019 and data has been used for seasonal comparisons.

Table 4-5 summarizes the ATP biomass values obtained from several sampling events that occurred in Winthrop, Maine. Biomass was initially measured and calculated in nanograms of ATP per gram dry weight, however, due to vast differences in densities between sand media and GAC media, comparative conversions were applied from surface area calculations based on gram dry weight and media densities. ATP per surface area can be seen in Table 4-6 and will be the focus of this discussion.

Table 4-5. ATP Biomass Concentrations for Various Sampling Dates and Filters as ng ATP/gdw.

Date	Filter	Average Water Temperature	Schmutzdecke	Mid-Sand	Sand Above GAC	GAC
11/6/19	2	10.8 (est.)	394.7 ± 22.1	-	-	245.6 ± 13.2
8/4/21	1	21.7	1859.3 ± 291.5	-	183.5 ± 47.0	1300.7 ± 328.8
9/27/21	1	21.3	676.8 ± 119.9	42.5 ± 8.7	14.2 ± 15.9	57.2 ± 9.7
2/23/22*	1	4.8	171.1 ± 47.8	-	-	-
5/19/22	3	11.6	64.9 ± 33.1	15.7 ± 2.5	17.3 ± 1.4	180.0 ± 19.1

**indicates Filter #1 was harrowed five days prior to sampling event.*

Table 4-6. ATP Biomass Concentrations for Various Sampling Dates and Filters Normalized to Surface Area as ng ATP/cm^2.

Date	Filter	Average Water Temperature	Schmutzdecke	Mid-Sand	Sand Above GAC	GAC
11/6/19	2	10.8 (est.)	12.1 ± 0.7	-	-	1.8 ± 0.1
8/4/21	1	21.7	55.0 ± 8.6	-	5.4 ± 1.4	14.6 ± 3.7
9/27/21	1	21.3	20.0 ± 4.2	1.3 ± 0.3	0.4 ± 0.5	0.6 ± 0.1
2/23/22	1	4.8	5.32 ± 1.6	-	-	-
5/19/22	3	11.6	1.9 ± 1.0	0.5 ± 0.1	0.5 ± 0.0	1.8 ± 0.2

In order to visualize the impact of biomass production within slow sand filters from a seasonal approach, Figure 4-1 displays the biomass results graphically, in both gram dry weight (a) and squared centimeter surface area (b). Optimal performances in slow sand filtration can be achieved when the filter is fully matured and acclimated with a steady biomass population (Arora, 2017). Media samples were obtained from various depths within the filter bed at various times through the study and include: the schmutzdecke at 0.2 cm (top of the filter bed), the mid-sand layer 20 cm below the filter surface, the sand above the GAC 33 cm below the filter surface, and the GAC which was obtained 38 cm below the filter surface.

Results are displaying variation of biomass production with respect to temperature and with filter media location. In particular, biomass accumulation per surface area has demonstrated that the GAC sublayer has the potential to accumulate higher biomass concentrations than adjacent sand layers. The warmest sampling event occurred in August and presents ATP biomass for sand media above the GAC as 5.4 ng ATP/cm^2 as compared to 14.6 ng ATP/cm^2 for GAC media. In another sampling event which occurred in September, similar trends can be seen where ATP biomass for sand media above the GAC was 0.4 ng ATP/cm^2 as compared to 0.6 ng ATP/cm^2 for GAC media. Sublette et al., (1982) reported that activated carbon can provide a surface for microorganisms to attach which provides a source of protection while microorganisms are simultaneously regenerating the activated carbon. According to the literature, biomass accumulation on the GAC sublayer is not well understood and will need further exploration to determine the potential for higher biomass accumulations on GAC as opposed to adjacent sand media.

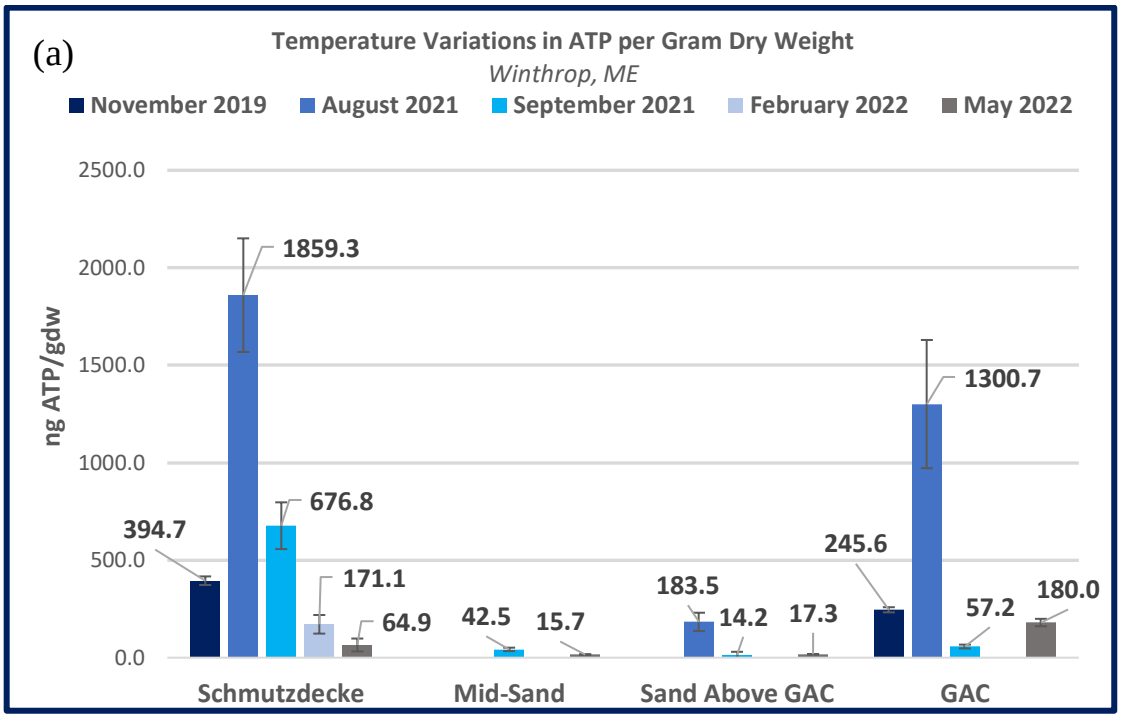

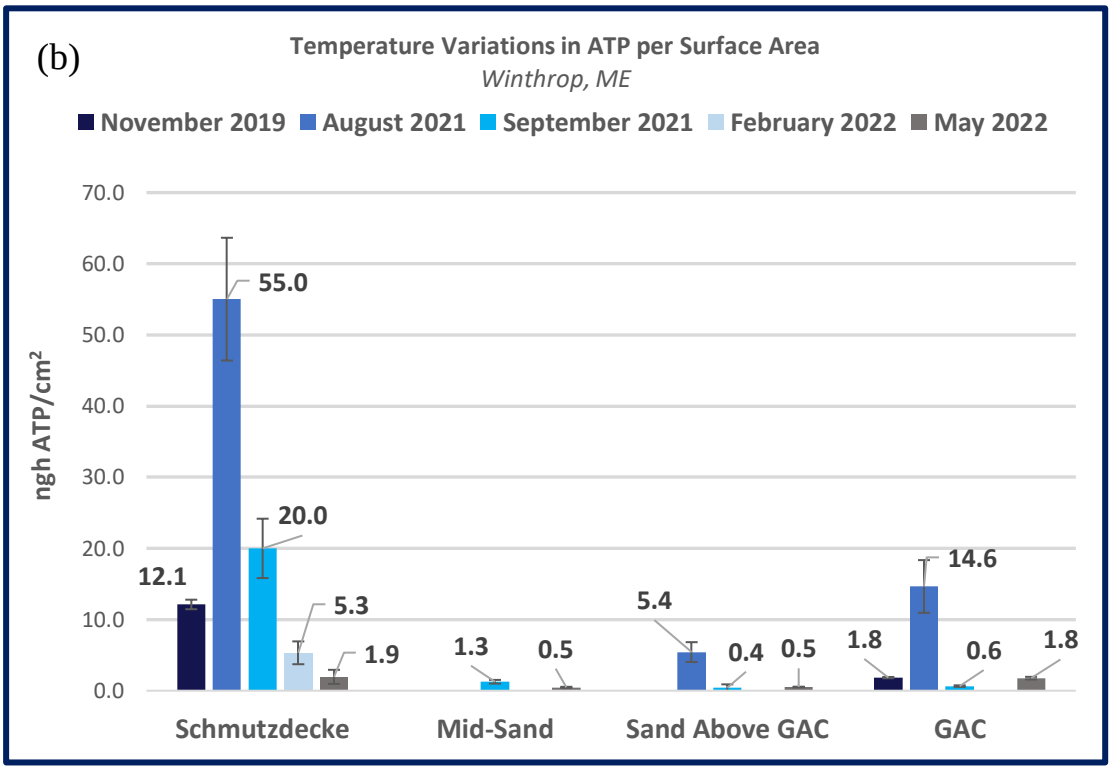

Figure 4-1. Temperature variations in ATP biomass for various media coatings from Filter #1 in Winthrop, (ME) normalized to (a) ng ATP/gdw and (b) ng ATP/cm^2 surface area.

Biomass production typically occurs within the schmutzdecke layer and top few centimeters of the sand bed. Duncan (1988) states that the biomass population can change dynamically in response to changes in temperature. Seasonal variations and biomass response to temperature changes within schmutzdecke and adjacent sand layers have been previously noted by Campos et al., (2002) and Partinoudi et al., (2006). Within this present study, biomass production, particularly within the schmutzdecke layer, responded abruptly to seasonal variations and demonstrated greater amounts ATP biomass in summer conditions as opposed to winter conditions.

4.2.2 Seasonal Variations in the Schmutzdecke ATP Content

Per Unger & Collins (2008), the schmutzdecke has been quantified in the upper 7.5 cm of the filter bed. Removal mechanisms associated with slow sand filtration can be dependent upon the microbial community present within the filter bed and the ripening period, which determines the biomass population and acclimation within the schmutzdecke layer. The development of the schmutzdecke layer depends upon the available microbes within raw water sources, food and oxygen supply, residence time, and wetting of the sand bed (Ranjan & Prem, 2018). Table 4-7 summarizes the average water temperatures during various sampling dates, as well as ATP biomass in nanograms per gram dry weight from the schmutzdecke layer only.

Table 4-7. Schmutzdecke ATP Biomass Concentrations as ng ATP/gdw.

Date	Filter	Average Water Temperature	Schmutzdecke
11/6/19	2	10.8 (est.)	394.7 ± 22.1
8/4/21	1	21.7	1859.9 ± 291.5
9/27/21	1	21.3	676.8 ± 119.9
2/23/22	1	4.8	171.1 ± 47.8
5/19/22	3	11.6	65.9 ± 33.1

Throughout the duration of this study, sampling of the schmutzdecke layer was most consistent. Figure 4-2 displays the variability of temperature within schmutzdecke sample averages obtained from Winthrop, Maine. In warmer months, particularly August and September where the average raw water temperature was 21.7 ºC and 21.3 ºC, biomass production was highest at 1859.9 ng ATP/gdw and 676.8 ng ATP/gdw respectively. In comparison, colder months included sampling events from November, February, and May where average water temperatures were 10.8ºC, 4.8 ºC, and 11.6ºC. Schmutzdecke biomass production within colder months included 394.7 ng ATP/gdw, 171.1 ng ATP/gdw, and 65.9 ng ATP/gdw.

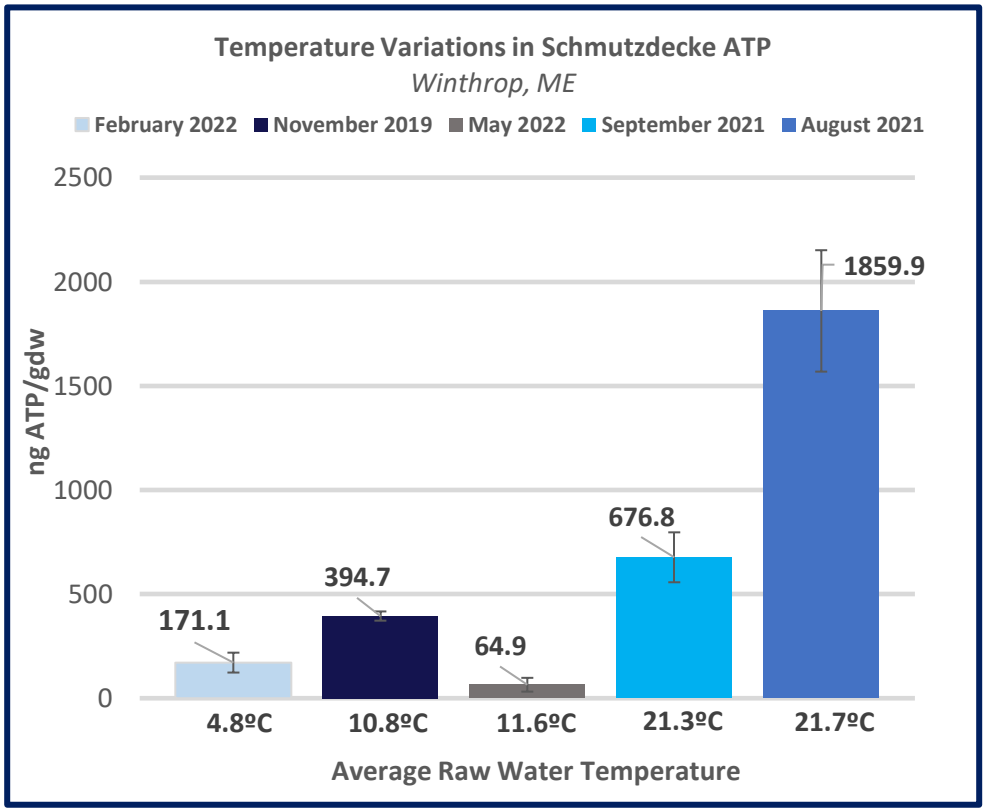

Figure 4-2. Temperature variations relating to ATP biomass production within the schmutzdecke.

Sampling restrictions pertaining to schmutzdecke media collection occurred in February. During this sampling event, six schmutzdecke samples were collected from Filter #1 and access was limited to adjacent filter sublayers. Schmutzdecke samples were collected from three different locations in Filter #1 just five days after Filter #1 was harrowed on February 18th, 2022. Harrowing, as previously mentioned in section 2.1.3, involves significantly draining the supernatant water layer in order to rake the sand medium which includes the schmutzdecke layer and top few centimeters of the sand bed. Figure 4-3 demonstrates the variability between filter location and biomass production in nanograms per gram dry weight after harrowing of the sand bed. Figure 4-4 displays the ATP biomass variability at various sampling dates and the days sampled after harrowing occurred for the duration of this study.

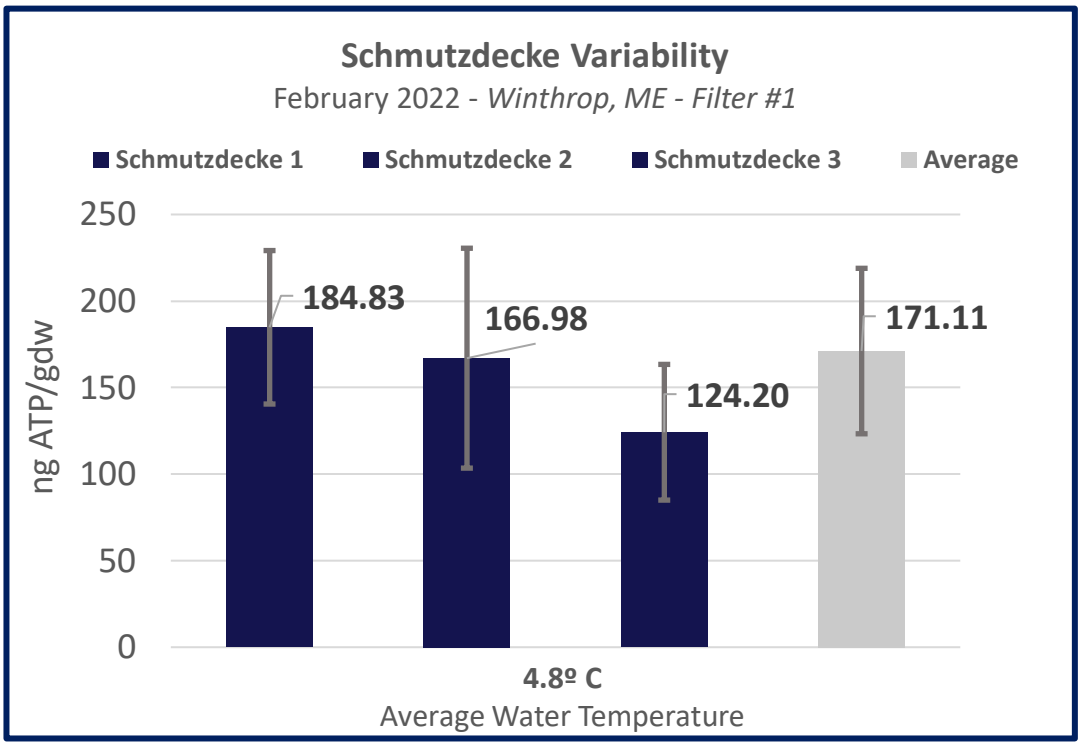

Figure 4-3. ATP biomass variability within schmutzdecke samples obtained five days after harrowing.

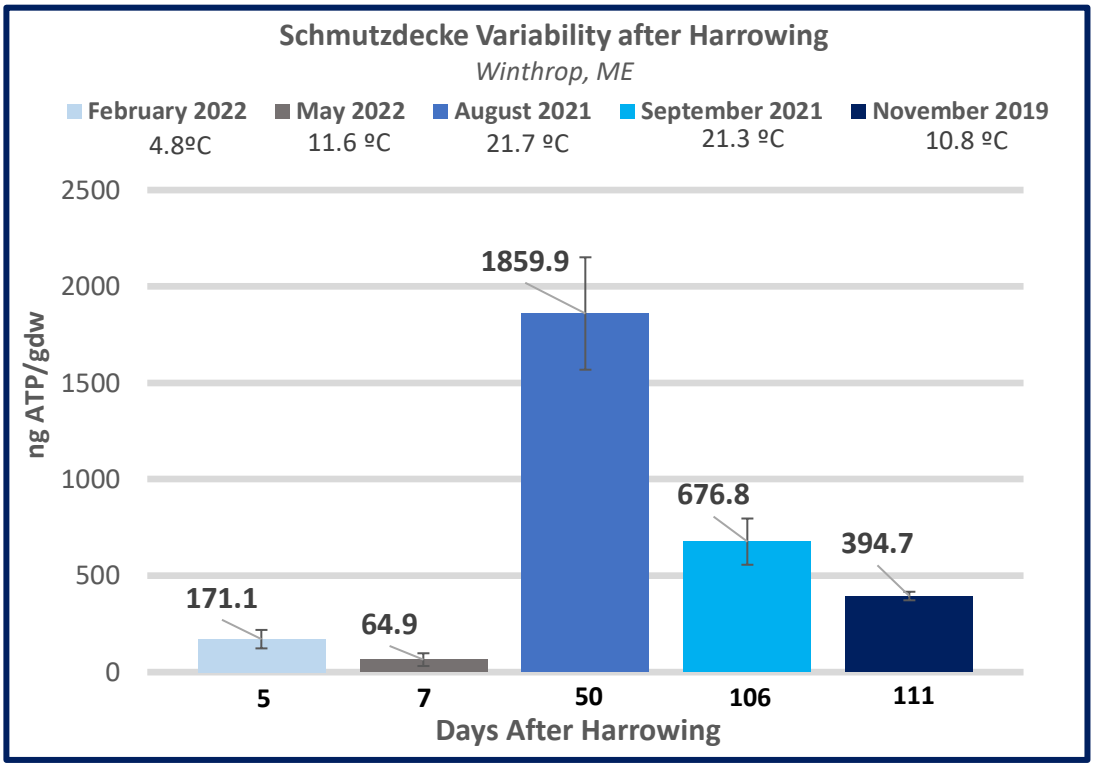

Figure 4-4. ATP biomass production in relation to harrowing events throughout the duration of this study.

As mentioned previously, ATP biomass production within the schmutzdecke layer responded promptly to seasonal changes during this present study. Partinoudi et al., (2006) also discovered that preferential microbial removal occurred when the study was conducted in summer conditions as opposed to winter conditions. In comparison, Campos et al., (2002) did not discover much variation in biomass production with the schmutzdecke layer over a time period between the months of May and August. Results from the present study verified that production of biomass within the schmutzdecke layer is dependent upon seasonal fluctuation and not from schmutzdecke location within the slow sand filter.

4.2.3 Microbial Community Composition by Media Type

Various media samples from Slow Sand Filter #1 at the Slow Sand Water Filtration Plant in Winthrop, Maine were analyzed for microbial composition in the months of August 2021, September 2021, and February 2022. DNA extractions and analyses were performed on samples obtained from the schmutzdecke layer, sand media above the granular activated carbon layer, and granular activated carbon. Slow sand filtration is successful based on the type of bacteria present within the schmutzdecke layer and adjacent filter layers. The microbial community formed within the schmutzdecke and adjacent filter layers is responsible for creating a zone of biological activity that can provide degradation of soluble organics from the raw water source. While the biomass population has been discovered to be most active in warmer temperatures and less active in colder temperatures, this section will place emphasis on the results from samples collected in August.

In order to gain insight on the species diversity present within the slow sand filter sampled in Winthrop, Maine, QIIME2 was used to generate an interactive tree of life based on extracted DNA from various media types. Figure 4-5 demonstrates the genetic diversity present within Filter #1 and is comprised of 36,610 sequence counts. To explore microbial community composition by layer and media type, data was obtained as amplicon sequence variants (ASVs) through QIIME2 coding. This measurement gives insight to the sequence variants present within each layer, as well as species abundance. For the purpose of this research, Level 2 frequencies were obtained from the QIIME2 database and displays species by the domain and phylum of which they belong to. Table 4-8 summarizes the three governing species by relative frequency found within the schmutzdecke media, sand media above the GAC, and granular activated

carbon media samples obtained in August of 2021. The three main bacterial species prevailing within all three media types were *Proteobacteria*, *Acidobacteriota*, and *Planctomycetota*.

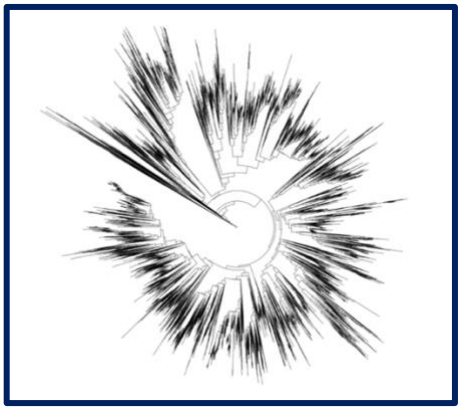

Figure 4-5. Interactive tree of life displaying genetic diversity within fifteen media samples from Winthrop, (ME) – Filter #1 August 2021.

Table 4-8. Percent Relative Frequency of Dominating Species - Filter #1 in Winthrop (ME), August 4th 2021.

Domain & Phylum	Schmutzdecke	Sand Above GAC	GAC
Bacteria – Proteobacteria	24 %	17%	32 %
Bacteria – Acidobacteriota	8 %	13%	8 %
Bacteria – Planctomycetota	34 %	27 %	19 %
% Relative Frequency Total	**66 %**	**57 %**	**59 %**

A visual representation of the diversity differences found within each filter media type is depicted in Figure 4-6. *Proteobacteria*, *Acidobacteriota*, and *Planctomycetota* account for over 50% of the relative abundance of species found by media type. Within the schmutzdecke, sand above the GAC, and GAC averages, these three species account for 67%, 57%, and 58% of relative frequency totals, respectively. Beyond the dominating species present in each layer, there are minor differences within species present in each sublayer and these can be seen in the top quadrants of the bar graphs in Figure 4-6 .

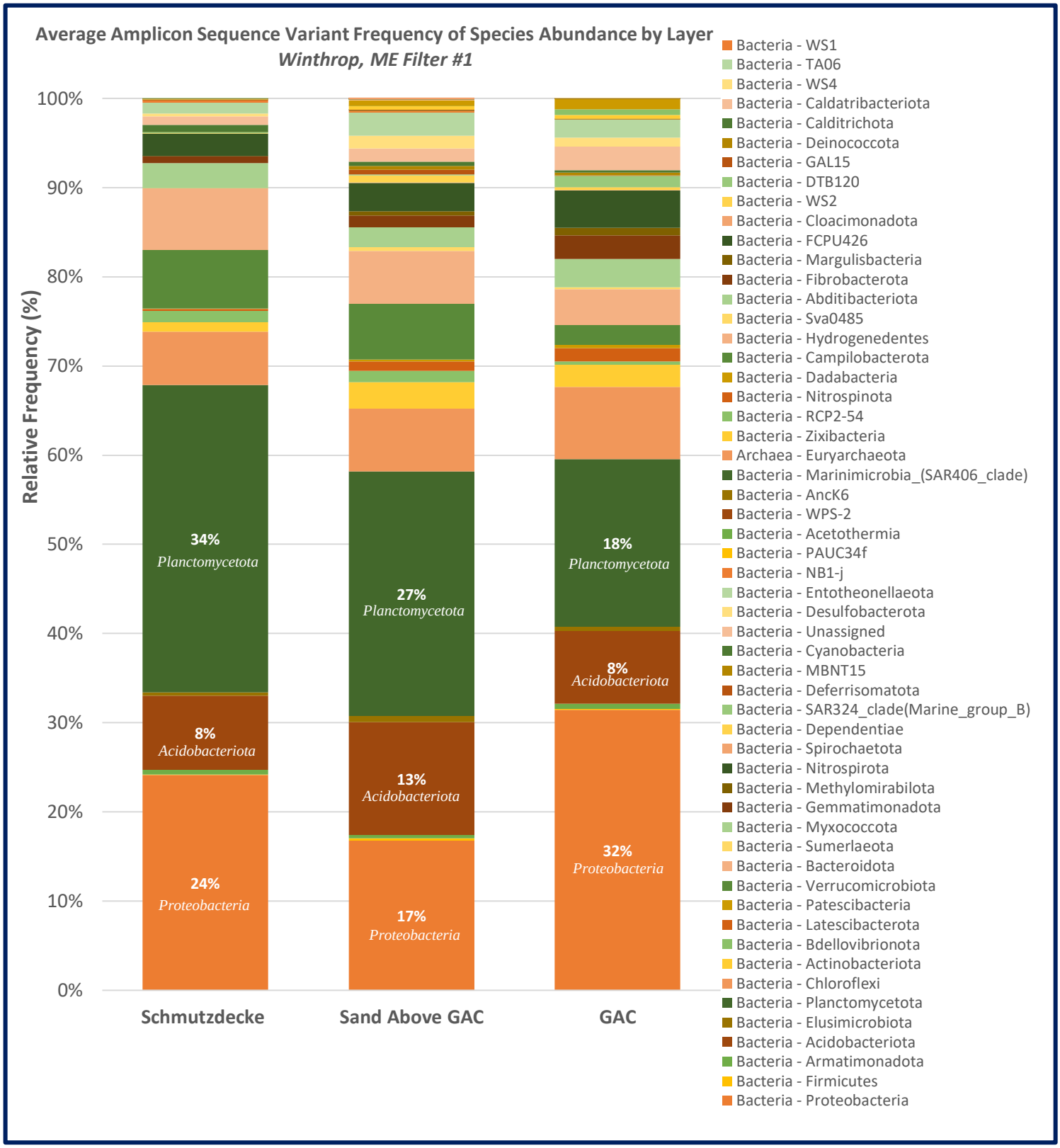

Figure 4-6. Average amplicon sequence variant frequency of species abundance by layer in Filter #1.

Statistical analyses were performed for sequence variants present within each layer. Alpha diversity analyses focus on taxa detected within each sample while beta diversity analyses focus on the difference in microbial composition between samples. Alpha diversity analyses were performed on QIIME2 using Faith's Phylogenetic Diversity to qualitatively measure community richness on the basis of phylogenetic relationships between features. A Kruskal-Wallis Pairwise analysis was also conducted by layer, which corresponds to media type. Figure 4-7 displays Faith's Phylogenetic Diversity by layer within Slow Sand Filter #1 in Winthrop, Maine from August of 2021. The schmutzdecke media and sand above the GAC are displaying higher values corresponding to phylogenetic diversity, signifying there is more species richness present within these two layers.

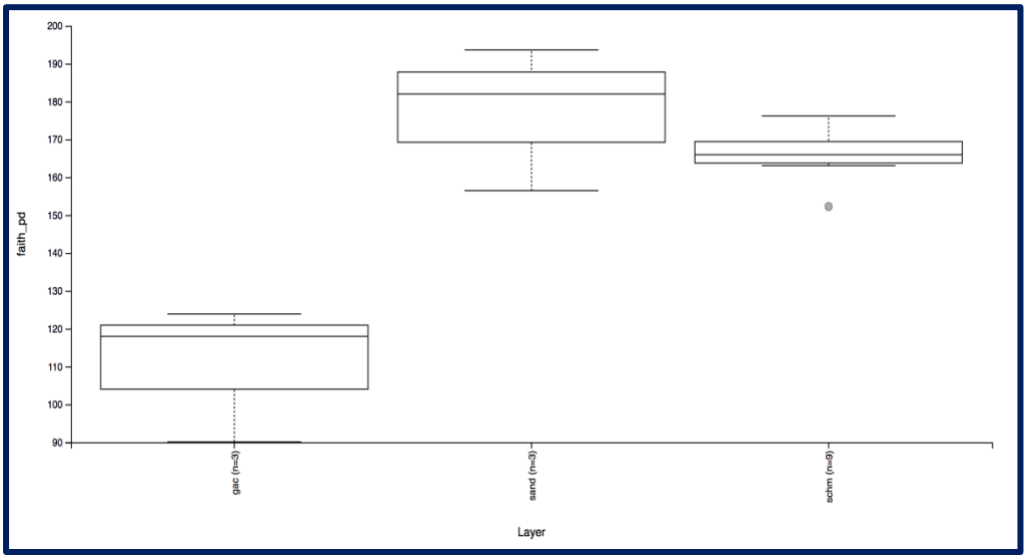

Figure 4-7. Faith's Phylogenetic diversity displayed by layer - Filter #1, August 2021.

The statistical results corresponding to alpha diversity using a Kruskal-Wallis pairwise test is summarized in Table 4-9. This test incorporates a significance level of p= 0.05 and a null hypothesis that there are no differences between phylogenetic diversity within each sample.

Results for comparisons between the sand and schmutzdecke layer produced a p-value of 0.049 and 0.012, respectively. Because these comparative values are less than 0.05 or 95 % confidence level, the medians between GAC and both the sand and schmutzdecke layers are statistically significant. The sand layer compared with the schmutzdecke layer produces a p-value of 0.309, which is greater than 0.05, signifying that the medians for these layers are not statistically significant. In light of the results pertaining to alpha diversity, species richness is greater within the sand and schmutzdecke layers, as compared to GAC. Bellamy et al, (1985a) reported that as filtration progresses, biological growth continues to occur within adjacent media layers. It is important to note that little differences were observed between the schmutzdecke and sand layers most likely due to harrowing processes. The schmutzdecke layer is raked during harrowing and this allows for mixing to occur between schmutzdecke and sand medias. While GAC did not show as much species richness compared to sand and schmutzdecke layers, results from this study suggest biological activity is continuing to occur within the GAC sublayer on the basis of ATP biomass production and potentially contributing to the bioregeneration process.

Table 4-9. Kruskal-Wallis Pairwise Statistical Analysis by Layer using Alpha Diversity, Filter #1 August 2021.

Group	H	p-value	q-value
gac (n=3) versus sand (n=3)	3.86	0.05	0.07
gac (n=3) versus schm (n=9)	6.23	0.01	0.04
sand (n=3) versus schm (n=9)	1.03	0.31	0.31

Beta diversity analyses conducted through QIIME2 and MATLAB software focused on a Principal Coordinate Analysis (PCoA) paired with a Permanova pairwise statistical analysis by layer group significance. Figure 4-8 displays the results of the PCoA plots which measure beta diversity based on phylogenetic differences. Results of the principal coordinate analysis plots

display the first two principal coordinates: axis 1 which accounts for a larger percentage of the observed variation by layer, and axis 2 which accounts for a smaller percentage of the observed variation by species These results suggests that microbial community composition is affected by layer location within the filter and are showing similar trends between two software applications

.

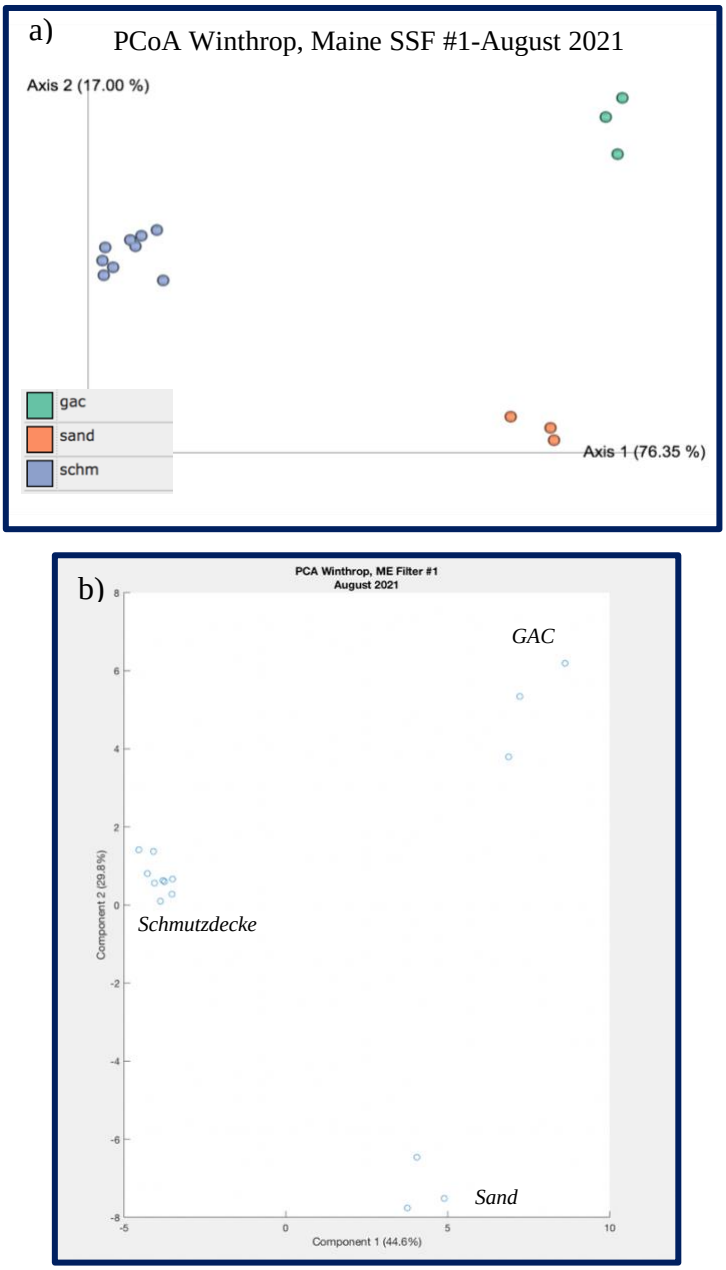

Figure 4-8. PCoA results from media samples obtained from Filter #1 in Winthrop, (ME) in August 2021 using (a) QIIME2 software and (b) MATLAB software.

The results of the statistical analysis related to beta diversity can been seen in Table 4-10 and coincide with results produced from the alpha diversity analyses. This test also incorporates a significance level of p= 0.05 and a null hypothesis that there are no differences between phylogenetic diversity within each layer.

Table 4-10. Permanova Pairwise Statistical Analysis by Layer Group Significance using Beta Diversity, Filter #1 August 2021.

Group	Sample Size	pseudo-F	p-value
gac versus sand	6	21.01	0.10
gac versus schm	12	88.92	0.008
sand versus schm	12	86.81	0.007

Pseudo-F values are a measure of effect size and typically the larger the F-value, the greater the difference in comparison. In this case, the distances between GAC and sand produced a pseudo-F value of 21.0, indicating a smaller difference in comparison. Comparisons between GAC and schmutzdecke distance produced a pseudo-F value of 88.9 while sand and schmutzdecke distances produced a pseudo-F value of 86.81, demonstrating a greater difference in comparison between these layer distances. In retrospect, the p-values produced in this Permanova demonstrate that the distance between GAC and sand is not statistically significant ($p = 0.05 < 0.1$), while the distances between GAC and schmutzdecke ($p=0.05 > 0.008$) and sand and schmutzdecke ($p=0.05 > 0.007$) are statistically significant. Due to sampling depths between the sand above the GAC and GAC media were within 2-inches of one another, this results further prove that species composition does not greatly differ between sand and GAC media types.

4.2.4 Assessment of Seasonal Variation on Microbial Community Composition

Various media coatings from Slow Sand Filter #1 at the Water Filtration Plant in Winthrop, Maine were analyzed for microbial community composition. Section 4.2 focused on the results from extracted samples in August, which included the schmutzdecke, sand above the GAC, and granular activated carbon media. Samples obtained in September included those three layers, plus an additional sample obtained from the middle sand layer within the filter. Due to restrictions in February, mentioned in *Section 4.2.2*, only schmutzdecke samples will be used for comparison within this section.

Microbial community composition was not expected to change drastically throughout the duration of this study due to the gradual accumulation of a biomass population and adhesion to the filter subsurface. Level 2 relative frequencies were obtained through QIIME2 for fifteen media samples collected in August, twelve media samples collected in September, and six schmutzdecke samples collected in February. Results are displayed in Figure 4-13 based on various sampling months and relative frequencies of taxonomy present within filter layers which include the schmutzdecke, sand above the GAC, and GAC.

Results in Figure 4-9 display minimal variation within taxonomy present in both the schmutzdecke and sand layers between August, September, and February sampling events concurring with the hypothesis that composition was not expected to alter greatly. The percent relative frequencies of the dominating species mentioned in Section 4.2.2 decreased slightly and can been seen in *Appendix B.* Between these sampling events, four species were present in very small amounts, below 1.0% relative frequency, within September and February samples. These

species include *Caldisericota, LCP-89, Fusobacteriota, and Halanaerobiaeota.* Due to such low relative frequencies, it can be concluded that these species are not driving factors within seasonal variability between filter layers. GAC comparisons are vastly different but could be attributed to errors within the lab during the PCR sequencing process, as DNA did not show up in the gel ladder for this sample. Further analyses will need to be conducted to determine these differences if they are present, or if this is attributable to error. Results verified that species composition within filter sublayers did not change drastically between winter and summer conditions, however, it demonstrates that microbial community composition is sensitive to location within the filter.

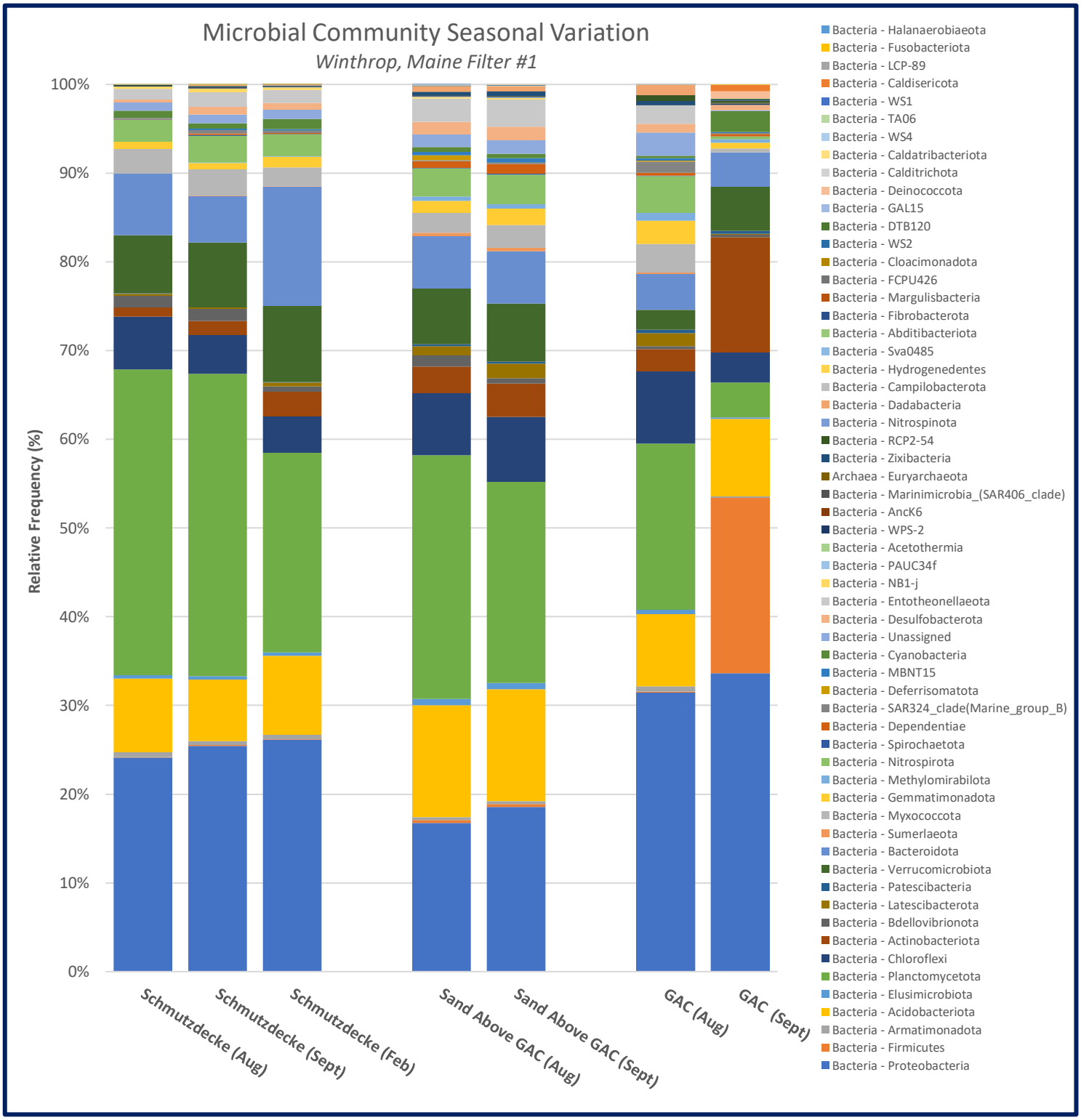

Figure 4-9. Seasonal comparisons of microbial community composition in Filter #1 in Winthrop, (ME), August 2021.

4.3 Assessing Metal Coating Accumulations as a Function of Media Type

Various media coatings from Slow Sand Filter #1 and Slow Sand Filter #3 from the Slow Sand Water Filtration Plant in Winthrop, Maine were analyzed for metals concentrations. Media coatings included samples from the schmutzdecke layer, sand media above the granular activated carbon layer, and granular activated carbon.

4.3.1 Metals Content for Various Media Coatings

Metals concentrations for Iron (Fe), Manganese (Mn), Calcium (Ca), and Aluminum (Al) are summarized in Table 4-11 as milligram per kilogram dry weight and normalized to surface area as milligram per centimeter squared in Table 4-10. Within the GAC sublayer, calcium content far exceeded any other metals concentrations present within various media coatings in Filter #1. Due to the vast differences between the densities of sand and GAC media, sand at 2.65 g/cm^3 and GAC at 0.52 g/cm^3, surface area calculations were performed to transform the data set (See *Appendix B*).

Table 4-11. Metals Concentrations for Various Media Coatings from Filter #1 as mg/kgdw.

Metal (mg/kgdw)	**Schmutzdecke**	**Sand Above GAC**	**GAC**
Iron	2190	3700	1960
Manganese	149	41	328
Calcium	333	381	15400
Aluminum	1120	1080	1840

Table 4-12. Metals Concentrations for Various Media Coatings from Filter #1 as mg/cm^2.

Metal (mg/cm^2)	**Schmutzdecke**	**Sand Above GAC**	**GAC**
Iron	64.8	109.5	22.1
Manganese	4.4	1.2	3.7
Calcium	9.9	11.3	173.5
Aluminum	33.1	32.0	20.7

Figure 4-10 (a) is a visual representation of the various media coatings and their respective metals concentrations as milligram per kilogram dry weight from Filter #1, while Figure 4-10 (b) is a representation of the metals concentrations after the surface area calculations were applied. Calcium still remained in greater concentrations within the GAC sublayer regardless of dry weight or surface area amounts.

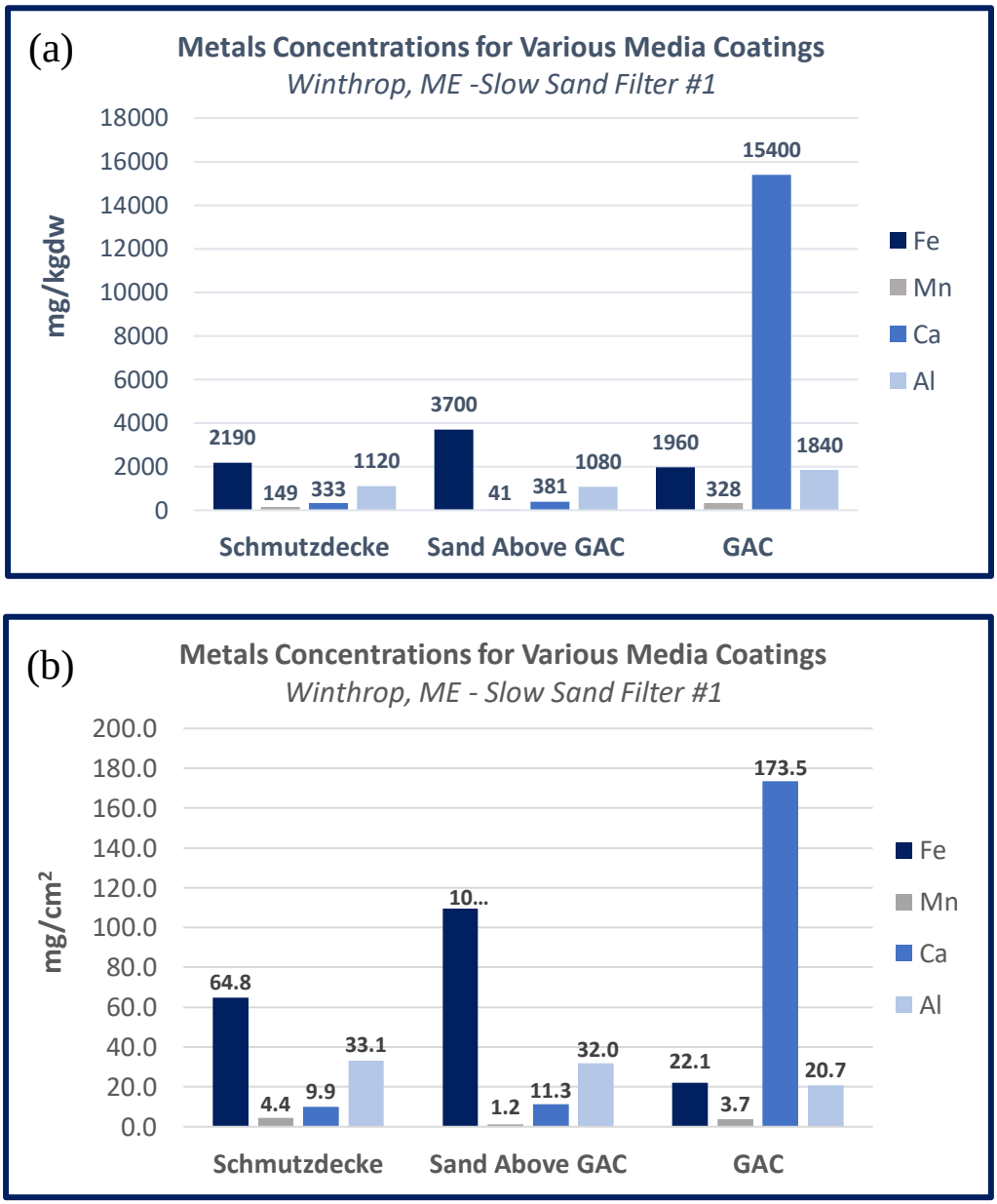

Figure 4-10. Metals concentrations for various media coatings from Filter #1 in Winthrop, (ME) normalized to (a) mg/kgdw and (b) mg/cm^2 surface area.

While metal coating accumulations are not expected to change drastically during the duration of this study due to gradual accumulations on filter media over time, comparing the total metal coating concentrations found in this study with other SSF studies may be of interest. Extractable metals content from various SSF surface sand media coatings obtained from Collins and Vaughan (1996), as well as metals content from this current study, are summarized in Table 4-13 and shown in Figure 4-11. Although the sand media samples are from vastly different locations, the source waters, length of service, and the overall metal content of the sand coatings were similar with iron being the most dominant.

Table 4-13. SSF Comparisons of Metals Surface Coating Concentrations (Collins & Vaughan, 1996).

Metal (mg/kgdw)	**Winthrop (ME) – SSF**	**West Hartford (CT) – SSF**	**Portsmouth (NH) – SSF**
Iron	3700	3732	2986
Manganese	41	200	45
Calcium	381	270	283
Aluminum	1080	1695	1148
Avg Metal Milliequivalents (meq/kgdw)	272	343	250

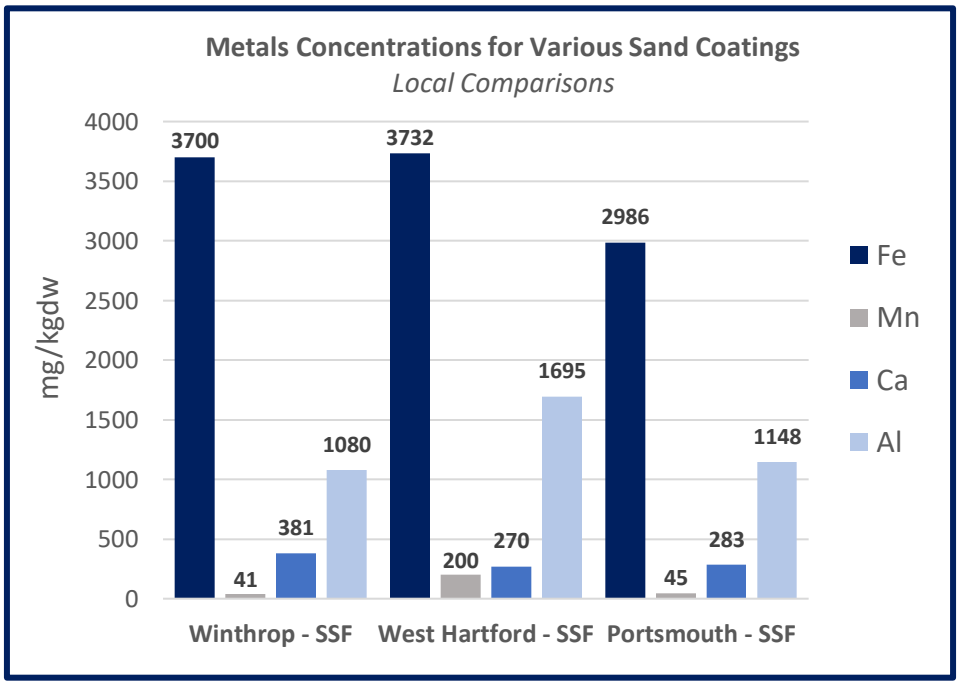

Figure 4-11. Visual comparison of metals concentrations found within various sand coatings from local slow sand filters.

4.3.2 Calcium Loading on GAC

Converting gram dry weight of filter media to metal content per surface area indicated large amounts of calcium accumulated on the GAC sublayer compared to the sand media in Filter #1 in Winthrop (ME). Results highlighted a theory that substantial amounts of calcium accumulation on the GAC sublayer could be contributing to higher removals associated with GAC through electrostatic attraction or binding. To further explore this theory, virgin GAC was analyzed for metals concentrations. Table 4-14 summarizes the metals concentrations found between virgin GAC and aged GAC, both obtained from the filtration plant in Winthrop (ME)

Table 4-14. Metals Concentrations for Virgin GAC and Aged GAC in mg/kgdw.

Metal (mg/kgdw)	**Virgin GAC**	**Aged GAC – Filter #1**	**Aged GAC – Filter #3**
Iron	2520	1960	2240
Manganese	26	328	13.6
Calcium	957	15400	15000
Aluminum	1560	1840	1660

Visual and statistical comparisons of the metals concentrations between virgin GAC and aged GAC for Iron (Fe), Manganese (Mn), Calcium (Ca), and Aluminum (Al) is displayed in Figure 4-12. The metals concentrations for Iron, Manganese, and Aluminum do not indicate variation between the two GAC types. However, calcium content for the virgin GAC was 957 mg/kgdw as compared to the aged GAC at 15,400 mg/kgdw. Comparisons between the metals content found on GAC that has not been used and aged GAC from Filter #1, which was installed in 2006, further verified the theory of significant calcium loading on the GAC sublayer.

Cannon et al., (1993) verified that metals accumulation on GAC can negatively affect the regeneration process. Within his study, it was discovered that GAC can accumulate heavy metals in significant quantities, particularly large amounts of calcium. Metals concentrations from the

current study verified calcium loading onto the GAC sublayer and that significant accumulation of calcium is occurring on aged GAC as opposed to virgin GAC. While calcium is a positively charged ion, portions of the bacterial population and NOM (possibly other negatively charged anions, e.g. HCO_3^-), could be attracted to the calcium coated GAC surfaces. Substantial amounts of calcium accumulations on the GAC sublayer could be contributing to the "renewal" of GAC adsorption sites through electrostatic attraction or binding, resulting in higher removal of TOC/DOC.

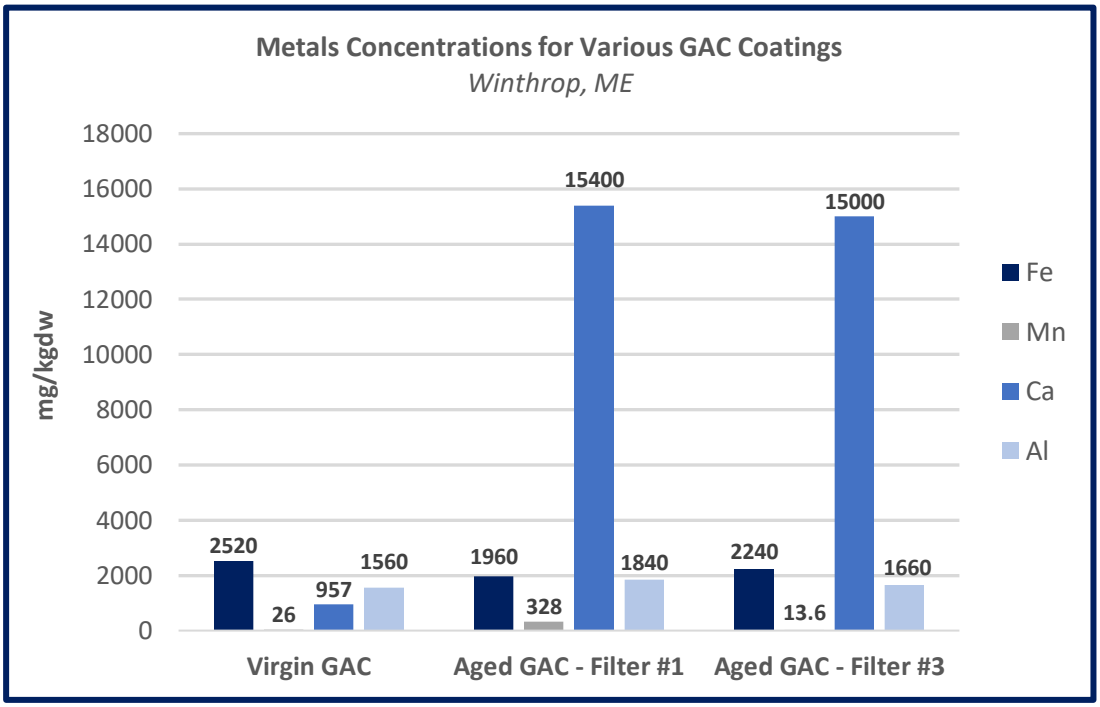

Figure 4-12. Metals concentrations for various GAC coatings from Winthrop, (ME).

4.4 Calcium Loading and Microbial Composition Relationship

Calcium loading on the GAC sublayer was discovered and verified throughout the duration of this study. To further explore microbial composition and its potential effects on the bioregeneration of GAC adsorption sites, a cluster analysis was conducted using data obtained

from the metal and DNA extractions. Principal component analyses were conducted in JMP in order to cluster data based on bacterial species, metals concentration, and media type. Table 4-15 provides the results of the cluster analysis with the four metals of focus and the relative frequencies corresponding to the bacterial population discovered in August of 2021. While there are 54 species of bacteria present amongst the three layers sampled in Filter #1, the cluster analysis verified species correlated to the metals concentrations for Iron, Manganese, Calcium, and Aluminum. Out of ten clusters, metals concentrations within the schmutzdecke, sand above the GAC, and GAC media types corresponded to three clusters.

Table 4-15. Cluster Analysis Results Corresponding to Media Type, Bacteria Present, and Metal Content.

Cluster	Members
1	**Iron**
1	Bacteria – PAUC34f
1	Bacteria – Caldatribacteriota
1	Bacteria – WS4
1	Bacteria – Firmicutes
1	Bacteria – Hydrogenedentes
1	Bacteria – Deferrisomatota
1	Bacteria – Acidobacteriota
1	Bacteria – Myxococcota
1	Bacteria – Proteobacteria
1	Bacteria – Armatimonadota
1	Bacteria – AncK6
2	Bacteria – Verrucomicrobiota
2	**Calcium**
2	**Aluminum**
2	Bacteria – Gemmatimonadota
2	Bacteria – Bdellovibrionota
2	Bacteria – Patescibacteria
3	Bacteria – RCP2-54
3	Bacteria – SAR324_clade(Marine_group_B)
3	Bacteria – Deinococcota
3	**Manganese**

Results of analysis conducted through MATLAB software for metals concentrations from various media types and their relation to bacterial species present within these three clusters are noted in Figure 4-13. Cluster two contains both calcium and aluminum metals concentrations along with the bacterial species: *Verrucomicrobiota, Gemmatimonadota, Bdellovibrionota, and Patescibacteria.* The four bacterial species present are gram negative, indicating the opportunity to greater adhere to the positively charged ion, calcium, that has been accumulated on the GAC sublayer. While this hypothesis has been produced based on metals accumulations discovered within the GAC sublayer, further analyses should be conducted to determine the effect, if any, of these four species on calcium accumulation.

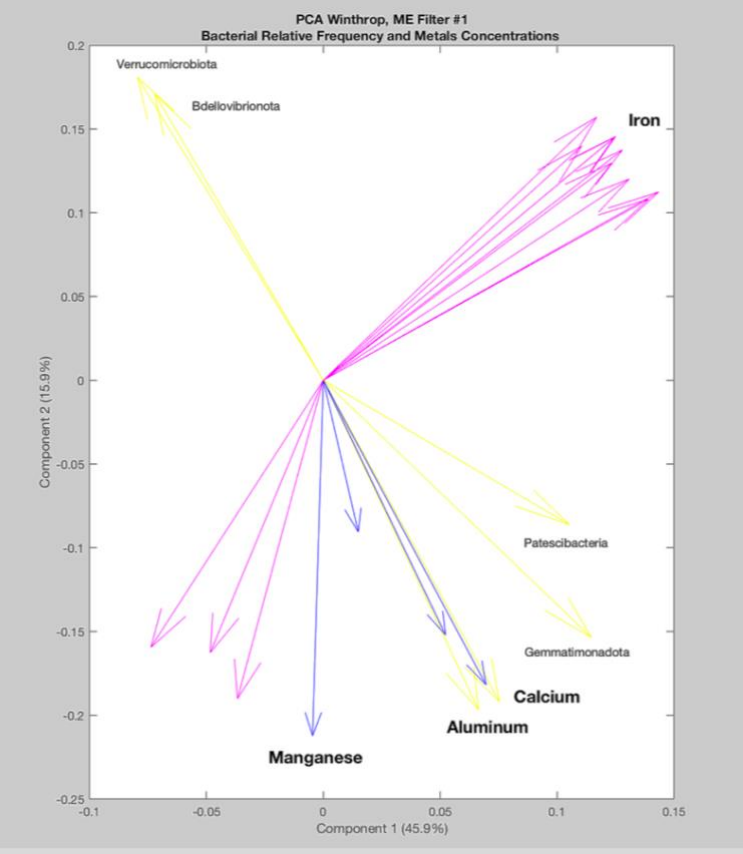

Figure 4-13. Principle component microbial composition analyses results corresponding to various metals concentrations.

4.5 Modeling DOC Removal Mechanisms in a SSF Sublayer of GAC

To further assess calcium loading on the GAC sublayer and its effect on SSF overall performance, relationships between calcium deposition and non-BDOC removals were investigated.

Calcium deposition efficiency was calculated in order to get an estimate of the deposition rates and calcium loading onto the GAC sublayer. The total calcium deposited on the GAC sublayer in Winthrop's SSF #1 was calculated as shown in equations [1] and [2].

Total Ca Deposited on GAC Sublayer, kg =

(SSF surface area x GAC depth) x (1- porosity) x (GAC density) x (Ca extractable from GAC) [1]

Total Ca Deposited on GAC Sublayer, kg =

$$(3000\ ft^2 \times 0.5\ ft) \times (1\text{-}0.4) \times \left(0.0153\ kg\ \frac{GAC}{ft^3}\right) \times \left(15.4\ \frac{kg\ Ca}{kg\ GAC}\right) = \mathbf{212\ kg} \quad [2]$$

The total Ca loading to the SSF was calculated as shown in equation [3] and [4].

Total Ca^{2+} Loaded to SSF Over 16 Year Service =

(Typical Ca^{2+} Concentration in Source Water) x (Filtration Rate) x (Total Time in SSF Service) [3]

Total Ca^{2+} Applied to SSF, kg =

$$\left(20\ \frac{mg}{L}\ \text{as}\ Ca^{2+} \times \frac{kg}{10^6\ mg}\right) \times \left(50\ \frac{gal}{min} \times 3.785\ \frac{L}{gal}\right) \times \left(1440\ \frac{min}{day} \times 365\ \frac{day}{year} \times 16\ \text{years}\right) = \mathbf{35 \times 10^3\ kg} \quad [4]$$

Thus, an estimated Ca deposition efficiency on the GAC sublayer was determined from equations [5] and [6].

$$\text{Ca Deposition Efficiency on GAC} = \left(\frac{Ca^{2+}\ Deposited}{Ca^{2+}\ Applied} \text{x}100 \right) \quad [5]$$

$$\text{Ca Deposition Efficiency on GAC} = \left(\frac{212\ kg}{35{,}000\ kg} \text{ x } 100 \right) = \mathbf{0.61\ \%} \quad [6]$$

The subsequent Ca dosage to the SSF GAC sublayer is estimated in Equation [7].

$$\left(\text{Ca Dosage, } \frac{meq}{L}\right) = \left(22\ \frac{mg}{L} \text{ as } Ca^{2+}\right) \text{ x } (0.61\%) \text{ x } \left(\frac{1\ meq}{20\ mg\ Ca^{2+}}\right) = \mathbf{0.0061}\ \boldsymbol{\frac{meq}{L}} \quad [7]$$

An assumption is made that the effective Ca dosing of the GAC will neutralize to an equivalent amount of negatively charged DOC due to minimal levels of SO_4^{2-} and HCO^-/CO_3^{2-} ($< 5\ \frac{mg}{L}$). The literature has depicted an equivalent (-) charge for NOM as 5-15 $\frac{ueq}{mg}$ DOC. A typical source water DOC in Winthrop (ME) is around 5 $\frac{mg}{L}$ with a SUVA close to 2.5 $\frac{L}{mg \bullet m}$. The negative charge associated with Winthrop's source water DOC, especially after schmutzdecke biodegradation process is estimated as 10 $\frac{ueq}{mg}$ DOC (assuming 10% removed by over burden sand):

$$= \left(10\ \frac{ueq}{mg}\right) \text{ x } \left(4.0\ \frac{mg}{L} \text{ DOC}\right) \text{ x } \left(\frac{1\ meq}{1000\ ueq}\right) = 0.040\ \frac{meq}{L} \quad [8]$$

Thusly, the amount of negatively-charged DOC that can be neutralized by the positively-charged calcium can be calculated as shown in Equation [9].

$$\text{Amount of DOC Neutralized by Ca} = \left(\frac{Equivalent\ (+)\ Ca\ Charge}{Equivalent\ (-)\ DOC\ Charge}\right) \text{ x } 100$$

Amount of DOC Neutralized by Ca = ($\frac{0.0061 \frac{meq}{L}(+)}{0.040 \frac{meq}{L}(-)}$) x 100 = 15 % x 4.0 $\frac{mg}{L}$ = **0.61** $\boldsymbol{\frac{mg}{L}}$ [9]

This 0.61 $\frac{mg}{L}$ estimated non-biodegradable removal of DOC by the GAC compares favorably with the measured DOC removal by the GAC sublayer of 0.53 $\frac{mg}{L}$ measured on 2-23-2022.

Biodegradation removals of DOC by biological filters has been modeled by Summers (1984) as shown in Equation [10].

$$\ln \frac{C_e}{C_o} = -kX\theta \quad [10]$$

where C_o = Influent DOC, $\frac{mg}{L}$

C_e = Filter Effluent DOC, $\frac{mg}{L}$

k = Biodegradation rate constant, $\frac{gdw}{ng\ ATP \bullet min}$

X = Biomass, $\frac{ng\ ATP}{gdw}$

Θ = EBCT, min

Biomass values were obtained from the 9-27-2021 sampling event due to sand media collected at various depths, along with a GAC media collection. For both the upper and lower layers of sand, ATP biomass resulted in a total weighted average of 244.5 ng ATP/gdw. Using the biofilter model, raw water DOC value of 4.69 mg/L (C_o) and the effluent sand DOC value of 3.95 mg/L (C_e), biomass concentration (x) of 244.5 ng ATP/gdw, and an EBCT (θ) of 600 minutes, resulted in the rate constant of 1.17 x 10^{-6} $\frac{gdw}{ng \bullet min}$.

The resulting rate constant (k) was applied to the GAC sublayer biofiltration model to determine a predicted effluent DOC concentration (C_e) using a (C_o) of 3.95 $\frac{mg}{L}$, a biomass concentration (x) of 57.2 $\frac{ng\ ATP}{gdw}$, and an EBCT (θ) of 224 minutes. The biofilter model predicts a (C_e) of 3.89 $\frac{mg}{L}$ signifying that biodegradation will account for removing < 2% or 0.06 $\frac{mg}{L}$ of the sand filtered DOC content. This 0.06 $\frac{mg}{L}$ predicted DOC removal by biodegradation closely matches the 0.10 $\frac{mg}{L}$ BDOC removal achieved by the GAC as reflected in Table 4-3.

DOC removals in the GAC sublayer of an amended SSF could be achieved by enhanced biodegradation in the GAC and DOC charge neutralization by Ca deposition and subsequent accumulation on the GAC. It was determined that charge neutralization mechanism was significantly (5x) more influential than enhanced biodegradation as depicted in Table 4-16 The reduction of the DOC functional-group charges by this charge neutralization mechanism appears to (i) enhance the hydrophobic adsorption tendencies of the NOM, and (ii) enhance electrostatic bridging of the divalent ion and competing negatively charged surfaces (Collins, 1985).

Table 4-16. Measured versus Predicted GAC Induced DOC Removals ($\frac{mg}{L}$).

Δ GAC Removal		**Enhanced Biodegradation**		**Charge Neutralization**	
Measured	Predicted	Measured	Predicted	Measured	Predicted
0.63	**0.67**	0.10	0.06	0.53	0.61

In most cases, GAC induced DOC removals are showing a correlation between measured and predicted values. It is possible there other chemical components present that may account for the slight differences being shown. Within slow sand filters, alkalinity, sulfate, chlorides, and other

competing anions could be contributing to the complexation of selected metal ions, reducing metals ability to attract natural organic matter, and of particular focus, calcium. Further analyses are required to expand comparisons between biodegradation removals associated with calcium and other metal deposition influences on DOC attachments.

5. CONCLUSIONS

The purpose of this research was to evaluate biologically and chemically active components within filter sublayers that may contribute to the GAC bioregenerative treatment process within a SSF amended with a GAC sublayer. Extensive biological and chemical analyses were performed to assess and analyze seasonal variation on BDOC and non-BDOC removals, biomass production between winter and summer conditions, and microbial community composition within the SSF sublayers. A major objective of this study was to gain a greater understanding of DOC removal mechanisms contributing to the maintenance of long-term GAC adsorption sites. Significant conclusions from each area of focus are summarized below.

5.1 Assessment of Seasonal Variations on BDOC and Non-BDOC Removals

- Removals associated with the biodegradable organic carbon fraction and the non-biodegradable organic carbon fraction remain significant for over 15 years of filter run-time and tens of thousands of GAC bed volumes.
- Performance of individual layers within the slow sand filtration process have various effects on BDOC and non-BDOC removals.
- The non-BDOC fraction removal is significant within the GAC sublayer and assists in highlighting the extended adsorption capacity of GAC.

5.2 Biomass Influence by Media Type

- ATP biomass production within slow sand filter layers responded promptly to changes in temperature.

- The schmutzdecke layer showed consistent patterns with seasonal variations, producing greater amounts of ATP biomass in warmer temperatures and smaller amounts of ATP biomass in colder temperatures.
- Biomass analyses and microbial community composition are sensitive to media location and seasonal changes.
- Metals concentrations for sand coatings remained consistent between Winthrop slow sand filters and local comparisons.
- Calcium accumulation on GAC has been verified.
- Cation calcium accumulation in GAC may also be correlated with higher removals of organic carbon.
- Calcium accumulation becomes problematic for regeneration processes associated with granular activated carbon.

5.3 Inorganic Deposition Influence by Media Type

- Microbial community composition did not vary significantly between summer and winter conditions.
- Cluster analyses indicated the influence of calcium and aluminum metals concentrations with the bacterial species *Verrucomicrobiota, Gemmatimonadota, Bdellovibrionota, and Patescibacteria.* Further studies should be conducted focused on these species.
- Species present with calcium accumulation are gram negative, indicating the opportunity to greater adhere to the positively charged ion, calcium, that has been accumulated on the GAC sublayer.

5.4 Assessing DOC Removal Mechanisms in the GAC Sublayer of a Slow Sand Filter

- DOC removals in the GAC sublayer of an amended SSF could be achieved by enhanced biodegradation in the GAC and DOC charge neutralization by Ca deposition and subsequent accumulation on the GAC.
- Charge neutralization mechanisms were significantly (5x) more influential than enhanced biodegradation.
- It is hypothesized that calcium induced charge neutralization could enhance DOC removals by (i) increasing the hydrophobic adsorption tendencies of the NOM carbon skeleton, and (ii) enhance electrostatic bridging of the divalent ion and competing negatively charged surfaces
- Further analyses are required to expand comparisons between biodegradation removals and calcium and other metal deposition influences on DOC attachments.

6. FUTURE RESEARCH RECOMMENDATIONS

The results of extensive biological and chemical analyses were used to analyze seasonal variation on BDOC and non-BDOC removals, biomass production between winter and summer conditions, and microbial community composition within filter sublayers. Additional research is required to further understand enhanced removals on the GAC sublayer, the mechanisms contributing to the bioregenerative treatment process, and the mechanisms contributing to the renewal of adsorption sites on the GAC sublayer. Based on the results of this study, the following are recommendations for continued research:

6.1 Increase Sampling Events

- Add additional sampling events which occur at greater frequency and consistency
- Sample every 2-3 months to fully capture seasonal patterns
- Remain consistent with sample collection by layer, filter effluents, and aqueous sample extraction above the GAC.

6.2 Explore Schmutzdecke Sampling Methods

- Schmutzdecke samples were obtained via a scraping method during this study, whereas previous studies have incorporated a coring method to analyze schmutzdecke media. Further exploration of sampling methods for the schmutzdecke and adjacent filter layers could assist in determining a more consistent method for filter sampling and the analysis of factors effecting slow sand filter performance

6.3 Explore Various GAC Ages

- Continue to collect aqueous and media samples from slow sand filters that contain GAC media of various ages.
- Performing extensive aqueous and media analyses on GAC media of various ages could assist in explaining the renewal of adsorption sites on GAC.

6.4 DOC Removal Mechanisms

- Continue to explore and model DOC removal mechanisms within slow sand filters amended with GAC.
- Determine the influence of alkalinity and sulfates to the competition of charge neutralization with the presence of calcium in various GAC ages.

List of References

Adeniran, A. E., and Akanmu, J. O. The Efficiency of Slow Sand Filters in the Treatment of Secondary Effluent from a Water Hyacinth Domestic Sewage Plan. *NSE Technical Transactions*, **2013**, 47(2).

Aktaş, Ö.; Çeçen, F. Bioregeneration of Activated Carbon: A Review. *International Biodeterioration & Biodegradation* **2007**, *59* (4), 257–272. https://doi.org/10.1016/j.ibiod.2007.01.003.

American Water Works Association. An Assessment of Microbial Activity on GAC. *Journal AWWA*, **1981**, 73(8), 447-454.

Arora, H. Optimising the Ripening Period of Slow Sand Filters. MS Thesis, Delft University of Technology, **2017**.

Artioli, Y. Adsorption. In *Encyclopedia of Ecology*; Jørgensen, S. E., Fath, B. D., Eds.; Academic Press: Oxford, **2008**; pp 60–65. https://doi.org/10.1016/B978-008045405-4.00252-4.

Balen, D. Enhancing *E.Coli* Removal from Slow-Rate Biofilters Treating Low-Carbon Source Waters. MS Thesis, University of New Hampshire, **2018**.

Baker. M.N. The Quest for Pure Water. *American Water Works Association*. **1949**.

Bauer, M.; Rachwal, A.; Buchanan, B.; Colbourne, J.; Foster, D.; Goodman, N.; Kay, A.; Sanders, T. The GAC/Slow Sand Filter Sandwich : From Concept to Commissioning. **1995**.

Baveye, P.; Vandevivere, P.; Hoyle, B. L.; DeLeo, P. C.; de Lozada, D. S. Environmental Impact and Mechanisms of the Biological Clogging of Saturated Soils and Aquifer Materials. *Critical Reviews in Environmental Science and Technology* **1998**, *28* (2), 123–191. https://doi.org/10.1080/10643389891254197.

Bellamy, W. D.; Hendricks, D. W.; Logsdon, G. S. Slow Sand Filtration: Influences of Selected Process Variables. *Journal AWWA* **1985a**, *77* (12), 62–66. https://doi.org/10.1002/j.1551-8833.1985.tb05659.x.

Campos, L. C.; Su, M. F. J.; Graham, N. J. D.; Smith, S. R. Biomass Development in Slow Sand Filters. *Water Research* **2002**, *36* (18), 4543–4551. https://doi.org/10.1016/S0043-1354(02)00167-7.

Cannon, F. S.; Snoeyink, V. L.; Lee, R. G.; Dagois, G.; DeWolfe, J. R. Effect of Calcium in Field-Spent GACs on Pore Development During Regeneration. *Journal - American*

Water Works Association **1993**, *85* (3), 76–89. https://doi.org/10.1002/j.1551-8833.1993.tb05959.x.

Carlson, M. A.; Heffernan, K. M.; Ziesemer, C. C.; Snyder, E. G. Comparing Two GACs for Adsorption and Biostabilization. *Journal AWWA* **1994**, *86* (3), 91–102. https://doi.org/10.1002/j.1551-8833.1994.tb06171.x.

Collins, M. R. Modifications to the Slow Sand Filtration Process for Improved Removals of Trihalomethane Precursors. *AWWARF*, **1989**.

Collins, M.R. Civil & Environmental Engineering Department, University of New Hampshire, Durham, NH. Personal Communication, **May 2022**.

Collins, M. R.; Eighmy, T. T.; Fenstermacher Jr., J. M.; Spanos, S. K. Removing Natural Organic Matter by Conventional Slow Sand Filtration. *Journal AWWA* **1993**, *84* (5), 80–90. https://doi.org/10.1002/j.1551-8833.1992.tb07357.x.

Collins, M. R.; Eighmy, T. T.; Jr., J. M. F.; Spanos, S. K. Using Granular Media Amendments to Enhance NOM Removal. *Journal - American Water Works Association* **1996**, *88*, 48–61. https://doi.org/10.1002/j.1551-8833.1996.tb06661.x.

Collins, M. R.; Eighmy, T. T.; Malley, J. P. Evaluating Modifications to Slow Sand Filters. *Journal - American Water Works Association* **1991**, *83* (9), 62–70. https://doi.org/10.1002/j.1551-8833.1991.tb07215.x.

Collins, M. R.; Vaughan, C. W. Characterization of NOM Removal by Biofiltration: Impact of Coagulation, Ozonation, and Sand Media Coating. In *Disinfection By-Products in Water Treatment*; CRC Press, **1996**.

Cullen, T. R.; Letterman, R. D. The Effect of Slow Sand Filter Maintenance on Water Quality. *Journal (American Water Works Association)* **1985**, *77* (12), 48–55.

Dullemont, Y. J.; Schijven, J.; Hijnen, W.; Colin, M.; Knezev, A.; Oorthuizen, W. Removal of Microorganisms by Slow Sand Filtration. *Recent Progress in Slow Sand and Alternative Biofiltration Processes* **2006**, 12–20.

Duncan, A. The Ecology of Slow Sand Filters. *Graham NJD (ed) Slow Sand Filtration: Recent Developments in Water Treatment Technology*. Ellis Horwood Ltd, Chichester, **1988**, 163– 180.

Eberhardt, M. Experience with the use of biologically effective activated carbon. *H. Sontheimer, (Ed.) Translation of Reports on Special Problems of Water Technology, Volume 9—Adsorption.* **1976**, 331-347.

Ellis, K. V.; White, G.; Warn, A. E. Surface Water Pollution and Its Control; *Macmillan International Higher Education*, **1989**.

Filtrasorb® 400 Granular Activated Carbon Data Sheet. *CalgonCarbon A Kuraray Company.* **2019.**

Frederick, H.T. Calcium Loading onto Granular Activated Carbon: The Influence of Organic Compounds. PhD Dissertation, The Pennsylvania State University, **1999**.

Glaze, W. H.; Wallace, J. L. Control of Trihalomethane Precursors in Drinking Water: Granular Activated Carbon With and Without Preozonation. *Journal AWWA* **1984**, *76* (2), 68–75. https://doi.org/10.1002/j.1551-8833.1984.tb05284.x.

Haig, S.-J.; Collins, G.; Davies, R.; Dorea, C.; Quince, C. Biological Aspects of Slow Sand Filtration: Past, Present and Future. *Water Science & Technology* **2011**, *11*. https://doi.org/10.2166/ws.2011.076.

Hendricks, D. W. *Manual of Design for Slow Sand Filtration*; The Foundation, **1991**.

Hirschi, S.D., and Sims, R.C. Particles and Microorganisms in Slow Rate Sand Filtration. *International Sand Filtration Workshop (USA)*, **1991**, 27-30.

Huisman, L. and Wood, W.E.. Slow Sand filtration. Geneva, *World Health Organization*. **1974**.

Ives, K. J. Rapid Filtration. *Water Research* **1970**, *4* (3), 201–223. https://doi.org/10.1016/0043-1354(70)90068-0.

Kapteijn, F.; Porre, H.; Moulijn, J. A. CO2 Gasification of Activated Carbon Catalyzed by Earth Alkaline Elements. *AIChE Journal* **1986**, *32*, 691–695. https://doi.org/10.1002/aic.690320421.

Karanfil, T.; Kilduff, J. E. Role of Granular Activated Carbon Surface Chemistry on the Adsorption of Organic Compounds. 1. Priority Pollutants. *Environ. Sci. Technol.* **1999**, *33* (18), 3217–3224. https://doi.org/10.1021/es981016g.

Kim, D.-J.; Miyahara, T.; Noike, T. Effect of C/N Ratio on the Bioregeneration of Biological Activated Carbon. *Water Science and Technology* **1997**, *36* (12), 239–249. https://doi.org/10.1016/S0273-1223(97)00720-8.

Klimenko, N.; Winther-Nielsen, M.; Smolin, S.; Nevynna, L.; Sydorenko, J. Role of the Physico-Chemical Factors in the Purification Process of Water from Surface-Active Matter by Biosorption. *Water Research* **2002**, *36* (20), 5132–5140. https://doi.org/10.1016/S0043-1354(02)00278-6.

Knappe, D. R. U.; Dagois, G.; DeWolfe, J. R. Effect of Calcium on Thermal Regeneration of GAC. *Journal - American Water Works Association* **1992**, *84* (8), 73–80. https://doi.org/10.1002/j.1551-8833.1992.tb07414.x.

Kutics, K.; Suzuki, M. Attachment and Growth of Biomass on Surface-Modified Activated Carbon Fibers. **1992**. https://doi.org/10.2166/WST.1992.0447.

Langlais, B.; Reckhow, D.; Brink, D. Ozone in Water Treatment. **1991**.

LeCraw, R.L. Personal Communication from Partinoudi et al., 2003. RAL Engineering, Newmarket, ON (CA), **2003**.

Li, J.; Zhou, Q.; Campos, L. C. The Application of GAC Sandwich Slow Sand Filtration to Remove Pharmaceutical and Personal Care Products. *Science of The Total Environment* **2018**, *635*, 1182–1190. https://doi.org/10.1016/j.scitotenv.2018.04.198.

Logsdon, G. S. Microbiology and Drinking Water Filtration. In *Drinking Water Microbiology: Progress and Recent Developments*; McFeters, G. A., Ed.; Brock/Springer Series in Contemporary Bioscience; Springer: New York, NY, **1990**; pp 120–146. https://doi.org/10.1007/978-1-4612-4464-6_6.

Logsdon, G.; Kohne, R.; Abel, S.; LaBonde, S. Slow Sand Filtration for Small Water Systems. *Journal of Environmental Engineering and Science - J ENVIRON ENG SCI* **2002**, *1*, 339–348. https://doi.org/10.1139/s02-025.

Lu, Z.; Sun, W.; Li, C.; Cao, W.; Jing, Z.; Li, S.; Ao, X.; Chen, C.; Liu, S. Effect of Granular Activated Carbon Pore-Size Distribution on Biological Activated Carbon Filter Performance. *Water Research* **2020**, *177*, 115768. https://doi.org/10.1016/j.watres.2020.115768.

Lubarsky, H.; Fava, N. de M. N.; Souza Freitas, B. L.; Terin, U. C.; Oliveira, M.; Lamon, A. W.; Pichel, N.; Byrne, J. A.; Sabogal-Paz, L. P.; Fernandez-Ibañez, P. Biological Layer in Household Slow Sand Filters: Characterization and Evaluation of the Impact on Systems Efficiency. *Water* **2022**, *14* (7), 1078. https://doi.org/10.3390/w14071078.

Manz, D.H. New Horizons for Slow Sand Filtration. *Eleventh Canadian National Conference and Second Policy Forum on Drinking Water*, **2004**, 682-692.

Maloney, S. W.; Bancroft, K.; Pipes, W. O.; Suffet, I. H. Bacterial TOC Removal on Sand and GAC. *Journal of Environmental Engineering* **1984**, *110* (3), 519–533. https://doi.org/10.1061/(ASCE)0733-9372(1984)110:3(519).

Marquis, R. E.; Mayzel, K.; Carstensen, E. L. Cation Exchange in Cell Walls of Gram-Positive Bacteria. *Can J Microbiol* **1976**, *22* (7), 975–982. https://doi.org/10.1139/m76-142.

Moona, N.; Wünsch, U. J.; Bondelind, M.; Bergstedt, O.; Sapmaz, T.; Pettersson, T. J. R.; Murphy, K. R. Temperature-Dependent Mechanisms of DOM Removal by Biological Activated Carbon Filters. *Environ. Sci.: Water Res. Technol.* **2019**, *5* (12), 2232–2241. https://doi.org/10.1039/C9EW00620F.

Muhammad, N. Removal of Heavy Metals by Slow Sand Filtration. PhD Dissertation, Loughborough University, **1998**.

Muhammad, N.; Parr, J.; Smith, M. D.; Wheatley, A. D. Microbial Uptake of Heavy Metals in Slow Sand Filters. *Environmental Technology* **1998**, *19* (6), 633–638. https://doi.org/10.1080/09593331908616720.

Nakamoto, N.; Graham, N.; Gimbel, R.; Collins, M. R. *Progress in Slow Sand and Alternative Biofiltration Processes: Chapter 1* ; IWA Publishing, 2014.

Nasser, A. M.; Oman, S. D. Quantitative Assessment of the Inactivation of Pathogenic and Indicator Viruses in Natural Water Sources. *Water Research* **1999**, *33* (7), 1748–1752. https://doi.org/10.1016/S0043-1354(98)00380-7.

Nowotny, N.; Epp, B.; von Sonntag, C.; Fahlenkamp, H. Quantification and Modeling of the Elimination Behavior of Ecologically Problematic Wastewater Micropollutants by Adsorption on Powdered and Granulated Activated Carbon. *Environ. Sci. Technol.* **2007**, *41* (6), 2050–2055. https://doi.org/10.1021/es0618595.

Page T.G. GAC Sandwich Modification to Slow Sand Filtration for Enhanced Removal of Natural Organic Matter. MS Thesis, University of New Hampshire, **1997**.

Palmateer, G. Toxicant and Parasite Challenge of Manz Intermittent Slow Sand Filter. *Environmental Toxicology*, **1998**, 14(2), 217-225.

Parada, A. E., Needham, D. M., & Fuhrman, J. A. Every base matters: assessing small subunit rRNA primers for marine microbiomes with mock communities, time series and global field samples. *Environmental Microbiology* **2016**, 18(5), 1403–1414. http://doi.org/10.1111/1462-2920.13023

Partinoudi, V.; Collins, M. R.; Martin-Doole, M.; Dwyer, P. Temperature Influences on Slow Sand Filtration Treatment Performance. *New England Water Treatment Technology Center*. **2006.**

Patil, A.; Hatch, G.; Michaud, C.; Brotman, M.; Regunathan, P.; Tallon, R.; Andrew, R.; Murphy, S.; Ver Strat, S.; Kim, M., Kappel, B.; Battenberg. Granular Activated Carbon (GAC) Fact Sheet. *Water Quality Association* **2013**.

Peel, R. G. The Roles of Slow Adsorption Kinetics and Bioactivity in Modelling of Activated Carbon Adsorbers. PhD Dissertation, McMaster University, **1979**.

Peel, R. G.; Benedek, A. Biodegradation and Adsorption within Activated Carbon Adsorbers. *Journal (Water Pollution Control Federation)* **1983**, *55* (9), 1168–1173.

Peel, R. G.; Benedek, A. Dual Rate Kinetic Model of Fixed Bed Adsorber. *Journal of Environmental Engineering* **1980**, 106(8), 797-813.

Perrotti, A. E. and Rodman, C. A. Factors Involved with Biological Regeneration of Activated Carbon. *American Institute of Chemical Engineering Symposium Series* – Water **1974**, 70, 316-325.

Poynter, S.F.B. and Slade, J.S. The Removal of Viruses by Slow Sand Filtration. *Prog. Water Technol.* **1977**, 9(1): 75-88.

Pradhan, A. A.; Levine, A. D. Experimental Evaluation of Microbial Metal Uptake by Individual Components of a Microbial Biosorption System. *Water Science and Technology* **1992**, *26* (9–11), 2145–2148. https://doi.org/10.2166/wst.1992.0682.

Quince, C., Lanzen, A., Davenport, R.J., & Turnbaugh, P.J. Removing noise from pyrosequenced amplicons. *BMC Bioinformatics* **2011**, 12: 38. https://doi.org/10.1186/1471-2105-12-38

Ranjan, P.; Prem, M. Schmutzdecke- A Filtration Layer of Slow Sand Filter. *Int.J.Curr.Microbiol.App.Sci* **2018**, *7* (07), 637–645. https://doi.org/10.20546/ijcmas.2018.707.077.

San Miguel, G.; Lambert, S. D.; Graham, N. J. D. The Regeneration of Field-Spent Granular-Activated Carbons. *Water Research* **2001**, *35* (11), 2740–2748. https://doi.org/10.1016/S0043-1354(00)00549-2.

Schuster, C. J.; Aramini, J. J.; Ellis, A. G.; Marshall, B. J.; Robertson, W. J.; Medeiros, D. T.; Charron, D. F. Infectious Disease Outbreaks Related to Drinking Water in Canada, 1974–2001. *Can J Public Health* **2005**, *96* (4), 254–258. https://doi.org/10.1007/BF03405157.

Seger, A. and Rothman, M. Slow Sand Filtration With and Without Ozonation in Nordic Climate. *Advances in Slow Sand and Alternative Biological Filtration* **1996**. Edited by N. Graham and R. Collins. John Wiley & Sons, Chichester, England.

Singer, P. C. Ozonation Research in Drinking Water. *AWWARF*, Denver , CO. **1988**.

Sirotkin, A. S.; Koshkina, L. Yu.; Ippolitov, K. G. The BAC-Process for Treatment of Waste Water Containing Non-Ionogenic Synthetic Surfactants. *Water Research* **2001**, *35* (13), 3265–3271. https://doi.org/10.1016/S0043-1354(01)00029-X.

Slow Sand Filtration Tech Brief 14. *A National Drinking Water Treatment Clearinghouse Fact Sheet.* **2000**, 1–4.

Sontheimer, H.; Crittenden, J. C.; Summers, R. S. *Activated Carbon for Water Treatment*; DVGW-Forschungsstelle, Engler-Bunte-Institut, Universitat Karlsruhe (TH): Karlsruhe, Germany, **1988**.

Stewart, M. H.; Wolfe, R. L.; Means, E. G. Assessment of the Bacteriological Activity Associated with Granular Activated Carbon Treatment of Drinking Water. *Applied Environmental Microbiol*ogy **1990**, *56* (12), 3822–3829. https://doi.org/10.1128/aem.56.12.3822-3829.1990.

Sublette, K. L.; Snider, E. H.; Sylvester, N. D. A Review of the Mechanism of Powdered Activated Carbon Enhancement of Activated Sludge Treatment. *Water Research* **1982**, *16* (7), 1075–1082. https://doi.org/10.1016/0043-1354(82)90122-1.

Summers, R.; Roberts, P. Simulation of DOC Removal in Activated Carbon Beds. **1984**. https://doi.org/10.1061/(ASCE)0733-9372(1984)110:1(73).

Sutherland, K. Filtration Overview: A Closer Look at Depth Filtration. *Filtration & Separation* **2008**, *45* (8), 25–28. https://doi.org/10.1016/S0015-1882(08)70296-9.

Tien, C.; Bai, R. An Assessment of the Conventional Cake Filtration Theory. *Chemical Engineering Science* **2003**, *58* (7), 1323–1336. https://doi.org/10.1016/S0009-2509(02)00655-3.

Toms, I.P. & Bayley, R.G. Slow Sand Filtration: Approach to Practical Issues *Slow Sand Filtration: Recent Developments in Water Treatment Technology, N.J.D. Graham (Ed.) Ellis Horwood Ltd., UK, 11-28.* **(1988)**

Unger, M. The Role of the Schmutzdecke in Escherichia coli Removal in Slow Sand and Riverbank Filtration. MS Thesis, University of New Hampshire, **2006**.

Unger, M.; Collins, M. R. Assessing *Escherichia Coli* Removal in the Schmutzdecke of Slow-Rate Biofilters. *Journal - American Water Works Association* **2008**, *100* (12), 60–73. https://doi.org/10.1002/j.1551-8833.2008.tb09799.x.

US EPA, O. Overview of Drinking Water Treatment Technologies https://www.epa.gov/sdwa/overview-drinking-water-treatment-technologies (accessed 2022 -05 -06).

Visscher, J. T. Slow Sand Filtration: Design, Operation, and Maintenance. *Journal AWWA* **1990**, *82* (6), 67–71. https://doi.org/10.1002/j.1551-8833.1990.tb06979.x.

Waer, M. A.; Snoeyink, V. L.; Mallon, K. L. Carbon Regeneration: Dependence on Time and Temperature. *Journal AWWA* **1992**, *84* (3), 82–91. https://doi.org/10.1002/j.1551-8833.1992.tb07324.x.

Wang, J. Z.; Summers, R. S.; Miltner, R. J. Biofiltration Performance: Part 1, Relationship to Biomass. *Journal AWWA* **1995**, *87* (12), 55–63. https://doi.org/10.1002/j.1551-8833.1995.tb06465.x.

Welté, B.; Montiel, A. The Influence of Temperature on the Removal of Biodegradable Organic Carbon. *rseau* **2005**, *9* (2), 163–187. https://doi.org/10.7202/705247ar.

Wholesale Activated Carbon Granular, Pellets & Powdered , Buy Activated Charcoal Bulk Online | Yongruida Activated Carbon https://www.yrdcarbon.com/products/activated-carbon/ (accessed 2022 -05 -05).

Xu, L.; Campos, L. C.; Li, J.; Karu, K.; Ciric, L. Removal of Antibiotics in Sand, GAC, GAC Sandwich and Anthracite/Sand Biofiltration Systems. *Chemosphere* **2021**, *275*, 130004. https://doi.org/10.1016/j.chemosphere.2021.130004.

Appendix A. Standard Operating Procedures

Total Organic Carbon/ Dissolved Organic Carbon

Biodegradable Organic Carbon

Ultraviolet (UV_{254}) Absorbance

Adenosine Triphosphate (ATP) Biomass Extraction

Deoxyribonucleic Acid (DNA) Extraction

Polymerase Chain Reaction (PCR) Amplfiication

Agarose Gel Set-Up

Metals Quantification by ICP-AES

Standard Operating Procedures

TOTAL ORGANIC CARBON

Principle

Organic carbon is oxidized to carbon dioxide by persulfate in the presence of ultraviolet light. The carbon dioxide produced is measured directly by a non-dispersive infrared analyzer.

Sample Collection and Storage

Collect samples in 40-mL amber TOC vials that have been washed with chromic acid and combusted at 550 degrees Celsius for 90 minutes to remove all organic matter.

Preserve with concentrated H_3PO_4 to pH < 2.

Refrigerate.

Holding time: < 2 weeks with acid preservation.

Equipment

a. Sievers Model 5310c Lab TOC Analyzer
b. Aluminum foil
c. Vials, 40 mL amber glass TOC vials

Reagents

a. Potassium persulfate solution, 15%. Shelf life: approximately 90 days.
b. Potassium acid phthalate (KHP), $KHC_8H_4O_8$ for standards

Method

Prepare KHP standards:

1. Prepare 1000 mg/L stock: dissolve 2.1254 g $KHC_8H_4O_8$ (dried to constant weight at 103 degrees Celsius) in RO lab water and dilute to 1000 mL.
2. Make standards according to the table below.

Table 1. Volumes of standard stock and RO lab water diluent to make TOC standards.

Standard Concentration, mg/L	Volume of 1000 mg/L Stock	Dilute to:
0.5	1 mL	2 L
1.0	1 mL	1 L
2.0	2 mL	1 L
5.0	5 mL	1 L
10.0	5 mL	500 mL

a. Start TOC analyzer, autosampler, computer, and printer.
b. Open TOC analyzer software program.
c. Fill TOC vials with standards: 1 for each point on the calibration curve and 1 standard of random concentration for every 8 samples.
d. Cover each vial with a small piece of aluminum foil in place of the cap. Be careful not to leave fingerprints on the foil over the vial opening. Fingerprints will be detected by the analyzer as the probe punctures the foil.
e. Arrange samples and standards. A typical run has the following sequence:

Table 2. Run order for TOC samples and standards.

Position	Sample or Standard
1-2	RO blank
3-7	Standards: one of each, randomized
8-15	Samples and/or sample duplicates, randomized
16	Randomly selected standard readback
{repeat 8 samples and 1 standard until all samples and duplicate have been analyzed}	
{last 3 spots}	RO blanks

f. Mount the samples and standards in the autosampler and enter their labels into the computer software.
g. Enter the oxidation and acid rates for each sample and standard:

Table 3. Acid and oxidation rate settings for standard or sample concentrations.

Concentration	Acid Rate	Oxidation Rate
RO blank	0.5	0.5
0.5 mg/L standard	0.5	1.0
All others	1.0	2.0

h. Run the collection program. The analyzer will take three readings from each sample or standard and calculate an average and standard deviation.

Calculations

a. Calibration Curve: Plot the measured concentrations against the expected standard concentrations and fit a calibration curve using linear regression as shown below.
b. Calculate the sample concentration by substituting the instrument reading (average of 3 readings for each sample) into the calibration curve equation.

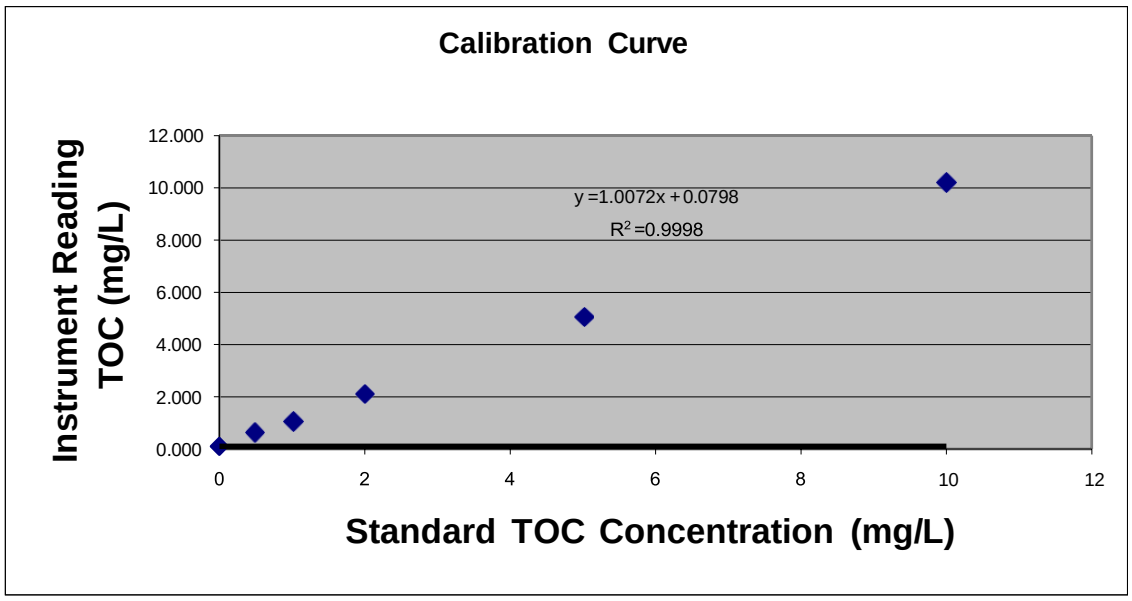

Figure 0.1. Sample TOC calibration curve (June 22, 2005).

Quality Control

Readbacks: random standard after every 8 samples. Duplicates:

analyzed at least 2 duplicate every run.

References

Mercier, David J (1998). Characterization and treatability of natural organic matter from the Croton Reservoir – Pilot Study II. M.S. Thesis. Univ. of New Hampshire.

Standard Operating Procedures
BIODEGRADABLE DISSOLVED ORGANIC CARBON (BDOC)
Summers/Shaker Batch Bioreactor Method

Principle

A water sample is applied to bioacclimated sand for 5 days in a batch reaction. The readily biodegradable portion of dissolved organic matter is expected to be consumed by microbial activity. The sample is agitated to promote mixing and aeration. Using fixed flora permits a rapid response. The difference between initial and final DOC is operationally defined as BDOC.

Apparatus

1. Reactors: 1L amber glass bottles with TFE lined caps. Wash with detergent, rinse, wash with chromic acid. Rinse 3x with DI water and 3x with Milli-Q water. Caps should not be chromic acid washed.
2. Sample vials, amber glass with TFE lined caps. Bake at 550°C for 2 hours.
3. Constant temperature room, 20 $\pm$ 1°C.
4. Glass filtration rig, or filter syringes with luer lock and 25 mm dia. Filter holders.
5. Filters, Whatman GF/F.
6. Shaker table; with modified platform to hold 1L bottles.

Reagents and materials

1. Bioacclimated sand: prepare per below.
2. Acclimation columns: 4" dia. PVC columns with stainless-steel screens, Masterflex pumps. Tubing, and carboys for reservoirs.
3. Glucose/Glutamic acid solution, 4, mg/l-C: Add 104 mg of glucose ($C_6H_{12}O_6H_2O$) and 104 mg glutamic acid ($C_5H_9NO_4$) to 200 ml Milli-Q water to make stock. Dilute 10 ml stock in 1000 ml Milli-Q or spike 10 ml into 1000 ml sample. Prepare G/GA stock immediately before use.
4. Phosphoric acid, concentrated.
5. Dechlorinated tap water: pass through GAC column or household type GAC water filter to remove chlorine and DOC. Store in carboy with spigot and keep it warm to room temperature. Verify no chlorine residual using HACH kit.

Method

Sand Acclimation

a. Prior to first use, wet-wash sand by swirling ~4 ld., vigorously in a bucket of water. After ~1 sec, of settling, decant off supernatant water. Repeat until decanted water is clear.
b. Bioacclimate sand with untreated natural water for at least 3-4 weeks in PVC columns using local water.
c. Recirculate raw water in up-flow mode at high rate to ensure penetration in sand bed.
d. Replace with fresh water at least 1x/week.
e. Preferably recirculate target water 1-3 days prior to testing.

Preparation of sand (immediately before use)

a. Remove sand from recirculating columns and place in plastic pan. Approximately 100 ml is required for each test.
b. Transfer ~200 g sand with plastic scoop into a large plastic dish or measuring cup. Wash sand with dechlorinated tap water 20x by gently swirling and decanting.
c. Optional: rinse sand 3x with Milli-Q water.
d. Sand is considered ready for use when UV absorbance of the final rinse water <0.02.
e. Homogenize acclimated sand to eliminate biomass selectively in separate reactors.

Sample application

a. Allow samples to warm to 20 $\pm$ 1°C. Samples need not be filtered prior to application.
b. Add ~150 g of wet sand to reactor.
c. Wash sand with 300 ml of sample to displace remaining water and then decant off.
d. Check the pH of the sample. If pH is outside the 6.0-9.0 range, adjust with 1N or 0.1N acid or base.
e. Add 500 ml of sample to each reactor. Approximately 400 ml of headspace will provide an oxygen source for the organisms.
f. Swirl bottle and sample for DOC.
g. Incubate at 20 degrees Celsius on a shaker table at ~150 RPM for 7 days. Keep in dark to prevent algal growth.
h. When the test is completed, return used sand to bioacclimating columns.

Sampling procedures

a. Prepare glass filtration rig or syringe filters per SOP.
b. Filter only ~25 ml if sampling at intermediate times.
c. Measure NPDOC and UV absorbance per SOPs.
d. Sample at 0 and 5 days to determine total BDOC. For kinetics studies and initial investigations of water sources, take additional samples at selected times during the run for up to 7-10 days.
e. If samples are not analyzed immediately, preserve by acidifying to pH<2, with 2 drops conc. H_3PO_4 and store at 4°C for up to 28 days.

Calculations

BDOC, mg C/L = $DOC_{INITIAL} - DOC_{FINAL}$

%BDOC = $[(DOC_{INITIAL} - DOC_{FINAL}) / DOC_{INITIAL}] * 100$

Quality Control

Method check

Sample final rinse water from sand for DOC to check for leaching. Sample for DOC both before and after placing the sample in the flask to check for contamination or dilution. Develop correlation of DOC with UV absorbance and use the more convenient UV abs measurement as a regular method check. Sample effluent from filter flashes to check filters for leaching (500 ml Milli-Q for 47 mm filters or 150 ml for 25 mm filters shown to be sufficient).

Glucose/glutamic acid control

Test Glucose/glutamic acid mixture with samples. Almost complete DOC removal should be seen if the sample in the reactor is biologically active and only carbon is limiting. Samples spiked with glucose should have the same DOC_{final} as unspiked sample aliquots.

Precision

a. Run duplicate BDOC tests. Calculate s=pooled standard deviation.
b. Collect random duplicate samples.
c. Determine minimum detectable difference in BDOC based on pooled s.

Acclimation of source water

Verify that no significant difference in results when sand is acclimated with local water vs. target water.

Notes from initial testing

Initial DOC samples immediately after adding the water to the sand may be inconclusive for checking for dilution or contamination. Tests show, depending on the state of the bugs, that DOC values can be higher or lower but nevertheless results appear consistent after 5 days of incubation.

Acclimating with target water may slightly improve kinetics but there was NSD in BDOC after 5 days.

Samples low in BDOC may reach a minimum level prior to 5 days then rise slightly.

Filter samples when collecting from bottles for analysis. Results were less consistent when sample water was prefiltered initially prior to application to the sand but not subsequently. NSD observed between samples initially prefiltered and not filtered as long as aliquots collected for analysis were filtered. Batch method is probably unsuitable for conducting conducive kinetics test because of the relatively low amount and variable state of the biomass.

References

a. Paige T.G. 1997. "GAC Sandwich Modification to Slow Sand Filtration for Enhanced Removal of Natural Organic Matter" Masters thesis, University of New Hampshire, Durham, NH.
b. Greenberg A.E., Clesceri L. S. and Eaton A. D (Editors). 1992. "Standard Methods for the Examination of Water and Wastewater" 18th edition. American Public Health Association, American Water Works Association and Water Environment Federation (publishers)

Standard Operating Procedures
ULTRAVIOLET ABSORBANCE (UV_{254})

Principle

Beers Law states that absorbance is proportional to the concentration of the analyte for a given absorption pathlength at any given wavelength. UV absorbance at 254 nm is a useful surrogate parameter for estimating the raw water concentrations of organic carbon and THM precursors (*Standard Methods* 2006).

Apparatus

Hach DR5000 spectrophotometer

a. Cuvettes, 1cm path length, 3 ml volume, matched quartz cells (Suprasil ®, Fisher Sci.)

Reagents and materials

DI Water

Collection of Samples

Collect samples in 40 mL amber TOC vials that have been washed with chromic acid and baked 90 min. in a muffle furnace at 550°C to mineralize all organic matter.

Store at 4°C.

Holding time: < 48 hours.

Method

a. Remove samples from refrigerator and allow to warm to room temp.
b. Set spectrophotometer to measure wavelength 254 nm.
c. Zero machine on RO lab water blank.
d. Rinse cuvette with RO water twice; then fill with at least 1.5 ml of sample.
e. Wipe cuvette with kimwipe to be sure it is dry and free of smudges.
f. Measure and record absorbance.
g. Analyze sample aliquots in duplicate (triplicate if discrepancy).

Quality Control

a. Blanks every 8 samples to check for drift.
b. Run duplicate samples from a random source each round of sampling.
c. For this method (not same instrument) the standard deviation of duplicate samples was ± 0.011 cm^{-1}. The standard deviation of duplicate measurements was ± 0.002 cm^{-1}. (Collins et al. 1989)

Hitachi UV2000 Specifications		
Range	Reproducibility	Accuracy
0-0.5 abs.	± 0.001	± 0.002
0.5-1.0 abs.	± 0.002	0.004±

Care for cuvettes

a. Periodically clean cells by rinsing with methanol then RO water, or use phosphate free soap.
b. Take care not to drop, scratch or in any way damage the cells.

Instrument Setup

a. Select Photometry in Main Menu using arrow keys; press ENTER.
b. Select Test Setup: set/check set to 254 nm wavelength.
c. Press FORWARD; machine will align to 254 nm. Wait for 30 minutes for the lamp to warm up.
d. Press AUTOZERO to zero on blanks.
e. Press start to measure absorbance of samples.

References

APHA, AWWA, WEF (2006). *Standard Methods for the Examination of Water and Wastewater*. 21st Ed.

Page T. G. 1997. "GAC Sandwich Modification to Slow Sand Filtration for Enhanced Removal of Natural Organic Matter" Master's thesis, University of New Hampshire, Durham, NH.

Standard Operating Procedures
ATP EXTRACTION

LUMINULTRA microbial monitoring

Test Kit Instructions
Deposit & Surface Analysis (DSA)

REHYDRATING LUMINASE

- Gently mix the buffer and **Luminase** enzyme.
- Wait 5 minutes for solution to dissolve.

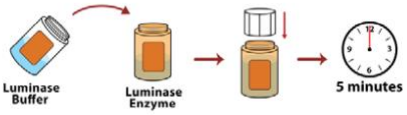

1. ULTRACHECK CALIBRATION (RLU_{ATP1})

- Hold the UltraCheck1 bottle vertical, add 2 drops (100µL) of **UltraCheck1** to a 12x55mm test tube.
- Pipet 100µL of **Luminase** into the test tube.
- Swirl tube and take reading within 10 seconds.

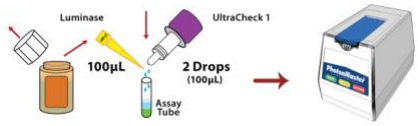

* If RLU_{ATP1} [illegible]

2. SAMPLE PREPARATION

A. **Surface Swab** – A measured area of the surface is swabbed to collect biofilm. ATP is then extracted from the swab.
B. **Measured Deposit** – A deposit is collected and measured. ATP is extracted from the deposit.
C. **Biofilm Collector** – ATP is extracted directly off a biofilm collection device (e.g. corrosion coupon).

2.A SURFACE SWAB

- Obtain a new Sterile Swab and wet with **LumiSolve.** Swab a surface area of approximately 5x5cm (2x2in).
- Insert swab in a **5mL UltraLyse 7 (Extraction) Tube**. Cap and mix the contents of the tube.

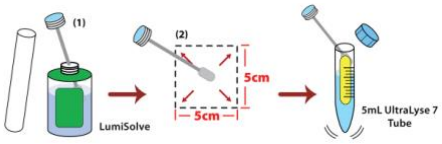

TIP: To increase analysis sensitivity, increase the swabbed surface area.

2.B MEASURED DEPOSIT

- Obtain a portion of the deposit and weigh 1g of sample.
- Add this to a **5mL UltraLyse 7 (Extraction) Tube**.
- Cap and mix the contents of the tube vigorously to disperse the deposit throughout the fluid.

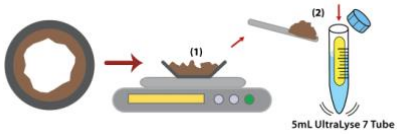

TIP: A measured volume of deposit (e.g. 1mL) can also be used instead of a weighed amount.

2.C BIOFILM COLLECTOR

- Obtain a biofilm collection device from the process and shake gently to remove excess fluid.
- Note the area of all biofilm-containing surfaces on the device and place it into a **5mL UltraLyse 7 (Extraction) Tube**.
- Cap and mix the contents of the tube vigorously to disperse the deposit throughout the fluid.

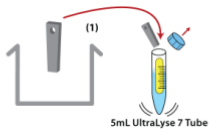

TIP: Attempt to test the biofilm collection device as quickly as possible following removal from process fluid.

3. TOTAL ATP (tATP) ANALYSIS

3.1 EXTRACTION

- ☐ Allow at least 5 minutes for ATP extraction in the **UltraLyse 7 (Extraction) Tube**.

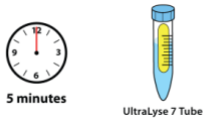

TIP: When using the biofilm collector method, ensure the device is submerged in the UltraLyse 7 during incubation.

3.2 DILUTION

- ☐ Transfer 1mL from the **UltraLyse 7 (Extraction) Tube** to a **9mL UltraLute (Dilution) Tube**.
- ☐ Cap and invert three times to mix.

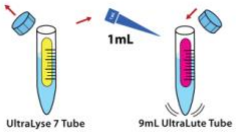

3.3 ASSAY

- ☐ Pipet 100µL of the **UltraLute (Dilution)** solution to a 12x55mm test tube.
- ☐ Using a new pipet tip, add 100µL of **Luminase** to the test tube.
- ☐ Swirl the tube and take reading within 10 seconds.

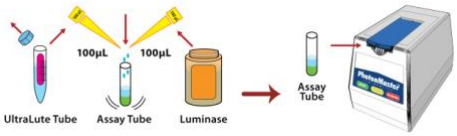

CALCULATIONS

The Total ATP (**tATP**) analysis measures all ATP within the deposit, including ATP from living cells as well as ATP released from dead cells.

A – Surface Swab (Default A_{Sample} = 25cm²):

$$tATP\left(pg\ ATP/cm^2\right) = \frac{RLU_{tATP}}{RLU_{ATP1}} \cdot \frac{50{,}000\left(pg\ ATP\right)}{A_{Sample}\left(cm^2\right)}$$

B – Measured Deposit (Default m_{Sample} = 1g):

$$tATP\left(pg\ ATP/g\right) = \frac{RLU_{tATP}}{RLU_{ATP1}} \cdot \frac{50{,}000\left(pg\ ATP\right)}{m_{Sample}\left(g\right)}$$

C – Biofilm Collector:

$$tATP\left(pg\ ATP/cm^2\right) = \frac{RLU_{tATP}}{RLU_{ATP1}} \cdot \frac{50{,}000\left(pg\ ATP\right)}{A_{Collector}\left(cm^2\right)}$$

TIP: You may also divide the result by the number of days the biofilm has had to evolve to obtain a growth rate.

Interpretation Guidelines

ATP-based measurements are extremely sensitive to changes in total microbial quantity. In general, processes will have the best microbial control when **tATP is minimized.**

It is recommend to compare surface/deposit results to bulk fluid results. Good control of biofilm is generally achieved when the biofilm/fluid ratio is <10x, and corrective action is required at levels of 100x or above:

Application	Good Control (pg tATP/cm² or g)	Preventive Action (pg tATP/cm² or g)	Corrective Action (pg tATP/cm² or g)
Potable & Sanitary Water	<10	10 to 1,000	>1,000
Raw, Cooling & Process Water (Oxidizing Biocide)	<100	100 to 10,000	>10,000
Cooling, Process, Bottom & Oilfield Water (Non-Oxidizing Biocide)	<1,000	1,000 to 100,000	>100,000
Bulk Fluid-to-Biofilm Ratio	<10x	10x to 100x	>100x
Biological Filter Media	Process Dependant		

Quick-Start Protocol May 2019

DNeasy® PowerSoil® Pro Kit

Solution CD2 should be stored at 2–8°C upon arrival. All other reagents and kit components should be stored at room temperature (15–25°C).

Further information

- *DNeasy® PowerSoil® Pro Kit Handbook*: **www.qiagen.com/HB-2495**
- Safety Data Sheets: **www.qiagen.com/safety**
- Technical assistance: **support.qiagen.com**

Notes before starting

- Ensure that the PowerBead Pro Tubes rotate freely in the centrifuge without rubbing.
- If Solution CD3 has precipitated, heat at 60°C until precipitate dissolves.
- Perform all centrifugation steps at room temperature (15–25°C).

1. Spin the PowerBead Pro Tube briefly to ensure that the beads have settled at the bottom. Add up to 250 mg of soil and 800 µl of Solution CD1. Vortex briefly to mix.
2. Secure the PowerBead Pro Tube horizontally on a Vortex Adapter for 1.5–2 ml tubes (cat. no. 13000-V1-24). Vortex at maximum speed for 10 min.
   Note: If using the Vortex Adapter for more than 12 preps simultaneously, increase the vortexing time by 5–10 min.
   Note: For more information about other bead beating methods, see the "Protocol: Detailed" section of *DNeasy® PowerSoil® Pro Kit Handbook*.
3. Centrifuge the PowerBead Pro Tube at 15,000 x *g* for 1 min.
4. Transfer the supernatant to a clean 2 ml Microcentrifuge Tube (provided).
   Note: Expect 500–600 µl. The supernatant may still contain some soil particles.
5. Add 200 µl of Solution CD2 and vortex for 5 s.
6. Centrifuge at 15,000 x *g* for 1 min at room temperature. Avoiding the pellet, transfer up to 700 µl of supernatant to a clean 2 ml Microcentrifuge Tube (provided).
   Note: Expect 500–600 µl.
7. Add 600 µl of Solution CD3 and vortex for 5 s.

8. Load 650 µl of the lysate onto an MB Spin Column and centrifuge at 15,000 x *g* for 1 min.
9. Discard the flow-through and repeat step 8 to ensure that all of the lysate has passed through the MB Spin Column.
10. Carefully place the MB Spin Column into a clean 2 ml Collection Tube (provided). Avoid splashing any flow-through onto the MB Spin Column.
11. Add 500 µl of Solution EA to the MB Spin Column. Centrifuge at 15,000 x *g* for 1 min.
12. Discard the flow-through and place the MB Spin Column back into the same 2 ml Collection Tube.
13. Add 500 µl of Solution C5 to the MB Spin Column. Centrifuge at 15,000 x *g* for 1 min.
14. Discard the flow-through and place the MB Spin Column into a new 2 ml Collection Tube (provided).
15. Centrifuge at up to 16,000 x *g* for 2 min. Carefully place the MB Spin Column into a new 1.5 ml Elution Tube (provided).
16. Add 50–100 µl of Solution C6 to the center of the white filter membrane.
17. Centrifuge at 15,000 x *g* for 1 min. Discard the MB Spin Column. The DNA is now ready for downstream applications.
    Note: We recommend storing the DNA frozen (–30 to –15°C or –90 to –65°C) as Solution C6 does not contain EDTA. To concentrate DNA, please refer to the Troubleshooting Guide.

Scan QR code for handbook.

For up-to-date licensing information and product specific disclaimers, see the respective QIAGEN kit handbook or user manual.

Standard Operating Procedures
PCR AMPLIFICATION

16S rRNA gene

Number of Reactions: 42

Cocktail Reagents

	Volume			Total Volume	
dH2O	17	uL		714	uL
Platinum PCR 2x Mix	25	uL		1050	uL
F Primer (5 uM)	3	uL		126	uL
R Primer (5 uM)	3	uL		126	uL
			Total	2016	uL
			Volume/tube	48	uL
			DNA	2	uL
			Total Volume	50	uL

Steps:		
	1	Clean Hood with bleach, ethanol, and DNAway
	2	UV Hood for 20-30 minutes
	3a	UV Reagents (highlighted) and tubes in Crosslinker for 600s
	3b	Thaw Reagents (unhighlighted) and DNA on ice
	3c	Add taq, Vortex and Aliquot cocktail.
	4	Add DNA template.
	5	Spin down and run on thermocycler (see below)
	6	Form Gel (2% for short segments, 1-1.5% for long)
	7	Run Gel
		Store at -20 C

General PCR Cycles:

	Temp	Time
1	94 C	3 mins
2	94 C	45 s
3	50 C	60 s
4	72 C	60 s
5	repeat steps 2-4	x 25
6	72 C	10 mins
7	4 C	Forever
8	End	

Standard Operating Procedures
AGAROSE GEL SETUP

Agarose Gel Setup

NOTE: Always wear dedicated gloves when using gel loading equipment and NEVER touch anything else around the lab with gloves. Make sure to wash hands after working with gels.

for 1.5%, 100 ml gel

1	Combine 1.5g agarose in 100 ml of 1x TBE buffer.
2	Microwave at 15 s intervals until agarose is dissolved.
3	Add 10 µl Gel Red (10,000x) directly to TBE-agarose solution.
4	Let cool to touch, then pour liquid in tray with comb, making sure tray is level and sides are sealed.
5	Inject 2 µl of 100 bp or 1 kb DNA ladder in respective well.
6	Dot gel loading dye (Blue 6X) on parafilm for each sample you plan to visualize. (Add 1 ul dye for every 2 ul sample you plan to load.)
7	Pipet 2 ul DNA samples onto dye dots, mixing contents with pipette tips. Inject carefully into submerged wells
8	Fill container with TBE buffer until the fill line, or just over the thickness of the gel.
9	Run gel to red for approximately 45 minutes at ~80V, or until fragments are properly sized with ladder.
10	Observe gel under transilluminator. Wear protective glasses when visualizing samples under UV light.

for 1.5%, 150 ml gel

1	Combine 2.25g agarose in 150 ml of 1x TBE buffer.
2	Microwave at 15 s intervals until agarose is dissolved.
3	Add 15 µl Gel Red (10,000x) directly to TBE-agarose solution.
4	Follow steps 4-10 above

for 1%, 100 ml gel

1	Combine 1g agarose in 100 ml of 1x TBE buffer.
2	Follow steps 2-10 above
3	Add 10 µl Gel Red (10,000x) directly to TBE-agarose solution.

Standard Operating Procedure
METHOD 6010B

INDUCTIVELY COUPLED PLASMA-ATOMIC EMISSION SPECTROMETRY

1.0 SCOPE AND APPLICATION

1.1 Inductively coupled plasma-atomic emission spectrometry (ICP-AES) determines trace elements, including metals, in solution. The method is applicable to all of the elements listed in Table 1. All matrices, excluding filtered groundwater samples but including ground water, aqueous samples, TCLP and EP extracts, industrial and organic wastes, soils, sludges, sediments, and other solid wastes, require digestion prior to analysis. Groundwater samples that have been prefiltered and acidified will not need acid digestion. Samples which are not digested must either use an internal standard or be matrix matched with the standards. Refer to Chapter Three for the appropriate digestion procedures.

1.2 Table 1 lists the elements for which this method is applicable. Detection limits, sensitivity, and the optimum and linear concentration ranges of the elements can vary with the wavelength, spectrometer, matrix and operating conditions. Table 1 lists the recommended analytical wavelengths and estimated instrumental detection limits for the elements in clean aqueous matrices. The instrument detection limit data may be used to estimate instrument and method performance for other sample matrices. Elements and matrices other than those listed in Table 1 may be analyzed by this method if performance at the concentration levels of interest (see Section 8.0) is demonstrated.

1.3 Users of the method should state the data quality objectives prior to analysis and must document and have on file the required initial demonstration performance data described in the following sections prior to using the method for analysis.

1.4 Use of this method is restricted to spectroscopists who are knowledgeable in the correction of spectral, chemical, and physical interferences described in this method.

2.0 SUMMARY OF METHOD

2.1 Prior to analysis, samples must be solubilized or digested using appropriate Sample Preparation Methods (e.g. Chapter Three). When analyzing groundwater samples for dissolved constituents, acid digestion is not necessary if the samples are filtered and acid preserved prior to analysis.

2.2 This method describes multielemental determinations by ICP-AES using sequential or simultaneous optical systems and axial or radial viewing of the plasma. The instrument measures characteristic emission spectra by optical spectrometry. Samples are nebulized and the resulting aerosol is transported to the plasma torch. Element-specific emission spectra are produced by a radio-frequency inductively coupled plasma. The spectra are dispersed by a grating spectrometer, and the intensities of the emission lines are monitored by photosensitive devices. Background correction is required for trace element determination. Background must be measured adjacent to analyte lines on samples during analysis. The position selected for the background-intensity measurement, on either or both sides of the analytical line, will be determined by the complexity of the spectrum adjacent to the analyte line. In one mode of analysis the position used should be as free as possible from spectral interference and should reflect the same change in background

intensity as occurs at the analyte wavelength measured. Background correction is not required in cases of line broadening where a background correction measurement would actually degrade the analytical result. The possibility of additional interferences named in Section 3.0 should also be recognized and appropriate corrections made; tests for their presence are described in Section 8.5. Alternatively, users may choose multivariate calibration methods. In this case, point selections for background correction are superfluous since whole spectral regions are processed.

3.0 INTERFERENCES

3.1 Spectral interferences are caused by background emission from continuous or recombination phenomena, stray light from the line emission of high concentration elements, overlap of a spectral line from another element, or unresolved overlap of molecular band spectra.

3.1.1 Background emission and stray light can usually be compensated for by subtracting the background emission determined by measurements adjacent to the analyte wavelength peak. Spectral scans of samples or single element solutions in the analyte regions may indicate when alternate wavelengths are desirable because of severe spectral interference. These scans will also show whether the most appropriate estimate of the background emission is provided by an interpolation from measurements on both sides of the wavelength peak or by measured emission on only one side. The locations selected for the measurement of background intensity will be determined by the complexity of the spectrum adjacent to the wavelength peak. The locations used for routine measurement must be free of off-line spectral interference (interelement or molecular) or adequately corrected to reflect the same change in background intensity as occurs at the wavelength peak. For multivariate methods using whole spectral regions, background scans should be included in the correction algorithm. Off-line spectral interferences are handled by including spectra on interfering species in the algorithm.

3.1.2 To determine the appropriate location for off-line background correction, the user must scan the area on either side adjacent to the wavelength and record the apparent emission intensity from all other method analytes. This spectral information must be documented and kept on file. The location selected for background correction must be either free of off-line interelement spectral interference or a computer routine must be used for automatic correction on all determinations. If a wavelength other than the recommended wavelength is used, the analyst must determine and document both the overlapping and nearby spectral interference effects from all method analytes and common elements and provide for their automatic correction on all analyses. Tests to determine spectral interference must be done using analyte concentrations that will adequately describe the interference. Normally, 100 mg/L single element solutions are sufficient; however, for analytes such as iron that may be found at high concentration, a more appropriate test would be to use a concentration near the upper analytical range limit.

3.1.3 Spectral overlaps may be avoided by using an alternate wavelength or can be compensated by equations that correct for interelement contributions. Instruments that use equations for interelement correction **require** the interfering elements be analyzed at the same time as the element of interest. When operative and uncorrected, interferences will produce false positive determinations and be reported as analyte concentrations. More extensive information on interferant effects at various wavelengths and resolutions is available in reference wavelength tables and books. Users may apply interelement

correction equations determined on their instruments with tested concentration ranges to compensate (off line or on line) for the effects of interfering elements. Some potential spectral interferences observed for the recommended wavelengths are given in Table 2. For multivariate methods using whole spectral regions, spectral interferences are handled by including spectra of the interfering elements in the algorithm. The interferences listed are only those that occur between method analytes. Only interferences of a direct overlap nature are listed. These overlaps were observed with a single instrument having a working resolution of 0.035 nm.

3.1.4 When using interelement correction equations, the interference may be expressed as analyte concentration equivalents (i.e. false analyte concentrations) arising from 100 mg/L of the interference element. For example, assume that As is to be determined (at 193.696 nm) in a sample containing approximately 10 mg/L of Al. According to Table 2, 100 mg/L of Al would yield a false signal for As equivalent to approximately 1.3 mg/L. Therefore, the presence of 10 mg/L of Al would result in a false signal for As equivalent to approximately 0.13 mg/L. The user is cautioned that other instruments may exhibit somewhat different levels of interference than those shown in Table 2. The interference effects must be evaluated for each individual instrument since the intensities will vary.

3.1.5 Interelement corrections will vary for the same emission line among instruments because of differences in resolution, as determined by the grating, the entrance and exit slit widths, and by the order of dispersion. Interelement corrections will also vary depending upon the choice of background correction points. Selecting a background correction point where an interfering emission line may appear should be avoided when practical. Interelement corrections that constitute a major portion of an emission signal may not yield accurate data. Users should not forget that some samples may contain uncommon elements that could contribute spectral interferences.

3.1.6 The interference effects must be evaluated for each individual instrument whether configured as a sequential or simultaneous instrument. For each instrument, intensities will vary not only with optical resolution but also with operating conditions (such as power, viewing height and argon flow rate). When using the recommended wavelengths, the analyst is required to determine and document for each wavelength the effect from referenced interferences (Table 2) as well as any other suspected interferences that may be specific to the instrument or matrix. The analyst is encouraged to utilize a computer routine for automatic correction on all analyses.

3.1.7 Users of sequential instruments must verify the absence of spectral interference by scanning over a range of 0.5 nm centered on the wavelength of interest for several samples. The range for lead, for example, would be from 220.6 to 220.1 nm. This procedure must be repeated whenever a new matrix is to be analyzed and when a new calibration curve using different instrumental conditions is to be prepared. Samples that show an elevated background emission across the range may be background corrected by applying a correction factor equal to the emission adjacent to the line or at two points on either side of the line and interpolating between them. An alternate wavelength that does not exhibit a background shift or spectral overlap may also be used.

3.1.8 If the correction routine is operating properly, the determined apparent analyte(s) concentration from analysis of each interference solution should fall within a specific concentration range around the calibration blank. The concentration range is calculated by multiplying the concentration of the interfering element by the value of the correction factor being tested and divided by 10. If after the subtraction of the calibration blank the apparent analyte concentration falls outside of this range in either a positive or negative direction, a change in the correction factor of more than 10% should be suspected. The cause of the change should be determined and corrected and the correction factor updated. The interference check solutions should be analyzed more than once to confirm a change has occurred. Adequate rinse time between solutions and before analysis of the calibration blank will assist in the confirmation.

3.1.9 When interelement corrections are applied, their accuracy should be verified, daily, by analyzing spectral interference check solutions. If the correction factors or multivariate correction matrices tested on a daily basis are found to be within the 20% criteria for 5 consecutive days, the required verification frequency of those factors in compliance may be extended to a weekly basis. Also, if the nature of the samples analyzed is such they do not contain concentrations of the interfering elements at ± one reporting limit from zero, daily verification is not required. All interelement spectral correction factors or multivariate correction matrices must be verified and updated every six months or when an instrumentation change, such as in the torch, nebulizer, injector, or plasma conditions occurs. Standard solution should be inspected to ensure that there is no contamination that may be perceived as a spectral interference.

3.1.10 When interelement corrections are <u>not</u> used, verification of absence of interferences is required.

3.1.10.1 One method is to use a computer software routine for comparing the determinative data to limits files for notifying the analyst when an interfering element is detected in the sample at a concentration that will produce either an apparent false positive concentration, (i.e., greater than) the analyte instrument detection limit, or false negative analyte concentration, (i.e., less than the lower control limit of the calibration blank defined for a 99% confidence interval).

3.1.10.2 Another method is to analyze an Interference Check Solution(s) which contains similar concentrations of the major components of the samples (>10 mg/L) on a continuing basis to verify the absence of effects at the wavelengths selected. These data must be kept on file with the sample analysis data. If the check solution confirms an operative interference that is $\geq$ 20% of the analyte concentration, the analyte must be determined using (1) analytical and background correction wavelengths (or spectral regions) free of the interference, (2) by an alternative wavelength, or (3) by another documented test procedure.

3.2 Physical interferences are effects associated with the sample nebulization and transport processes. Changes in viscosity and surface tension can cause significant inaccuracies, especially in samples containing high dissolved solids or high acid concentrations. If physical interferences are present, they must be reduced by diluting the sample or by using a peristaltic pump, by using an internal standard or by using a high solids nebulizer. Another problem that can occur with high dissolved solids is salt buildup at the tip of the nebulizer, affecting aerosol flow rate

and causing instrumental drift. The problem can be controlled by wetting the argon prior to nebulization, using a tip washer, using a high solids nebulizer or diluting the sample. Also, it has been reported that better control of the argon flow rate, especially to the nebulizer, improves instrument performance: this may be accomplished with the use of mass flow controllers. The test described in Section 8.5.1 will help determine if a physical interference is present.

3.3 Chemical interferences include molecular compound formation, ionization effects, and solute vaporization effects. Normally, these effects are not significant with the ICP technique, but if observed, can be minimized by careful selection of operating conditions (incident power, observation position, and so forth), by buffering of the sample, by matrix matching, and by standard addition procedures. Chemical interferences are highly dependent on matrix type and the specific analyte element.

3.4 Memory interferences result when analytes in a previous sample contribute to the signals measured in a new sample. Memory effects can result from sample deposition on the uptake tubing to the nebulizer and from the build up of sample material in the plasma torch and spray chamber. The site where these effects occur is dependent on the element and can be minimized by flushing the system with a rinse blank between samples. The possibility of memory interferences should be recognized within an analytical run and suitable rinse times should be used to reduce them. The rinse times necessary for a particular element must be estimated prior to analysis. This may be achieved by aspirating a standard containing elements at a concentration ten times the usual amount or at the top of the linear dynamic range. The aspiration time for this sample should be the same as a normal sample analysis period, followed by analysis of the rinse blank at designated intervals. The length of time required to reduce analyte signals to within a factor of two of the method detection limit should be noted. Until the required rinse time is established, this method suggests a rinse period of at least 60 seconds between samples and standards. If a memory interference is suspected, the sample must be reanalyzed after a rinse period of sufficient length. Alternate rinse times may be established by the analyst based upon their DQOs.

3.5 Users are advised that high salt concentrations can cause analyte signal suppressions and confuse interference tests. If the instrument does not display negative values, fortify the interference check solution with the elements of interest at 0.5 to 1 mg/L and measure the added standard concentration accordingly. Concentrations should be within 20% of the true spiked concentration or dilution of the samples will be necessary. In the absence of measurable analyte, overcorrection could go undetected if a negative value is reported as zero.

3.6 The dashes in Table 2 indicate that no measurable interferences were observed even at higher interferant concentrations. Generally, interferences were discernible if they produced peaks, or background shifts, corresponding to 2 to 5% of the peaks generated by the analyte concentrations.

4.0 APPARATUS AND MATERIALS

4.1 Inductively coupled argon plasma emission spectrometer:

4.1.1 Computer-controlled emission spectrometer with background correction.

4.1.2 Radio-frequency generator compliant with FCC regulations.

4.1.3 Optional mass flow controller for argon nebulizer gas supply.

4.1.4 Optional peristaltic pump.

4.1.5 Optional Autosampler.

4.1.6 Argon gas supply - high purity.

4.2 Volumetric flasks of suitable precision and accuracy.

4.3 Volumetric pipets of suitable precision and accuracy.

5.0 REAGENTS

5.1 Reagent or trace metals grade chemicals shall be used in all tests. Unless otherwise indicated, it is intended that all reagents shall conform to the specifications of the Committee on Analytical Reagents of the American Chemical Society, where such specifications are available. Other grades may be used, provided it is first ascertained that the reagent is of sufficiently high purity to permit its use without lessening the accuracy of the determination. If the purity of a reagent is in question analyze for contamination. If the concentration of the contamination is less than the MDL then the reagent is acceptable.

5.1.1 Hydrochloric acid (conc), HCl.

5.1.2 Hydrochloric acid (1:1), HCl. Add 500 mL concentrated HCl to 400 mL water and dilute to 1 liter in an appropriately sized beaker.

5.1.3 Nitric acid (conc), HNO_3.

5.1.4 Nitric acid (1:1), HNO_3. Add 500 mL concentrated HNO_3 to 400 mL water and dilute to 1 liter in an appropriately sized beaker.

5.2 Reagent Water. All references to water in the method refer to reagent water unless otherwise specified. Reagent water will be interference free. Refer to Chapter One for a definition of reagent water.

5.3 Standard stock solutions may be purchased or prepared from ultra- high purity grade chemicals or metals (99.99% pure or greater). All salts must be dried for 1 hour at 105°C, unless otherwise specified.

Note: This section does not apply when analyzing samples that have been prepared by Method 3040.

CAUTION: Many metal salts are extremely toxic if inhaled or swallowed. Wash hands thoroughly after handling.

Typical stock solution preparation procedures follow. Concentrations are calculated based upon the weight of pure metal added, or with the use of the element fraction and the weight of the metal salt added.

For metals:

$$\text{Concentration (ppm)} = \frac{\text{weight (mg)}}{\text{volume (L)}}$$

For metal salts:

$$\text{Concentration (ppm)} = \frac{\text{weight (mg) x mole fraction}}{\text{volume (L)}}$$

5.3.1 Aluminum solution, stock, 1 mL = 1000 µg Al: Dissolve 1.000 g of aluminum metal, weighed accurately to at least four significant figures, in an acid mixture of 4.0 mL of (1:1) HCl and 1.0 mL of concentrated $HN0_3$ in a beaker. Warm beaker slowly to effect solution. When dissolution is complete, transfer solution quantitatively to a 1-liter flask, add an additional 10.0 mL of (1:1) HCl and dilute to volume with reagent water.

NOTE: Weight of analyte is expressed to four significant figures for consistency with the weights below because rounding to two decimal places can contribute up to 4 % error for some of the compounds.

5.3.2 Antimony solution, stock, 1 mL = 1000 µg Sb: Dissolve 2.6673 g $K(SbO)C_4H_4O_6$ (element fraction Sb = 0.3749), weighed accurately to at least four significant figures, in water, add 10 mL (1:1) HCl, and dilute to volume in a 1,000 mL volumetric flask with water.

5.3.3 Arsenic solution, stock, 1 mL = 1000 µg As: Dissolve 1.3203 g of As_2O_3 (element fraction As = 0.7574), weighed accurately to at least four significant figures, in 100 mL of water containing 0.4 g NaOH. Acidify the solution with 2 mL concentrated HNO_3 and dilute to volume in a 1,000 mL volumetric flask with water.

5.3.4 Barium solution, stock, 1 mL = 1000 µg Ba: Dissolve 1.5163 g $BaCl_2$ (element fraction Ba = 0.6595), dried at 250°C for 2 hours, weighed accurately to at least four significant figures, in 10 mL water with 1 mL (1:1) HCl. Add 10.0 mL (1:1) HCl and dilute to volume in a 1,000 mL volumetric flask with water.

5.3.5 Beryllium solution, stock, 1 mL = 1000 µg Be: Do not dry. Dissolve 19.6463 g $BeSO_4{\cdot}4H_2O$ (element fraction Be = 0.0509), weighed accurately to at least four significant figures, in water, add 10.0 mL concentrated HNO_3, and dilute to volume in a 1,000 mL volumetric flask with water.

5.3.6 Boron solution, stock, 1 mL = 1000 µg B: Do not dry. Dissolve 5.716 g anhydrous H_3BO_3 (B fraction = 0.1749), weighed accurately to at least four significant figures, in reagent water and dilute in a 1-L volumetric flask with reagent water. Transfer immediately after mixing in a clean polytetrafluoroethylene (PTFE) bottle to minimize any leaching of boron from the glass volumetric container. Use of a non-glass volumetric flask is recommended to avoid boron contamination from glassware.

5.3.7 Cadmium solution, stock, 1 mL = 1000 µg Cd: Dissolve 1.1423 g CdO (element fraction Cd = 0.8754), weighed accurately to at least four significant figures, in a

minimum amount of (1:1) HNO_3. Heat to increase rate of dissolution. Add 10.0 mL concentrated HNO_3 and dilute to volume in a 1,000 mL volumetric flask with water.

5.3.8 Calcium solution, stock, 1 mL = 1000 µg Ca: Suspend 2.4969 g $CaCO_3$ (element Ca fraction = 0.4005), dried at 180°C for 1 hour before weighing, weighed accurately to at least four significant figures, in water and dissolve cautiously with a minimum amount of (1:1) HNO_3. Add 10.0 mL concentrated HNO_3 and dilute to volume in a 1,000 mL volumetric flask with water.

5.3.9 Chromium solution, stock, 1 mL = 1000 µg Cr: Dissolve 1.9231 g CrO_3 (element fraction Cr = 0.5200), weighed accurately to at least four significant figures, in water. When solution is complete, acidify with 10 mL concentrated HNO_3 and dilute to volume in a 1,000 mL volumetric flask with water.

5.3.10 Cobalt solution, stock, 1 mL = 1000 µg Co: Dissolve 1.00 g of cobalt metal, weighed accurately to at least four significant figures, in a minimum amount of (1:1) HNO_3. Add 10.0 mL (1:1) HCl and dilute to volume in a 1,000 mL volumetric flask with water.

5.3.11 Copper solution, stock, 1 mL = 1000 µg Cu: Dissolve 1.2564 g CuO (element fraction Cu = 0.7989), weighed accurately to at least four significant figures), in a minimum amount of (1:1) HNO_3. Add 10.0 mL concentrated HNO_3 and dilute to volume in a 1,000 mL volumetric flask with water.

5.3.12 Iron solution, stock, 1 mL = 1000 µg Fe: Dissolve 1.4298 g Fe_2O_3 (element fraction Fe = 0.6994), weighed accurately to at least four significant figures, in a warm mixture of 20 mL (1:1) HCl and 2 mL of concentrated HNO_3. Cool, add an additional 5.0 mL of concentrated HNO_3, and dilute to volume in a 1,000 mL volumetric flask with water.

5.3.13 Lead solution, stock, 1 mL = 1000 µg Pb: Dissolve 1.5985 g $Pb(NO_3)_2$ (element fraction Pb = 0.6256), weighed accurately to at least four significant figures, in a minimum amount of (1:1) HNO_3. Add 10 mL (1:1) HNO_3 and dilute to volume in a 1,000 mL volumetric flask with water.

5.3.14 Lithium solution, stock, 1 mL = 1000 µg Li: Dissolve 5.3248 g lithium carbonate (element fraction Li = 0.1878), weighed accurately to at least four significant figures, in a minimum amount of (1:1) HCl and dilute to volume in a 1,000 mL volumetric flask with water.

5.3.15 Magnesium solution, stock, 1 mL = 1000 µg Mg: Dissolve 1.6584 g MgO (element fraction Mg = 0.6030), weighed accurately to at least four significant figures, in a minimum amount of (1:1) HNO_3. Add 10.0 mL (1:1) concentrated HNO_3 and dilute to volume in a 1,000 mL volumetric flask with water.

5.3.16 Manganese solution, stock, 1 mL = 1000 µg Mn: Dissolve 1.00 g of manganese metal, weighed accurately to at least four significant figures, in acid mixture (10 mL concentrated HCl and 1 mL concentrated HNO_3) and dilute to volume in a 1,000 mL volumetric flask with water.

5.3.17 Mercury solution, stock, 1 mL = 1000 µg Hg: Do not dry, highly toxic element. Dissolve 1.354 g $HgCl_2$ (Hg fraction = 0.7388) in reagent water. Add 50.0 mL concentrated HNO_3 and dilute to volume in 1-L volumetric flask with reagent water.

5.3.18 Molybdenum solution, stock, 1 mL = 1000 µg Mo: Dissolve 1.7325 g $(NH_4)_6Mo_7O_{24}.4H_2O$ (element fraction Mo = 0.5772), weighed accurately to at least four significant figures, in water and dilute to volume in a 1,000 mL volumetric flask with water.

5.3.19 Nickel solution, stock, 1 mL = 1000 µg Ni: Dissolve 1.00 g of nickel metal, weighed accurately to at least four significant figures, in 10.0 mL hot concentrated HNO_3, cool, and dilute to volume in a 1,000 mL volumetric flask with water.

5.3.20 Phosphate solution, stock, 1 mL = 1000 µg P: Dissolve 4.3937 g anhydrous KH_2PO_4 (element fraction P = 0.2276), weighed accurately to at least four significant figures, in water. Dilute to volume in a 1,000 mL volumetric flask with water.

5.3.21 Potassium solution, stock, 1 mL = 1000 µg K: Dissolve 1.9069 g KCl (element fraction K = 0.5244) dried at 110°C, weighed accurately to at least four significant figures, in water, and dilute to volume in a 1,000 mL volumetric flask with water.

5.3.22 Selenium solution, stock, 1 mL = 1000 µg Se: Do not dry. Dissolve 1.6332 g H_2SeO_3 (element fraction Se = 0.6123), weighed accurately to at least four significant figures, in water and dilute to volume in a 1,000 mL volumetric flask with water.

5.3.23 Silica solution, stock, 1 mL = 1000 µg SiO_2: Do not dry. Dissolve 2.964 g NH_4SiF_6, weighed accurately to at least four significant figures, in 200 mL (1:20) HCl with heating at 85°C to effect dissolution. Let solution cool and dilute to volume in a 1-L volumetric flask with reagent water.

5.3.24 Silver solution, stock, 1 mL = 1000 µg Ag: Dissolve 1.5748 g $AgNO_3$ (element fraction Ag = 0.6350), weighed accurately to at least four significant figures, in water and 10 mL concentrated HNO_3. Dilute to volume in a 1,000 mL volumetric flask with water.

5.3.25 Sodium solution, stock, 1 mL = 1000 µg Na: Dissolve 2.5419 g NaCl (element fraction Na = 0.3934), weighed accurately to at least four significant figures, in water. Add 10.0 mL concentrated HNO_3 and dilute to volume in a 1,000 mL volumetric flask with water.

5.3.26 Strontium solution, stock, 1 mL = 1000 µg Sr: Dissolve 2.4154 g of strontium nitrate ($Sr(NO_3)_2$) (element fraction Sr = 0.4140), weighed accurately to at least four significant figures, in a 1-liter flask containing 10 mL of concentrated HCl and 700 mL of water. Dilute to volume in a 1,000 mL volumetric flask with water.

5.3.27 Thallium solution, stock, 1 mL = 1000 µg Tl: Dissolve 1.3034 g $TlNO_3$ (element fraction Tl = 0.7672), weighed accurately to at least four significant figures, in water. Add 10.0 mL concentrated HNO_3 and dilute to volume in a 1,000 mL volumetric flask with water.

5.3.28 Tin solution, stock, 1 mL = 1000 µg Sn: Dissolve 1.000 g Sn shot, weighed accurately to at least 4 significant figures, in 200 mL (1:1) HCl with heating to effect dissolution. Let solution cool and dilute with (1:1) HCl in a 1-L volumetric flask.

5.3.29 Vanadium solution, stock, 1 mL = 1000 µg V: Dissolve 2.2957 g NH_4VO_3 (element fraction V = 0.4356), weighed accurately to at least four significant figures, in a minimum amount of concentrated HNO_3. Heat to increase rate of dissolution. Add 10.0 mL concentrated HNO_3 and dilute to volume in a 1,000 mL volumetric flask with water.

5.3.30 Zinc solution, stock, 1 mL = 1000 µg Zn: Dissolve 1.2447 g ZnO (element fraction Zn = 0.8034), weighed accurately to at least four significant figures, in a minimum amount of dilute HNO_3. Add 10.0 mL concentrated HNO_3 and dilute to volume in a 1,000 mL volumetric flask with water.

5.4 Mixed calibration standard solutions - Prepare mixed calibration standard solutions by combining appropriate volumes of the stock solutions in volumetric flasks (see Table 3). Add the appropriate types and volumes of acids so that the standards are matrix matched with the sample digestates. Prior to preparing the mixed standards, each stock solution should be analyzed separately to determine possible spectral interference or the presence of impurities. Care should be taken when preparing the mixed standards to ensure that the elements are compatible and stable together. Transfer the mixed standard solutions to FEP fluorocarbon or previously unused polyethylene or polypropylene bottles for storage. Fresh mixed standards should be prepared, as needed, with the realization that concentration can change on aging. Some typical calibration standard combinations are listed in Table 3.

NOTE: If the addition of silver to the recommended acid combination results in an initial precipitation, add 15 mL of water and warm the flask until the solution clears. Cool and dilute to 100 mL with water. For this acid combination, the silver concentration should be limited to 2 mg/L. Silver under these conditions is stable in a tap-water matrix for 30 days. Higher concentrations of silver require additional HCl.

5.5 Two types of blanks are required for the analysis for samples prepared by any method other than 3040. The calibration blank is used in establishing the analytical curve, and the method blank is used to identify possible contamination resulting from varying amounts of the acids used in the sample processing.

5.5.1 The calibration blank is prepared by acidifying reagent water to the same concentrations of the acids found in the standards and samples. Prepare a sufficient quantity to flush the system between standards and samples. The calibration blank will also be used for all initial and continuing calibration blank determinations (see Sections 7.3 and 7.4).

5.5.2 The method blank must contain all of the reagents in the same volumes as used in the processing of the samples. The method blank must be carried through the complete procedure and contain the same acid concentration in the final solution as the sample solution used for analysis.

5.6 The Initial Calibration Verification (ICV) is prepared by the analyst by combining compatible elements from a standard source different than that of the calibration standard and at concentrations within the linear working range of the instrument (see Section 8.6.1 for use).

5.7 The Continuing Calibration Verification (CCV)) should be prepared in the same acid matrix using the same standards used for calibration at a concentration near the mid-point of the calibration curve (see Section 8.6.1 for use).

5.8 The interference check solution is prepared to contain known concentrations of interfering elements that will provide an adequate test of the correction factors. Spike the sample with the elements of interest, particularly those with known interferences at 0.5 to 1 mg/L. In the absence of measurable analyte, overcorrection could go undetected because a negative value could be reported as zero. If the particular instrument will display overcorrection as a negative number, this spiking procedure will not be necessary.

6.0 SAMPLE COLLECTION, PRESERVATION, AND HANDLING

6.1 See the introductory material in Chapter Three, Inorganic Analytes, Sections 3.1 through 3.3.

7.0 PROCEDURE

7.1 Preliminary treatment of most matrices is necessary because of the complexity and variability of sample matrices. Groundwater samples which have been prefiltered and acidified will not need acid digestion. Samples which are not digested must either use an internal standard or be matrix matched with the standards**.** Solubilization and digestion procedures are presented in Sample Preparation Methods (Chapter Three, Inorganic Analytes).

7.2 Set up the instrument with proper operating parameters established as detailed below. The instrument must be allowed to become thermally stable before beginning (usually requiring at least 30 minutes of operation prior to calibration). Operating conditions - The analyst should follow the instructions provided by the instrument manufacturer.

7.2.1 Before using this procedure to analyze samples, there must be data available documenting initial demonstration of performance. The required data document the selection criteria of background correction points; analytical dynamic ranges, the applicable equations, and the upper limits of those ranges; the method and instrument detection limits; and the determination and verification of interelement correction equations or other routines for correcting spectral interferences. This data must be generated using the same instrument, operating conditions and calibration routine to be used for sample analysis. These documented data must be kept on file and be available for review by the data user or auditor.

7.2.2 Specific wavelengths are listed in Table 1. Other wavelengths may be substituted if they can provide the needed sensitivity and are corrected for spectral interference. Because of differences among various makes and models of spectrometers, specific instrument operating conditions cannot be provided. The instrument and operating conditions utilized for determination must be capable of providing data of acceptable quality to the program and data user. The analyst should follow the instructions provided by the instrument manufacturer unless other conditions provide similar or better performance for

a task. Operating conditions for aqueous solutions usually vary from 1100 to 1200 watts forward power, 14 to 18 mm viewing height, 15 to 19 liters/min argon coolant flow, 0.6 to 1.5 L/min argon nebulizer flow, 1 to 1.8 mL/min sample pumping rate with a 1 minute preflush time and measurement time near 1 second per wavelength peak for sequential instruments and 10 seconds per sample for simultaneous instruments. For an axial plasma, the conditions will usually vary from 1100-1500 watts forward power, 15-19 liters/min argon coolant flow, 0.6-1.5 L/min argon nebulizer flow, 1-1.8 mL/min sample pumping rate with a 1 minute preflush time and measurement time near 1 second per wavelength peak for sequential instruments and 10 seconds per sample for simultaneous instruments. Reproduction of the Cu/Mn intensity ratio at 324.754 nm and 257.610 nm respectively, by adjusting the argon aerosol flow has been recommended as a way to achieve repeatable interference correction factors.

7.2.3 The plasma operating conditions need to be optimized prior to use of the instrument. This routine is not required on a daily basis, but only when first setting up a new instrument or following a change in operating conditions. The following procedure is recommended or follow manufacturer's recommendations. The purpose of plasma optimization is to provide a maximum signal to background ratio for some of the least sensitive elements in the analytical array. The use of a mass flow controller to regulate the nebulizer gas flow or source optimization software greatly facilitates the procedure.

7.2.3.1 Ignite the radial plasma and select an appropriate incident RF power. Allow the instrument to become thermally stable before beginning, about 30 to 60 minutes of operation. While aspirating a 1000 ug/L solution of yttrium, follow the instrument manufacturer's instructions and adjust the aerosol carrier gas flow rate through the nebulizer so a definitive blue emission region of the plasma extends approximately from 5 to 20 mm above the top of the load coil. Record the nebulizer gas flow rate or pressure setting for future reference. The yttrium solution can also be used for coarse optical alignment of the torch by observing the overlay of the blue light over the entrance slit to the optical system.

7.2.3.2 After establishing the nebulizer gas flow rate, determine the solution uptake rate of the nebulizer in mL/min by aspirating a known volume of calibration blank for a period of at least three minutes. Divide the volume aspirated by the time in minutes and record the uptake rate; set the peristaltic pump to deliver the rate in a steady even flow.

7.2.3.3 Profile the instrument to align it optically as it will be used during analysis. The following procedure can be used for both horizontal and vertical optimization in the radial mode, but is written for vertical. Aspirate a solution containing 10 ug/L of several selected elements. These elements can be As, Se, Tl or Pb as the least sensitive of the elements and most needing to be optimize or others representing analytical judgement (V, Cr, Cu, Li and Mn are also used with success). Collect intensity data at the wavelength peak for each analyte at 1 mm intervals from 14 to 18 mm above the load coil. (This region of the plasma is referred to as the analytical zone.) Repeat the process using the calibration blank. Determine the net signal to blank intensity ratio for each analyte for each viewing height setting. Choose the height for viewing the plasma that provides the best net intensity ratios for the elements analyzed or the highest intensity ratio for the least

sensitive element. For optimization in the axial mode, follow the instrument manufacturer's instructions.

7.2.3.4 The instrument operating condition finally selected as being optimum should provide the lowest reliable instrument detection limits and method detection limits.

7.2.3.5 If either the instrument operating conditions, such as incident power or nebulizer gas flow rate are changed, or a new torch injector tube with a different orifice internal diameter is installed, the plasma and viewing height should be re-optimized.

7.2.3.6 After completing the initial optimization of operating conditions, but before analyzing samples, the laboratory must establish and initially verify an interelement spectral interference correction routine to be used during sample analysis. A general description concerning spectral interference and the analytical requirements for background correction in particular are discussed in the section on interferences. Criteria for determining an interelement spectral interference is an apparent positive or negative concentration for the analyte that falls within ± one reporting limit from zero. The upper control limit is the analyte instrument detection limit. Once established the entire routine must be periodically verified every six months. Only a portion of the correction routine must be verified more frequently or on a daily basis. Initial and periodic verification of the routine should be kept on file. Special cases where continual verification is required are described elsewhere.

7.2.3.7 Before daily calibration and after the instrument warmup period, the nebulizer gas flow rate must be reset to the determined optimized flow. If a mass flow controller is being used, it should be set to the recorded optimized flow rate, In order to maintain valid spectral interelement correction routines the nebulizer gas flow rate should be the same (< 2% change) from day to day.

7.2.4 For operation with organic solvents, use of the auxiliary argon inlet is recommended, as are solvent-resistant tubing, increased plasma (coolant) argon flow, decreased nebulizer flow, and increased RF power to obtain stable operation and precise measurements.

7.2.5 Sensitivity, instrumental detection limit, precision, linear dynamic range, and interference effects must be established for each individual analyte line on each particular instrument. All measurements must be within the instrument linear range where the correction equations are valid.

7.2.5.1 Method detection limits must be established for all wavelengths utilized for each type of matrix commonly analyzed. The matrix used for the MDL calculation must contain analytes of known concentrations within 3-5 times the anticipated detection limit. Refer to Chapter One for additional guidance on the performance of MDL studies.

7.2.5.2 Determination of limits using reagent water represent a best case situation and do not represent possible matrix effects of real world samples.

7.2.5.3 If additional confirmation is desired, reanalyze the seven replicate aliquots on two more non consecutive days and again calculate the method detection limit values for each day. An average of the three values for each analyte may provide for a more appropriate estimate. Successful analysis of samples with added analytes or using method of standard additions can give confidence in the method detection limit values determined in reagent water.

7.2.5.4 The upper limit of the linear dynamic range must be established for each wavelength utilized by determining the signal responses from a minimum for three, preferably five, different concentration standards across the range. One of these should be near the upper limit of the range. The ranges which may be used for the analysis of samples should be judged by the analyst from the resulting data. The data, calculations and rationale for the choice of range made should be documented and kept on file. The upper range limit should be an observed signal no more than 10% below the level extrapolated from lower standards. Determined analyte concentrations that are above the upper range limit must be diluted and reanalyzed. The analyst should also be aware that if an interelement correction from an analyte above the linear range exists, a second analyte where the interelement correction has been applied may be inaccurately reported. New dynamic ranges should be determined whenever there is a significant change in instrument response. For those analytes that periodically approach the upper limit, the range should be checked every six months. For those analytes that are known interferences, and are present at above the linear range, the analyst should ensure that the interelement correction has not been inaccurately applied.

NOTE: Many of the alkali and alkaline earth metals have non-linear response curves due to ionization and self absorption effects. These curves may be used if the instrument allows; however the effective range must be checked and the second order curve fit should have a correlation coefficient of 0.995 or better. Third order fits are not acceptable. These non-linear response curves should be revalidated and recalculated every six months. These curves are much more sensitive to changes in operating conditions than the linear lines and should be checked whenever there have been moderate equipment changes.

7.2.6 The analyst must (1) verify that the instrument configuration and operating conditions satisfy the analytical requirements and (2) maintain quality control data confirming instrument performance and analytical results.

7.3 Profile and calibrate the instrument according to the instrument manufacturer's recommended procedures, using the typical mixed calibration standard solutions described in Section 5.4. Flush the system with the calibration blank (Section 5.5.1) between each standard or as the manufacturer recommends. (Use the average intensity of multiple exposures for both standardization and sample analysis to reduce random error.) The calibration curve must consist of a minimum of a blank and a standard.

7.4 For all analytes and determinations, the laboratory must analyze an ICV (Section 5.6), a calibration blank (Section 5.5.1), and a continuing calibration verification (CCV) (Section 5.7) immediately following daily calibration. A calibration blank and either a calibration verification (CCV) or an ICV must be analyzed after every tenth sample and at the end of the sample run. Analysis of

the check standard and calibration verification must verify that the instrument is within ± 10% of calibration with relative standard deviation < 5% from replicate (minimum of two) integrations. If the calibration cannot be verified within the specified limits, the sample analysis must be discontinued, the cause determined and the instrument recalibrated. All samples following the last acceptable ICV, CCV or check standard must be reanalyzed. The analysis data of the calibration blank, check standard, and ICV or CCV must be kept on file with the sample analysis data.

7.5 Rinse the system with the calibration blank solution (Section 5.5.1) before the analysis of each sample. The rinse time will be one minute. Each laboratory may establish a reduction in this rinse time through a suitable demonstration.

7.6 Calculations: If dilutions were performed, the appropriate factors must be applied to sample values. All results should be reported with up to three significant figures.

7.7 The MSA should be used if an interference is suspected or a new matrix is encountered. When the method of standard additions is used, standards are added at one or more levels to portions of a prepared sample. This technique compensates for enhancement or depression of an analyte signal by a matrix. It will not correct for additive interferences, such as contamination, interelement interferences, or baseline shifts. This technique is valid in the linear range when the interference effect is constant over the range, the added analyte responds the same as the endogenous analyte, and the signal is corrected for additive interferences. The simplest version of this technique is the single addition method. This procedure calls for two identical aliquots of the sample solution to be taken. To the first aliquot, a small volume of standard is added; while to the second aliquot, a volume of acid blank is added equal to the standard addition. The sample concentration is calculated by: multiplying the intensity value for the unfortified aliquot by the volume (Liters) and concentration (mg/L or mg/kg) of the standard addition to make the numerator; the difference in intensities for the fortified sample and unfortified sample is multiplied by the volume (Liters) of the sample aliquot for the denominator. The quotient is the sample concentration.

For more than one fortified portion of the prepared sample, linear regression analysis can be applied using a computer or calculator program to obtain the concentration of the sample solution.

NOTE: Refer to Method 7000 for a more detailed discussion of the MSA.

7.8 An alternative to using the method of standard additions is the internal standard technique. Add one or more elements not in the samples and verified not to cause an interelement spectral interference to the samples, standards and blanks; yttrium or scandium are often used. The concentration should be sufficient for optimum precision but not so high as to alter the salt concentration of the matrix. The element intensity is used by the instrument as an internal standard to ratio the analyte intensity signals for both calibration and quantitation. This technique is very useful in overcoming matrix interferences especially in high solids matrices.

8.0 QUALITY CONTROL

8.1 All quality control data should be maintained and available for easy reference or inspection. All quality control measures described in Chapter One should be followed.

8.2 Dilute and reanalyze samples that exceed the linear calibration range or use an alternate, less sensitive line for which quality control data is already established.

8.3 Employ a minimum of one method blank per sample batch to determine if contamination or any memory effects are occurring. A method blank is a volume of reagent water carried through the same preparation process as a sample (refer to Chapter One).

8.4 Analyze matrix spiked duplicate samples at a frequency of one per matrix batch. A matrix duplicate sample is a sample brought through the entire sample preparation and analytical process in duplicate.

8.4.1.1 The relative percent difference between spiked matrix duplicate determinations is to be calculated as follows:

$$RPD = \frac{|D_1 - D_2|}{(|D_1 + D_2|)/2} \times 100$$

where:

RPD = relative percent difference.
D_1 = first sample value.
D_2 = second sample value (replicate).

(A control limit of ± 20% RPD or within the documented historical acceptance limits for each matrix shall be used for sample values greater than ten times the instrument detection limit.)

8.4.1.2 The spiked sample or spiked duplicate sample recovery is to be within ± 25% of the actual value or within the documented historical acceptance limits for each matrix.

8.5 It is recommended that whenever a new or unusual sample matrix is encountered, a series of tests be performed prior to reporting concentration data for analyte elements. These tests, as outlined in Sections 8.5.1 and 8.5.2, will ensure that neither positive nor negative interferences are operating on any of the analyte elements to distort the accuracy of the reported values.

8.5.1 Dilution Test: If the analyte concentration is sufficiently high (minimally, a factor of 10 above the instrumental detection limit after dilution), an analysis of a 1:5 dilution should agree within ± 10% of the original determination. If not, a chemical or physical interference effect should be suspected.

8.5.2 Post Digestion Spike Addition: An analyte spike added to a portion of a prepared sample, or its dilution, should be recovered to within 75% to 125% of the known value. The spike addition should produce a minimum level of 10 times and a maximum of 100 times the instrumental detection limit. If the spike is not recovered within the specified limits, a matrix effect should be suspected.

CAUTION: If spectral overlap is suspected, use of computerized compensation, an alternate wavelength, or comparison with an alternate method is recommended.

8.6 Check the instrument standardization by analyzing appropriate QC samples as follows.

8.6.1 Verify calibration with the Continuing Calibration Verification (CCV) Standard immediately following daily calibration, after every ten samples, and at the end of an analytical run. Check calibration with an ICV following the initial calibration (Section 5.6). At the laboratory's discretion, an ICV may be used in lieu of the continuing calibration verifications. If used in this manner, the ICV should be at a concentration near the mid-point of the calibration curve. Use a calibration blank (Section 5.5.1) immediately following daily calibration, after every 10 samples and at the end of the analytical run.

8.6.1.1 The results of the ICV and CCVs are to agree within 10% of the expected value; if not, terminate the analysis, correct the problem, and recalibrate the instrument.

8.6.1.2 The results of the check standard are to agree within 10% of the expected value; if not, terminate the analysis, correct the problem, and recalibrate the instrument.

8.6.1.3 The results of the calibration blank are to agree within three times the IDL. If not, repeat the analysis two more times and average the results. If the average is not within three standard deviations of the background mean, terminate the analysis, correct the problem, recalibrate, and reanalyze the previous 10 samples. If the blank is less than 1/10 the concentration of the action level of interest, and no sample is within ten percent of the action limit, analyses need not be rerun and recalibration need not be performed before continuation of the run.

8.6.2 Verify the interelement and background correction factors at the beginning of each analytical run. Do this by analyzing the interference check sample (Section 5.8). Results should be within ± 20% of the true value.

9.0 METHOD PERFORMANCE

9.1 In an EPA round-robin Phase 1 study, seven laboratories applied the ICP technique to acid-distilled water matrices that had been spiked with various metal concentrates. Table 4 lists the true values, the mean reported values, and the mean percent relative standard deviations.

9.2 Performance data for aqueous solutions and solid samples from a multilaboratory study (9) are provided in Tables 5 and 6.

10.0 REFERENCES

1. Boumans, P.W.J.M. Line Coincidence Tables for Inductively Coupled Plasma Atomic Emission Spectrometry, 2nd Edition. Pergamon Press, Oxford, United Kingdom, 1984.

2. Sampling and Analysis Methods for Hazardous Waste Combustion; U.S. Environmental Protection Agency; Air and Energy Engineering Research Laboratory, Office of Research and Development: Research Triangle Park, NC, 1984; Prepared by Arthur D. Little, Inc.

3. Rohrbough, W.G.; et al. Reagent Chemicals, American Chemical Society Specifications, 7th ed.; American Chemical Society: Washington, DC, 1986.

4. 1985 Annual Book of ASTM Standards, Vol. 11.01; "Standard Specification for Reagent Water"; ASTM: Philadelphia, PA, 1985; D1193-77.

5. Jones, C.L. et al. An Interlaboratory Study of Inductively Coupled Plasma Atomic Emission Spectroscopy Method 6010 and Digestion Method 3050. EPA-600/4-87-032, U.S. Environmental Protection Agency, Las Vegas, Nevada, 1987.

TABLE 1
RECOMMENDED WAVELENGTHS AND ESTIMATED INSTRUMENTAL DETECTION LIMITS

Detection Element	Wavelength[a] (nm)	Estimated IDL[b] (µg/L)
Aluminum	308.215	30
Antimony	206.833	21
Arsenic	193.696	35
Barium	455.403	0.87
Beryllium	313.042	0.18
Boron	249.678x2	3.8
Cadmium	226.502	2.3
Calcium	317.933	6.7
Chromium	267.716	4.7
Cobalt	228.616	4.7
Copper	324.754	3.6
Iron	259.940	4.1
Lead	220.353	28
Lithium	670.784	2.8
Magnesium	279.079	20
Manganese	257.610	0.93
Mercury	194.227x2	17
Molybdenum	202.030	5.3
Nickel	231.604x2	10
Phosphorus	213.618	51
Potassium	766.491	See note c
Selenium	196.026	50
Silica (SiO_2)	251.611	17
Silver	328.068	4.7
Sodium	588.995	19
Strontium	407.771	0.28
Thallium	190.864	27
Tin	189.980x2	17
Titanium	334.941	5.0
Vanadium	292.402	5.0
Zinc	213.856x2	1.2

[a]The wavelengths listed (where x2 indicates second order) are recommended because of their sensitivity and overall acceptance. Other wavelengths may be substituted (e.g., in the case of an interference) if they can provide the needed sensitivity and are treated with the same corrective techniques for spectral interference (see Section 3.1). In time, other elements may be added as more information becomes available and as required.

[b]The estimated instrumental detection limits shown are provided as a guide for an instrumental limit. The actual method detection limits are sample dependent and may vary as the sample matrix varies.

[c]Highly dependent on operating conditions and plasma position.

TABLE 2
POTENTIAL INTERFERENCES
ANALYTE CONCENTRATION EQUIVALENTS ARISING FROM
INTERFERENCE AT THE 100-mg/L LEVEL[c]

Analyte	Wavelength (nm)	Interferant[a,b] Al	Ca	Cr	Cu	Fe	Mg	Mn	Ni	Ti	V
Aluminum	308.215	--	--	--	--	--	--	0.21	--	--	1.4
Antimony	206.833	0.47	--	2.9	--	0.08	--	--	--	0.25	0.45
Arsenic	193.696	1.3	--	0.44	--	--	--	--	--	--	1.1
Barium	455.403	--	--	--	--	--	--	--	--	--	--
Beryllium	313.042	--	--	--	--	--	--	--	--	0.04	0.05
Cadmium	226.502	--	--	--	--	0.03	--	--	0.02	--	--
Calcium	317.933	--	--	0.08	--	0.01	0.01	0.04	--	0.03	0.03
Chromium	267.716	--	--	--	--	0.003	--	0.04	--	--	0.04
Cobalt	228.616	--	--	0.03	--	0.005	--	--	0.03	0.15	--
Copper	324.754	--	--	--	--	0.003	--	--	--	0.05	0.02
Iron	259.940	--	--	--	--	--	--	0.12	--	--	--
Lead	220.353	0.17	--	--	--	--	--	--	--	--	--
Magnesium	279.079	--	0.02	0.11	--	0.13	--	0.25	--	0.07	0.12
Manganese	257.610	0.005	--	0.01	--	0.002	0.002	--	--	--	--
Molybdenum	202.030	0.05	--	--	--	0.03	--	--	--	--	--
Nickel	231.604	--	--	--	--	--	--	--	--	--	--
Selenium	196.026	0.23	--	--	--	0.09	--	--	--	--	--
Sodium	588.995	--	--	--	--	--	--	--	--	0.08	--
Thallium	190.864	0.30	--	--	--	--	--	--	--	--	--
Vanadium	292.402	--	--	0.05	--	0.005	--	--	--	0.02	--
Zinc	213.856	--	--	--	0.14	--	--	--	0.29	--	--

[a] Dashes indicate that no interference was observed even when interferents were introduced at the following levels:

Al -	1000 mg/L	Mg -	1000 mg/L
Ca -	1000 mg/L	Mn -	200 mg/L
Cr -	200 mg/L	Tl -	200 mg/L
Cu -	200 mg/L	V -	200 mg/L
Fe -	1000 mg/L		

[b] The figures recorded as analyte concentrations are not the actual observed concentrations; to obtain those figures, add the listed concentration to the interferant figure.

[c] Interferences will be affected by background choice and other interferences may be present.

TABLE 3
MIXED STANDARD SOLUTIONS

Solution	Elements
I	Be, Cd, Mn, Pb, Se and Zn
II	Ba, Co, Cu, Fe, and V
III	As, Mo
IV	Al, Ca, Cr, K, Na, Ni,Li, and Sr
V	Ag (see “NOTE” to Section 5.4), Mg, Sb, and Tl
VI	P

TABLE 4. ICP PRECISION AND ACCURACY DATA[a]

Element	Sample No. 1				Sample No. 2				Sample No. 3			
	True Conc. (ug/L)	Mean Conc. (ug/L)	RSD[b] (%)	Accuracy[d] (%)	True Conc. (ug/L)	Mean Conc. (ug/L)	RSD[b]	Accuracy[d] (%)	True Conc. (ug/L)	Mean Conc. (ug/L)	RSD[b] (%)	Accuracy[d] (%)
Be	750	733	6.2	98	20	20	9.8	100	180	176	5.2	98
Mn	350	345	2.7	99	15	15	6.7	100	100	99	3.3	99
V	750	749	1.8	100	70	69	2.9	99	170	169	1.1	99
As	200	208	7.5	104	22	19	23	86	60	63	17	105
Cr	150	149	3.8	99	10	10	18	100	50	50	3.3	100
Cu	250	235	5.1	94	11	11	40	100	70	67	7.9	96
Fe	600	594	3.0	99	20	19	15	95	180	178	6.0	99
Al	700	696	5.6	99	60	62	33	103	160	161	13	101
Cd	50	48	12	96	2.5	2.9	16	116	14	13	16	93
Co	700	512	10	73	20	20	4.1	100	120	108	21	90
Ni	250	245	5.8	98	30	28	11	93	60	55	14	92
Pb	250	236	16	94	24	30	32	125	80	80	14	100
Zn	200	201	5.6	100	16	19	45	119	80	82	9.4	102
Se[c]	40	32	21.9	80	6	8.5	42	142	10	8.5	8.3	85

[a]Not all elements were analyzed by all laboratories.
[b]RSD = relative standard deviation.
[c]Results for Se are from two laboratories.
[d]Accuracy is expressed as the mean concentration divided by the true concentration times 100.

TABLE 5

ICP-AES PRECISION AND ACCURACY FOR AQUEOUS SOLUTIONS[a]

Element	Mean Conc. (mg/L)	N[b]	RSD[b] (%)	Accuracy[c] (%)
Al	14.8	8	6.3	100
Sb	15.1	8	7.7	102
As	14.7	7	6.4	99
Ba	3.66	7	3.1	99
Be	3.78	8	5.8	102
Cd	3.61	8	7.0	97
Ca	15.0	8	7.4	101
Cr	3.75	8	8.2	101
Co	3.52	8	5.9	95
Cu	3.58	8	5.6	97
Fe	14.8	8	5.9	100
Pb	14.4	7	5.9	97
Mg	14.1	8	6.5	96
Mn	3.70	8	4.3	100
Mo	3.70	8	6.9	100
Ni	3.70	7	5.7	100
K	14.1	8	6.6	95
Se	15.3	8	7.5	104
Ag	3.69	6	9.1	100
Na	14.0	8	4.2	95
Tl	15.1	7	8.5	102
V	3.51	8	6.6	95
Zn	3.57	8	8.3	96

[a]these performance values are independent of sample preparation because the labs analyzed portions of the same solutions

[b]N = Number of measurements for mean and relative standard deviation (RSD).

[c]Accuracy is expressed as a percentage of the nominal value for each analyte in acidified, multi-element solutions.

TABLE 6

ICP-AES PRECISION AND BIAS FOR SOLID WASTE DIGESTS[a]

Element	Spiked Coal Fly Ash (NIST-SRM 1633a) Mean Conc. (mg/L)	N[b]	RSD[b] (%)	Bias[c] (%AAS)	Spiked Electroplating Sludge Mean Conc. (mg/L)	N[b]	RSD[b] (%)	Bias[c] (%AAS)
Al	330	8	16	104	127	8	13	110
Sb	3.4	6	73	96	5.3	7	24	120
As	21	8	83	270	5.2	7	8.6	87
Ba	133	8	8.7	101	1.6	8	20	58
Be	4.0	8	57	460	0.9	7	9.9	110
Cd	0.97	6	5.7	101	2.9	7	9.9	90
Ca	87	6	5.6	208	954	7	7.0	97
Cr	2.1	7	36	106	154	7	7.8	93
Co	1.2	6	21	94	1.0	7	11	85
Cu	1.9	6	9.7	118	156	8	7.8	97
Fe	602	8	8.8	102	603	7	5.6	98
Pb	4.6	7	22	94	25	7	5.6	98
Mg	15	8	15	110	35	8	20	84
Mn	1.8	7	14	104	5.9	7	9.6	95
Mo	891	8	19	105	1.4	7	36	110
Ni	1.6	6	8.1	91	9.5	7	9.6	90
K	46	8	4.2	98	51	8	5.8	82
Se	6.4	5	16	73	8.7	7	13	101
Ag	1.4	3	17	140	0.75	7	19	270
Na	20	8	49	130	1380	8	9.8	95
Tl	6.7	4	22	260	5.0	7	20	180
V	1010	5	7.5	100	1.2	6	11	80
Zn	2.2	6	7.6	93	266	7	2.5	101

[a]These performance values are independent of sample preparation because the labs analyzed portions of the same digests.

[b]N = Number of measurements for mean and relative standard deviation (RSD).

[c]Bias for the ICP-AES data is expressed as a percentage of atomic absorption spectroscopy (AA) data for the same digests.

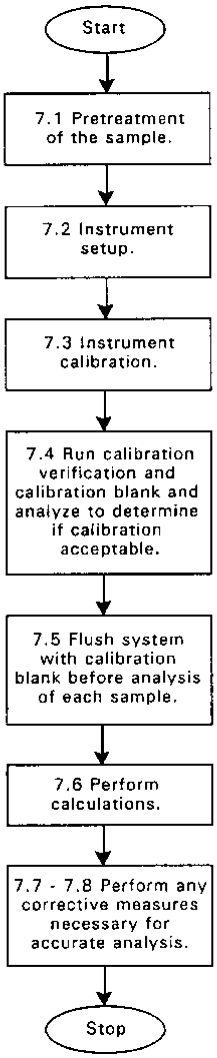
Start
7.1 Pretreatment of the sample.
7.2 Instrument setup.
7.3 Instrument calibration.
7.4 Run calibration verification and calibration blank and analyze to determine if calibration acceptable.
7.5 Flush system with calibration blank before analysis of each sample.
7.6 Perform calculations.
7.7 - 7.8 Perform any corrective measures necessary for accurate analysis.
Stop

Appendix B. Raw Data & Statistics

Total Organic Carbon/ Dissolved Organic Carbon Data

Adenosine Triphosphate (ATP) Data

Gram Dry Weight and Surface Area Conversions

Metals Data

Bed Volume Calculations

Winthrop, Maine August 2021

	D 0 TOC (mg/L) **Average** *St Dev*	D 1 TOC (mg/L) **Average** *St Dev*	D 2 TOC (mg/L) **Average** *St Dev*	D 5 TOC (mg/L) **Average** *St Dev*	D 7 TOC (mg/L) **Average** *St Dev*
Influent A	5.45	5.22	5.03	4.62	4.44
Influent B	5.44	5.29	5.13	4.60	4.58
Effluent A	4.34	4.21	4.05	3.76	3.66
Effluent B	4.37	4.20	4.04	3.78	3.65
Control A	4.40	3.77	1.79	0.67	0.63
Control B	4.36	3.76	1.84	0.61	0.64

Kate Morsefield
Winthrop Maine August 2021

D 1 BDOC (mg/L)	**D2 BDOC** (mg/L)	**D 5 BDOC** (mg/L)	**D 7 BDOC** (mg/L)
0.23	0.42	0.84	1.01
0.16	0.31	0.85	0.86
0.12	0.29	0.58	0.67
0.17	0.33	0.60	0.73
0.63	2.61	3.73	3.77
0.60	2.52	3.75	3.72

Winthrop, ME September 2021

	D0 TOC (mg/L) **Average** *St Dev*	**D1 TOC** (mg/L) **Average** *St Dev*	**D2 TOC** (mg/L) **Average** *St Dev*	**D5 TOC** (mg/L) **Average** *St Dev*	**D7 TOC** (mg/L) **Average** *St Dev*	**D1 BDOC** (mg/L)	**D2 BDOC** (mg/L)	**D5 BDOC** (mg/L)	**D7 BDOC** (mg/L)
Influent A	5.06	4.69	4.45	4.01	3.76	0.37	0.61	1.05	1.30
Influent B	5.04	4.71	4.47	4.04	3.84	0.33	0.57	1.00	1.20
Filter 1 Effluent A	2.79	2.71	2.59	2.57	2.56	0.08	0.2	0.22	0.23
Filter 1 Effluent B	2.89	2.63	2.59	2.66	2.64	0.26	0.3	0.23	0.25
Filter 2 Effluent A	0.49	0.41	0.45	0.57	0.69	0.08	0.04	-0.08	-0.20
Filter 2 Effluent B	0.51	0.42	0.53	0.56	0.68	0.09	-0.02	-0.05	-0.17
Filter 3 Effluent A	2.66	2.41	2.41	2.45	2.53	0.25	0.25	0.21	0.13
Filter 3 Effluent B	3.16	2.43	2.44	2.53	2.53	0.73	0.72	0.63	0.63
Control A	4.95	2.85	0.83	0.02	0.70	2.10	4.12	4.93	4.25
Control B	3.94	2.79	0.76	0.02	0.68	1.15	3.18	3.92	3.26

Katie Morsefield
BDOC
Winthrop, Maine
February 23, 2022 Samples

	Day 1 BDOC (mg/L)	Day 2 BDOC (mg/L)	Day 5 BDOC (mg/L)	Day 7 BDOC (mg/L)
Feed A	0.02	0.46	0.78	0.94
Feed B	0.32	0.44	0.78	1.08
Filter 1 A	0.17	0.15	0.29	0.39
Filter 1 B	0.32	0.28	0.45	0.44
Filter 2 A	0.01	-0.11	-0.13	-0.09
Filter 2 B	0.02	-0.01	-0.09	-0.07
Filter 3 A	0.04	0.12	0.18	0.25
Filter 3 B	0.05	-0.40	0.17	0.23
Sand A	0.19	0.34	0.45	0.48
Sand B	0.23	0.20	0.22	0.53
Control A	1.85	3.25	3.19	3.20
Control B	1.50	2.87	2.88	2.89

Katie Morsefield
BDOC
Winthrop, Maine
February 23, 2022 Samples

	Initial TOC (mg/L)	Day 1 TOC (mg/L)	Day 2 TOC (mg/L)	Day 5 TOC (mg/L)	Day 7 TOC (mg/L)
Feed A	4.61	4.59	4.14	3.83	3.67
Feed B	4.76	4.44	4.32	3.98	3.68
Filter 1 A	3.23	3.06	3.07	2.94	2.84
Filter 1 B	3.40	3.08	3.12	2.95	2.96
Filter 2 A	0.47	0.45	0.57	0.60	0.55
Filter 2 B	0.47	0.46	0.48	0.56	0.54
Filter 3 A	3.02	2.98	2.91	2.85	2.77
Filter 3 B	3.08	3.04	3.49	2.91	2.85
Sand A	3.95	3.76	3.61	3.50	3.47
Sand B	3.94	3.71	3.74	3.71	3.41
Control A	3.88	2.03	0.64	0.69	0.68
Control B	3.57	2.07	0.70	0.68	0.68

TOC samples Winthrop, Maine Revised 18-May-22

Analyzed 5/24/2022

y= 1.1585X - 0.1106

	TOC (mg/L)	corrected TOC (mg/L)	corrected TOC (mg/L) **Average** *St Dev*	Location TOC (mg/L) **Average** *St Dev*
Winthrop Influent	4.60	5.22	**5.23**	**5.23**
	4.6	5.22	*0.01*	*0.00*
	4.62	5.24		
Winthrop Influent dup	4.61	5.23	**5.23**	
	4.62	5.24	*0.02*	
	4.59	5.21		
Effluent Filter 1	3.00	3.36	**3.35**	**3.36**
	2.98	3.34	*0.01*	*0.02*
	2.98	3.34		
Effluent Filter 1 dup	3.01	3.38	**3.38**	
	3.01	3.38	*0.00*	
	3.01	3.38		
Effluent Filter 2	0.249	0.18	**0.17**	**0.19**
	0.244	0.17	*0.00*	*0.02*
	0.241	0.17		
Effluent Filter 2 dup	0.274	0.21	**0.20**	
	0.272	0.20	*0.00*	
	0.271	0.20		
Effluent Filter 3	3.05	3.42	**3.43**	**3.39**
	3.06	3.43	*0.01*	*0.06*
	3.06	3.43		
Effluent Filter 3 d	2.99	3.35	**3.35**	
	2.98	3.34	*0.01*	
	2.99	3.35		
Above GAC Filter 3	3.47	3.91	**3.91**	**3.95**
	3.47	3.91	*0.01*	*0.06*
	3.48	3.92		
Above GAC Filter 3 dup	3.55	4.00	**3.99**	
	3.56	4.01	*0.02*	
	3.52	3.97		

(2)

Katie Morsefield
BDOC
Winthrop, Maine
May 18, 2022 Samples

	Initial TOC (mg/L)	Day 1 TOC (mg/L)	Day 2 TOC (mg/L)	Day 5 TOC (mg/L)	Day 7 TOC (mg/L)
Feed A	5.63	4.90	4.53	4.05	3.92
				3.96	
Feed B	5.37	4.95	4.47	3.95	3.92
Filter 1 A	3.46	3.38	3.24	3.36	3.08
					3.12
Filter 1 B	3.48	3.32	3.24	3.23	3.17
Filter 2 A	0.63	0.41	0.41	0.46	0.78
					0.43
Filter 2 B	0.44	0.37	0.36	0.42	0.48
Filter 3 A	3.73	3.34	3.27	3.00	3.10
					3.06
Filter 3 B	3.44	3.28	3.25	3.05	3.12
Above GAC 3A	4.13	3.89	3.64	3.58	3.47
					3.53
Above GAC 3B	4.04	3.84	3.65	3.46	3.61
Control A	5.13	3.18	1.80	0.66	0.66
Control B	4.82	3.23	1.00	0.61	0.66

ATP Raw Data – August 4th, 2021

		weight (g)	RLU	average	ATP(pg ATP/g)	ATP (ng ATP/g)	ATP (ng ATP/gdw)	ATP (ng ATP/cm^2)
2	Schmutzdecke 1A	1.02	260851	279423	1504685.07	1504.68507	1770.217729	52.37330561
3	Schmutzdecke 1B	1.02	258740		1492508.041	1492.508041	1755.891813	51.94946193
4	Schmutzdecke 1C	1.01	318678		1856453.12	1856.45312	2184.062494	64.61723355
5	Schmutzdecke 2A	1.01	219615	255124.3333	1279363.345	1279.363345	1505.133347	44.53057239
6	Schmutzdecke 2B	1.01	243674		1419518.629	1419.518629	1670.021916	49.40893243
7	Schmutzdecke 2C	1.01	302084		1759785.063	1759.785063	2070.335368	61.25252569
8	Schmutzdecke 3A	1.02	327977	281670.3333	1891892.671	1891.892671	2225.756084	65.85077172
9	Schmutzdecke 3B	1.01	306001		1782603.478	1782.603478	2097.180562	62.0467622
10	Schmutzdecke 3C	1.00	211033		1241662.744	1241.662744	1460.779699	43.21833429
11	Sand 1	1.02	25043	26856	144457.2887	144.4572887	169.9497514	5.028099154
12	Sand 2	1.01	21124		123057.4929	123.0574929	144.773521	4.283240266
13	Sand 3	1.01	34401		200402.4243	200.4024243	235.767558	6.97537154
14	GAC 1	1.02	83260	116372.6667	480274.4821	480.2744821	923.6047733	10.40095465
15	GAC 2	1.01	129464		754190.2696	754.1902696	1450.365903	16.33294936
16	GAC 3	1.01	136394		794560.8635	794.5608635	1528.001661	17.20722591
17								
18								
19	**RLU ATP1**	8498.00						

ATP Raw Data – September 29th, 2021

		weight (g)	RLU	ATP(pg ATP/g)	ATP (ng ATP/g)	ATP (ng ATP/gdw)	ATP (ng ATP/cm^2)
2	Schmutzdecke 1A	1.00	269994	643425.0036	643.4250036	756.9705924	22.39557966
3	Schmutzdecke 1B	1.00	218268	520156.3319	520.1563319	611.9486258	18.10498893
4	Schmutzdecke 2A	1.00	182896	435861.0171	435.8610171	512.7776672	15.1709369
5	Schmutzdecke 2B	1.01	297429	701787.7089	701.7877089	825.6325987	24.42699996
6	Schmutzdecke 3A	1.01	16447	38806.91677	38.80691677	45.6551962	1.35074545
7	Schmutzdecke 3B	1.01	46909	110682.4137	110.6824137	130.2146044	3.852503089
8	Mid-Sand 1	1.01	17546	41400.02199	41.40002199	48.70590822	1.441003202
9	Mid-Sand 2	1.01	13096	30900.18739	30.90018739	36.35316164	1.075537327
10	Sand 1	1.00	9054	21576.6646	21.5766646	25.3843113	0.751015127
11	Sand 2	1.01	1049	2475.129549	2.475129549	2.911917117	0.086151394
12	GAC 1	1.01	11085	26155.20596	26.15520596	50.298473	0.566424245
13	GAC 2	1.00	13975	33303.94166	33.30394166	64.04604166	0.721239208
14							
15							
16	**RLU ATP1**	20981.00					

ATP Raw Data – February 23rd, 2022

	weight (g)	RLU	ATP(pg ATP/g)	ATP(ng ATP/g)	ATP (ng ATP/gdw)	ATP (ng ATP/cm^2)
Schmutzdecke 1A	1.01	60622	162422.9642	162.4229642	216.1796329	7.254350096
Schmutzdecke 1B	1.01	43040	115315.9641	115.3159641	153.4817624	5.150394711
Schmutzdecke 2A	1.00	33891	91711.31677	91.71131677	122.0647517	4.096132607
Schmutzdecke 2B	1.00	58832	159203.3339	159.2033339	211.8944107	7.110550693
Schmutzdecke 3A	1.01	42602	114142.442	114.142442	151.919843	5.097981307
Schmutzdecke 3B	1.00	26788	72490.12286	72.49012286	96.48197363	3.237650122
RLU ATP1	18477					

ATP Raw Data – May 19th, 2022

	weight (g)	RLU	ATP(pg ATP/g)	ATP (ng ATP/g)	ATP (ng ATP/gdw)	ATP (ng ATP/cm^2)
Schmutzdecke 1A	1.01	13940	40278.93597	40.27893597	52.31030645	1.56617684
Schmutzdecke 1B	1.01	20288	58621.16592	58.62116592	76.13138431	2.279382764
Schmutzdecke 2A	1.01	11725	33878.80374	33.87880374	43.99844642	1.317318755
Schmutzdecke 2B	1.01	1945	5619.980664	5.619980664	7.298676187	0.218523239
Schmutzdecke 3A	1.01	31234	90249.08795	90.24908795	117.2066077	3.509179872
Schmutzdecke 3B	1.01	9241	26701.40942	26.70140942	34.67715509	1.038238176
Mid-Sand 1	1.01	3759	10861.44335	10.86144335	13.92492737	0.416913993
Mid-Sand 2	1.01	4722	13643.9839	13.6439839	17.49228706	0.523721169
Sand 1	1.01	5133	14831.54794	14.83154794	16.29840433	0.487976178
Sand 2	1.01	5777	16692.35388	16.69235388	18.34324602	0.549198983
GAC 1	1.01	34580	99917.18836	99.91718836	166.5286473	1.627846014
GAC 2	1.01	40192	116132.783	116.132783	193.5546383	1.892029699
RLU ATP1	17133.00					

Gram Dry Weight and Surface Area Conversions

ATP results were converted from $\frac{pg\ ATP}{g\ (wet\ media)}$ to $\frac{ng\ ATP}{gdw}$ using the following equation:

$$Sand\ Media:\ \frac{pg\ tATP}{1.0\ g\ (wet\ media)} * \frac{1.0\ g\ (wet\ media)}{0.87\ g\ (dry\ weight)} * \frac{1000\ ng}{1\ pg} = \frac{ng\ tATP}{gdw}$$

$$GAC\ Media:\ \frac{pg\ tATP}{1.0\ g\ (wet\ media)} * \frac{1.0\ g\ (wet\ media)}{0.52\ g\ (dry\ weight)} * \frac{1000\ ng}{1\ pg} = \frac{ng\ tATP}{gdw}$$

ATP results were converted from $\frac{ng\ tATP}{gdw}$ to $\frac{ng\ tATP}{cm^2}$ for both sand and GAC media using the following equations:

Sand Media:

$$\frac{0.85\ gdw}{2.65\frac{g}{cm^3}} = 0.321\ cm^3$$

$$V = \frac{1}{6}\pi\ (0.057\ cm)^3\ = 9.7\ x\ 10^{-5}\ cm^3\ \ per\ sand\ grain$$

$$\#\ of\ GAC\ particles = \frac{0.321\ cm^3}{9.7\ x\ 10^{-5} cm^3} = 3{,}309\ sand\ grains$$

$$surface\ area = 3{,}309\ sand\ grains\ \pi(0.057\ cm)^2 = \ 33.8\ cm^2 \text{ / gdw}$$

$$\frac{ng\ tATP}{gdw} * \frac{gdw}{33.8\ cm^2} = \frac{ng\ tATP}{cm^2}$$

GAC Media:

$$\frac{0.52\ gdw}{0.54\frac{g}{cm^3}} = 0.963\ cm^3$$

$$V = \frac{1}{6}\pi\ (0.065\ cm)^3\ = 1.44\ x\ 10^{-4}\ cm^3\ \ per\ GAC\ particle$$

$$\#\ of\ GAC\ particles = \frac{0.963\ cm^3}{1.44\ x\ 10^{-4} cm^3} = 6{,}697\ GAC\ particles$$

$$surface\ area = 6{,}697\ GAC\ particles\ \pi(0.065\ cm)^2 = 88.8\ cm^2\ /\ \text{gdw}$$

$$\frac{ng\ tATP}{gdw}\ *\frac{gdw}{88.8\ cm^2} = \frac{ng\ tATP}{cm^2}$$

ACE Products and Consulting, LLC.

Date: *22-Sep-21*

CLIENT:	New Hampshire University	**Client Sample ID:**	KM Schm 2021
Lab Order:	2108007	**Tag Number:**	
Project:	Research	**Collection Date:**	8/5/2021
Lab ID:	2108007-006A	**Date Received:** 8/11/2021	**Matrix:** SOIL

Analyses	Result	Limit	Qual	Units	Date Analyzed
METALS IN SOLID BY ICP		**SW6010A**		**(SW3050A)**	Analyst: **TL**
Aluminum	1120	11.4		mg/Kg-dry	8/13/2021
Antimony	ND	5.71		mg/Kg-dry	8/13/2021
Arsenic	ND	5.71		mg/Kg-dry	8/13/2021
Barium	4.85	0.571		mg/Kg-dry	8/13/2021
Beryllium	ND	0.571		mg/Kg-dry	8/13/2021
Boron	ND	5.71		mg/Kg-dry	8/13/2021
Cadmium	ND	0.571		mg/Kg-dry	8/13/2021
Calcium	333	57.1		mg/Kg-dry	8/13/2021
Chromium	1.08	0.571		mg/Kg-dry	8/13/2021
Cobalt	0.576	0.571		mg/Kg-dry	8/13/2021
Copper	ND	5.71		mg/Kg-dry	8/13/2021
Iron	2190	5.71		mg/Kg-dry	8/13/2021
Lead	ND	1.14		mg/Kg-dry	8/13/2021
Magnesium	381	57.1		mg/Kg-dry	8/13/2021
Manganese	149	0.571		mg/Kg-dry	8/13/2021
Molybdenum	ND	1.14		mg/Kg-dry	8/13/2021
Nickel	1.08	0.571		mg/Kg-dry	8/13/2021
Potassium	182	57.1		mg/Kg-dry	8/13/2021
Selenium	ND	5.71		mg/Kg-dry	8/13/2021
Silver	ND	0.571		mg/Kg-dry	8/13/2021
Sodium	ND	57.1		mg/Kg-dry	8/13/2021
Strontium	1.93	1.14		mg/Kg-dry	8/13/2021
Thallium	ND	5.71		mg/Kg-dry	8/13/2021
Titanium	83.7	0.571		mg/Kg-dry	8/13/2021
Vanadium	1.71	0.571		mg/Kg-dry	8/13/2021
Zinc	6.18	2.28		mg/Kg-dry	8/13/2021

Qualifiers:

*	Value exceeds Maximum Contaminant Level	B	Analyte detected in the associated Method Blank
E	Value above quantitation range	H	Holding times for preparation or analysis exceeded
J	Analyte detected below quantitation limits	ND	Not Detected at the Reporting Limit
S	Spike Recovery outside accepted recovery limits		

ACE Products and Consulting, LLC.

Date: *22-Sep-21*

CLIENT:	New Hampshire University	**Client Sample ID:**	KM SAND 2021
Lab Order:	2108007	**Tag Number:**	
Project:	Research	**Collection Date:**	8/5/2021
Lab ID:	2108007-005A **Date Received:** 8/11/2021	**Matrix:**	SOIL

Analyses	Result	Limit	Qual	Units	Date Analyzed
METALS IN SOLID BY ICP		**SW6010A**		**(SW3050A)**	Analyst: **TL**
Aluminum	1080	11.4		mg/Kg-dry	8/13/2021
Antimony	ND	5.72		mg/Kg-dry	8/13/2021
Arsenic	ND	5.72		mg/Kg-dry	8/13/2021
Barium	5.70	0.572		mg/Kg-dry	8/13/2021
Beryllium	ND	0.572		mg/Kg-dry	8/13/2021
Boron	7.88	5.72		mg/Kg-dry	8/13/2021
Cadmium	ND	0.572		mg/Kg-dry	8/13/2021
Calcium	381	57.2		mg/Kg-dry	8/13/2021
Chromium	2.01	0.572		mg/Kg-dry	8/13/2021
Cobalt	0.794	0.572		mg/Kg-dry	8/13/2021
Copper	ND	5.72		mg/Kg-dry	8/13/2021
Iron	3700	5.72		mg/Kg-dry	8/13/2021
Lead	ND	1.14		mg/Kg-dry	8/13/2021
Magnesium	362	57.2		mg/Kg-dry	8/13/2021
Manganese	41.2	0.572		mg/Kg-dry	8/13/2021
Molybdenum	ND	1.14		mg/Kg-dry	8/13/2021
Nickel	1.16	0.572		mg/Kg-dry	8/13/2021
Potassium	224	57.2		mg/Kg-dry	8/13/2021
Selenium	ND	5.72		mg/Kg-dry	8/13/2021
Silver	ND	0.572		mg/Kg-dry	8/13/2021
Sodium	ND	57.2		mg/Kg-dry	8/13/2021
Strontium	2.01	1.14		mg/Kg-dry	8/13/2021
Thallium	ND	5.72		mg/Kg-dry	8/13/2021
Titanium	102	0.572		mg/Kg-dry	8/13/2021
Vanadium	3.71	0.572		mg/Kg-dry	8/13/2021
Zinc	5.43	2.29		mg/Kg-dry	8/13/2021

Qualifiers:

*	Value exceeds Maximum Contaminant Level	B	Analyte detected in the associated Method Blank
E	Value above quantitation range	H	Holding times for preparation or analysis exceeded
J	Analyte detected below quantitation limits	ND	Not Detected at the Reporting Limit
S	Spike Recovery outside accepted recovery limits		

ACE Products and Consulting, LLC.

Date: *22-Sep-21*

CLIENT:	New Hampshire University	**Client Sample ID:**	KM GAC 2021
Lab Order:	2108007	**Tag Number:**	
Project:	Research	**Collection Date:**	8/5/2021
Lab ID:	2108007-004A **Date Received:** 8/11/2021	**Matrix:**	SOIL

Analyses	Result	Limit	Qual	Units	Date Analyzed
METALS IN SOLID BY ICP		**SW6010A**		**(SW3050A)**	Analyst: TL
Aluminum	1840	18.3		mg/Kg-dry	8/13/2021
Antimony	ND	9.13		mg/Kg-dry	8/13/2021
Arsenic	ND	9.13		mg/Kg-dry	8/13/2021
Barium	113	0.913		mg/Kg-dry	8/13/2021
Beryllium	1.32	0.913		mg/Kg-dry	8/13/2021
Boron	ND	9.13		mg/Kg-dry	8/13/2021
Cadmium	ND	0.913		mg/Kg-dry	8/13/2021
Calcium	15400	91.3		mg/Kg-dry	8/13/2021
Chromium	12.8	0.913		mg/Kg-dry	8/13/2021
Cobalt	7.53	0.913		mg/Kg-dry	8/13/2021
Copper	108	9.13		mg/Kg-dry	8/13/2021
Iron	1960	9.13		mg/Kg-dry	8/13/2021
Lead	ND	1.83		mg/Kg-dry	8/13/2021
Magnesium	764	91.3		mg/Kg-dry	8/13/2021
Manganese	328	0.913		mg/Kg-dry	8/13/2021
Molybdenum	ND	1.83		mg/Kg-dry	8/13/2021
Nickel	14.8	0.913		mg/Kg-dry	8/13/2021
Potassium	141	91.3		mg/Kg-dry	8/13/2021
Selenium	ND	9.13		mg/Kg-dry	8/13/2021
Silver	ND	0.913		mg/Kg-dry	8/13/2021
Sodium	260	91.3		mg/Kg-dry	8/13/2021
Strontium	112	1.83		mg/Kg-dry	8/13/2021
Thallium	ND	9.13		mg/Kg-dry	8/13/2021
Titanium	218	0.913		mg/Kg-dry	8/13/2021
Vanadium	40.2	0.913		mg/Kg-dry	8/13/2021
Zinc	21.2	3.65		mg/Kg-dry	8/13/2021

Qualifiers:

*	Value exceeds Maximum Contaminant Level	B	Analyte detected in the associated Method Blank
E	Value above quantitation range	H	Holding times for preparation or analysis exceeded
J	Analyte detected below quantitation limits	ND	Not Detected at the Reporting Limit
S	Spike Recovery outside accepted recovery limits		

ACE Products and Consulting, LLC.

Date: *07-Apr-22*

CLIENT:	New Hampshire University	**Client Sample ID:**	Virgin GAC
Lab Order:	2204002	**Tag Number:**	
Project:	Virgin GAC	**Collection Date:**	8/14/2021
Lab ID:	2204002-001A **Date Received:** 3/31/2022	**Matrix:**	SOLID

Analyses	Result	Limit	Qual	Units	Date Analyzed
METALS IN SOLID BY ICP		SW6010A		(SW3050A)	Analyst: TL
Aluminum	1560	13.5		mg/Kg-dry	4/5/2022
Antimony	ND	6.74		mg/Kg-dry	4/5/2022
Arsenic	ND	6.74		mg/Kg-dry	4/5/2022
Barium	68.0	0.674		mg/Kg-dry	4/5/2022
Beryllium	ND	0.674		mg/Kg-dry	4/5/2022
Boron	24.5	13.5		mg/Kg-dry	4/5/2022
Cadmium	ND	0.674		mg/Kg-dry	4/5/2022
Calcium	957	67.4		mg/Kg-dry	4/5/2022
Chromium	5.89	0.674		mg/Kg-dry	4/5/2022
Cobalt	7.11	0.674		mg/Kg-dry	4/5/2022
Copper	23.2	6.74		mg/Kg-dry	4/5/2022
Iron	2520	6.74		mg/Kg-dry	4/5/2022
Lead	ND	1.35		mg/Kg-dry	4/5/2022
Lithium	2.60	0.674		mg/Kg-dry	4/5/2022
Magnesium	176	67.4		mg/Kg-dry	4/5/2022
Manganese	25.5	0.674		mg/Kg-dry	4/5/2022
Molybdenum	1.40	1.35		mg/Kg-dry	4/5/2022
Nickel	15.3	0.674		mg/Kg-dry	4/5/2022
Potassium	198	67.4		mg/Kg-dry	4/5/2022
Selenium	ND	6.74		mg/Kg-dry	4/5/2022
Silver	ND	0.674		mg/Kg-dry	4/5/2022
Sodium	248	67.4		mg/Kg-dry	4/5/2022
Strontium	110	1.35		mg/Kg-dry	4/5/2022
Sulfur	3190	67.4		mg/Kg-dry	4/5/2022
Thallium	ND	6.74		mg/Kg-dry	4/5/2022
Titanium	238	0.674		mg/Kg-dry	4/5/2022
Vanadium	30.9	0.674		mg/Kg-dry	4/5/2022
Zinc	6.23	2.70		mg/Kg-dry	4/5/2022
PERCENT MOISTURE		D2216			Analyst: TL
Percent Moisture	25.8	0.100		wt%	4/5/2022 3:00:00 PM

Qualifiers:

*	Value exceeds Maximum Contaminant Level	B	Analyte detected in the associated Method Blank
E	Value above quantitation range	H	Holding times for preparation or analysis exceeded
J	Analyte detected below quantitation limits	ND	Not Detected at the Reporting Limit
S	Spike Recovery outside accepted recovery limits		

ACE Products and Consulting, LLC.

Date: *02-Jun-22*

CLIENT:	New Hampshire University	**Client Sample ID:**	GAC
Lab Order:	2205011	**Tag Number:**	
Project:	ICP METALS	**Collection Date:**	5/25/2022
Lab ID:	2205011-001A **Date Received:** 5/25/2022	**Matrix:**	SOLID

Analyses	Result	Limit	Qual	Units	Date Analyzed
METALS IN SOLID BY ICP		**SW6010A**		**(SW3050A)**	Analyst: TL
Aluminum	1660	16.9		mg/Kg-dry	5/26/2022
Antimony	ND	8.45		mg/Kg-dry	5/26/2022
Arsenic	ND	8.45		mg/Kg-dry	5/26/2022
Barium	91.3	0.845		mg/Kg-dry	5/26/2022
Beryllium	1.34	0.845		mg/Kg-dry	5/26/2022
Boron	19.4	16.9		mg/Kg-dry	5/26/2022
Cadmium	ND	0.845		mg/Kg-dry	5/26/2022
Calcium	15000	84.5		mg/Kg-dry	5/26/2022
Chromium	10.8	0.845		mg/Kg-dry	5/26/2022
Cobalt	8.90	0.845		mg/Kg-dry	5/26/2022
Copper	49.8	8.45		mg/Kg-dry	5/26/2022
Iron	2240	8.45		mg/Kg-dry	5/26/2022
Lead	ND	1.69		mg/Kg-dry	5/26/2022
Lithium	0.989	0.845		mg/Kg-dry	5/26/2022
Magnesium	706	84.5		mg/Kg-dry	5/26/2022
Manganese	13.6	0.845		mg/Kg-dry	5/26/2022
Molybdenum	ND	1.69		mg/Kg-dry	5/26/2022
Nickel	15.3	0.845		mg/Kg-dry	5/26/2022
Potassium	128	84.5		mg/Kg-dry	5/26/2022
Selenium	ND	8.45		mg/Kg-dry	5/26/2022
Silver	ND	0.845		mg/Kg-dry	5/26/2022
Sodium	271	84.5		mg/Kg-dry	5/26/2022
Strontium	108	1.69		mg/Kg-dry	5/26/2022
Sulfur	2730	84.5		mg/Kg-dry	5/26/2022
Thallium	ND	8.45		mg/Kg-dry	5/26/2022
Titanium	256	0.845		mg/Kg-dry	5/26/2022
Vanadium	35.4	0.845		mg/Kg-dry	5/26/2022
Zinc	14.7	3.38		mg/Kg-dry	5/26/2022

Qualifiers:

*	Value exceeds Maximum Contaminant Level	B	Analyte detected in the associated Method Blank
E	Value above quantitation range	H	Holding times for preparation or analysis exceeded
J	Analyte detected below quantitation limits	ND	Not Detected at the Reporting Limit
S	Spike Recovery outside accepted recovery limits		

Bed Volume Calculations

Bed Volumes were calculated for each filter using surface area and flow rates applied in Winthrop (ME):

$$70\ ft\ x\ 47.67\ ft = 3{,}336.9\ ft^2$$

$$3{,}336.9\ ft^2 - 288\ ft^2 \text{(ramp)} = 3{,}050\ ft^2$$

$$3{,}050\ ft^2\ x\ 0.5\ ft = 1{,}525\ ft^3$$

$$1{,}525\ ft^3\ x\ \frac{7.48\ gal}{ft^3} = 11{,}407\ \frac{gal}{bed\ volume}$$

*Filters in Winthrop (ME) operated within 50-60 gpm

$$\textbf{Yearly Q} = 50\ \frac{gal}{min}\ x\ 60\ \frac{min}{hr}\ x\ 24\ \frac{hr}{day}\ x\ 355\ \frac{day}{year} = 25.56\ x\ 10^6\ \frac{gal}{year}$$

Thus,

$$\frac{\#\ of\ bed\ volumes}{year} = 25.56\ x\ 10^6\ \frac{gal}{year}\ x\ \frac{1\ BV}{11{,}407\ gal} = 2{,}241\ \frac{bed\ volumes}{year}$$

Filter #1 – GAC installed in 2006:

$$2{,}241\ \frac{bed\ volumes}{year}\ x\ 16\ years = 35,\ 856\ bed\ volumes$$

Filter #2 – GAC installed in 2020:

$$2{,}241\ \frac{bed\ volumes}{year}\ x\ 2\ years = 4{,}482\ bed\ volumes$$

Filter #3 – GAC installed in 2011:

$$2{,}241\ \frac{bed\ volumes}{year}\ x\ 11\ years = 24{,}651\ bed\ volumes$$